U-Pb geochronology of the Duluth Complex and related hypabyssal intrusions: investigating the emplacement history of a large multiphase intrusive complex related to the 1.1 Ga Midcontinent Rift

A THESIS
SUBMITTED TO THE FACULTY OF THE GRADUATE SCHOOL
OF THE UNIVERSITY OF MINNESOTA
BY

Steven Arthur Hoaglund

IN PARTIAL FULFILLMENT OF THE REQUIREMENTS
FOR THE DEGREE OF
MASTER OF SCIENCE

James D. Miller Jr.

July, 2010

Acknowledgements

- The Precambrian Research Center, for their financial and moral support
- Jim Crowley, Mark Schmitz, and Debbie Pierce from the Boise State Isotope Geology Laboratory for access to their lab, training and help for analyses
- Christina Gallup, for her assistance with initial project development
- UMD's Swenson College of Science and Engineering, for their financial support to travel to the 2009 Geological Society of America annual meeting and present my initial results
- UMD's Department of Geological Sciences, for their financial support for both project costs and registration costs for professional meetings
- The Institute on Lake Superior Geology (ILSG), for the Eisenbrey Student Travel award that allowed me to present my final results at the 56^{th} annual meeting
- The Mesabi Range Geological Society, for their travel award which also helped me attend the 56^{th} annual ILSG meeting
- UMD's Natural Resource Research Institute, for use of their rock crushing equipment
- Dan Costello for his help with collecting field samples
- Teddy Berg, undergraduate geology student at UMD, for his tireless assistance
- My entire Committee: Jim Miller, Christina Gallup, and Paul Kiprof, for supporting the initial project proposal
- My Mom and Dad, for their encouragement and support
- Lastly, my lovely wife Jenny for her endless love, patience, and support throughout this entire study

Abstract

Paces and Miller (1993) precisely established the main intrusive periods that created the Duluth Complex and related intrusions associated with the 1.1 Ga Midcontinent Rift in NE Minnesota. They did not, however, resolve differences in emplacement ages within and between major intrusive units due to a small number of dated samples. New high-precision U-Pb baddeleyite and zircon ages from five mafic intrusions related to the Duluth Complex builds on the work of Paces and Miller (1993).

Ages from three intrusions that span the entire range of Duluth Complex layered series intrusive activity indicate that the layered series and anorthositic series were synchronously emplaced around 1098 Ma. Moreover, zircon ages obtained from the perceived oldest (Partridge River, $^{206}Pb/^{238}U$ age 1095.94 ± 0.18 Ma) and youngest (Bald Eagle, $^{206}Pb/^{238}U$ age 1095.64 ± 0.19 Ma) layered series intrusions suggest the bulk of layered series activity occurred within a period of 670 ka. The Tuscarora intrusion (early layered series) has a distinctly older $^{207}Pb/^{206}Pb$ baddeleytie age than the Partridge River intrusion (1098.81 ± 0.32 and 1097.98 ± 0.37 Ma, respectively). However, in light of new information regarding the incompatibility between zircon and baddeleyite ages, its temporal relationship with other layered series intrusions remains unclear.

Zircon ages obtained from two early Beaver Bay Complex (BBC) intrusions indicate Duluth Complex and BBC magmatism likely overlap. The Houghtaling Creek troctolite is indistinguishable from the other layered series intrusions. Moreover, the Wilson Lake ferrogabbro, long interpreted to be older than the Houghtaling Creek, is distinctly younger ($^{207}Pb/^{206}Pb$ zircon ages 1095.75 ± 0.92 and 1098.62 ± 0.50 Ma, respectively). There still exists an approximate 2 Ma gap between early Beaver Bay and Duluth Complex, and late BBC.

A reasonable estimate based on the geometry of layered series intrusions indicate that over 16,000 km^3 of mafic magma intruded during layered series emplacement (excluding unknowable amounts of erosion). With over 16,000 km^3 of mafic magma being intruded over a period of 670 ka, emplacement rates were at least 0.024 km^3/yr, which is similar to estimates for other large continental flood basalt provinces.

Table of Contents

List of Tables —— v

List of Figures —— vi

Chapter 1 Introduction —— 1

Chapter 2 Geologic Setting —— 4

2.1 The Midcontinent Rift —— 4
2.2 Midcontinent Rift-related Geology in the Lake Superior Region —— 11
2.3 North Shore Volcanic Group —— 13
2.4 Duluth Complex —— 17
2.5 Beaver Bay Complex —— 20

Chapter 3 Previous Geochronologic Studies —— 23

3.1 Davis and Sutcliffe (1985) —— 24
3.2 Palmer and Davis (1987) —— 26
3.3 Davis and Paces (1990) —— 27
3.4 Heaman and Machado (1992) —— 28
3.5 Paces and Miller (1993) —— 29
3.6 Zartman et al. (1997) —— 31
3.7 Davis and Green (1997) —— 33
3.8 Vervoort et al. (2007) —— 36
3.9 Heaman et al. (2007) —— 39
3.10 Summary —— 42

Chapter 4 Purpose of Study —— 44

Chapter 5 Methods —— 47

5.1 Sampling Strategy —— 47
5.2 Mineral Separations and Analytical Procedure —— 56

Chapter 6 Results —— 59

6.1 Duluth Complex: Partridge River intrusion - *Sample PRI* —— 63
6.2 Duluth Complex: Tuscarora intrusion - *Sample TI* —— 63
6.3 Duluth Complex: Duluth Layered Series - *Sample DLS* —— 64
6.4 Duluth Complex: Greenwood Lake intrusion - *Sample GLI* —— 65
6.5 Duluth Complex: Bald Eagle intrusion - *Sample BEI* —— 65
6.6 Beaver Bay Complex: Wilson Lake ferrogabbro - *Sample WLFG* —— 66

6.7 Beaver Bay Complex: Houghtaling Creek troctolite - *Sample HCT* 67
6.8 Miscellaneous Intrusion: Endion Sill - *Sample ES* 68

Chapter 7 Discussion 69

7.1 Differences in $^{207}Pb/^{206}Pb$ and $^{206}Pb/^{238}U$ ages 69
7.2 Baddeleyite vs. Zircon 72
7.3 Relative Ages of Layered Series Intrusions 74
7.4 Overlap of Duluth Complex and Beaver Bay Complex Magmatism 80
7.5 Periodicity of Main Stage MCR Magmatism 88
7.6 Age of Endion Sill 90
7.7 Rate of Emplacement of Layered Series Intrusions 91

Chapter 8 Conclusions 94

Chapter 9 References 97

List of Tables

Chapter 3 Tables

3.1 Davis and Sutcliffe (1985) $^{207}Pb/^{206}Pb$ ages — 25
3.2 Davis and Paces (1990) $^{207}Pb/^{206}Pb$ ages — 27
3.3 Paces and Miller (1993) $^{207}Pb/^{206}Pb$ ages — 29
3.4 Zartman et al. (1997) $^{207}Pb/^{206}Pb$ ages — 32
3.5 Davis and Green (1997) $^{207}Pb/^{206}Pb$ ages — 34
3.6 Heaman et al. (2007) $^{207}Pb/^{206}Pb$ ages — 40

Chapter 5 Tables

5.1 Sample locations — 48

Chapter 6 Tables

6.1 Isotopic data — 60
6.2 Summary of U-Pb ages obtained in this study — 62

Chapter 7 Tables

7.1 U-Pb ages from the Duluth and Beaver Bay Complex — 80
7.2 Summary of layered series volume calculations — 92

List of Figures

Chapter 2 Figures

2.1 Bouger gravity anomaly of the Midcontinent Rift (MCR) ———6
2.2 Interpretive model for magmatic stages MCR system ———10
2.3 General geology of the MCR in the Lake Superior region ———13
2.4 General geologic of the North Shore Volcanic Group (NSVG) ——15
2.5 Lithostratigraphy of the NSVG ———16
2.6 General geology of the Duluth Complex (DC) ———18
2.7 General geology of the Beaver Bay Complex (BBC) ———22

Chapter 3 Figures

3.1 U-Pb zircon ages for DC granophyres from Vervoort et al. (2007) –37
3.2 Summary of previous $^{207}Pb/^{206}Pb$ ages pertaining to DC and BBC –38
3.3 Correlation diagram for age studies of the MCR ———44

Chapter 4 Figures

4.1 Aeromagnetic data and geologic interpretation of layered series intrusions for the western DC ——45

Chapter 5 Figures

5.1 Geologic map of DC containing sample locations ———49
5.2 Flow chart for zircon/baddeleyite separations and CA-TIMS ———57

Chapter 6 Figures

6.1 Zircon and baddeleyite photomicrographs ———62
6.2 Concordia plot of Partridge River intrusion with ages ———63
6.3 Concordia plot of Tuscarora intrusion with ages ———64
6.4 Concordia plot of Bald Eagle intrusion with ages ———66
6.5 Concordia plot of Wilson Lake ferrogabbro with ages ———67
6.6 Concordia plot of Houghtaling Creek troctolite with ages ———68

Chapter 7 Figures

7.1 Zircon concordia plots from Schoene et al. (2006) ———71
7.2 Concordia plot for zircon FC1, FC4b, and baddeleyite FC4b from Boise State Isotope Geology Laboratory ———74
7.3 Summary of $^{207}Pb/^{206}Pb$ ages related to the DC and BBC ———77

7.4 $^{207}Pb/^{206}Pb$ weighted mean ages for layered series and anorthositic series intrusions ——78
7.5 $^{206}Pb/^{238}U$ weighted mean ages for layered series and anorthositic series intrusions ——79
7.6 $^{207}Pb/^{206}Pb$ weighted mean ages for DC layered series and anorthositic series intrusions and BBC intrusions ——82
7.7 Aeromagnetic field images along with corresponding geologic maps of the southern and northern BBC ——83
7.8 $^{206}Pb/^{238}U$ weighted mean ages for DC layered series and anorthositic series intrusions and BBC intrusions ——84
7.9 Geology of a portion of the Wilson Lake area ——86
7.10 Volume estimation method for DC layered series intrusions ——93

Chapter 8 Figures

8.1 Distribution of weighted mean $^{207}Pb/^{206}Pb$ ages for intrusions related to the DC and BBC ——96

1. Introduction

Geochronologic studies of the Midcontinent Rift in the Lake Superior region, a 1.1 Ga failed attempt at continental rifting, have played a critical role in understanding the tectonomagmatic evolution of this major geological province. Before the development of high-precision, single-grain zircon geochronology, many conventional low-precision Rb-Sr, K-Ar, and bulk U-Pb studies were conducted on rocks associated with the Midcontinent Rift (e.g. Silver and Green, 1972; Baragar, 1978; Chaudhuri, 1972; Chaudhuri and Brookins, 1969; **See Sum paper**). As methods that increased the precision of U-Pb zircon dates, such as the air-abrasion method of Krogh (1982), it was revealed that the MCR evolved over a period of at least 23 million years and did so in several distinct tectonomagmatic stages (Davis and Sutcliffe, 1985; Palmer and Davis, 1987; Heaman and Machado, 1992; Paces and Miller, 1993; Zartman et al. 1997; Davis and Green, 1997; Vervoort et al., 2007; Heaman et al., 2007).

Miller and Vervoort (1996) termed the magmatic stages evident in the geochronologic data as Early, Latent, Main and Late. The early magmatic stage, from 1109 to 1107 Ma, occurred during a period of reversed magnetic polarity and was characterized by voluminous volcanism of an initially primitive source, giving rise to more evolved magmas towards the end of the stage. The latent magmatic stage, from 1107 to 1102 Ma, was a time of limited felsic magmatism occurred. Mafic magmatism resumed during the main magmatic stage from 1102 to 1094 Ma, at a time of normal magnetic polarity that was characterized by a diverse range of mostly uncontaminated magma compositions. The late magmatic stage (1094 to 1086 Ma) is characterized by waning volcanic activity, and continued rift basin subsidence resulting in interbedded sedimentary and volcanic sequences (Miller and Severson, 2002). Recent data by Heaman et al. (2007) of intrusive rock in the Lake Nipigon/Thunder Bay area of Ontario suggest that early rift-related magmatism may extend as far back 1115 Ma.

In northeastern Minnesota, several modern geochronologic studies have been conducted on MCR-related intrusive and volcanic rocks that have been critical to understanding the evolution of the rift in the western Lake Superior region. The first systematic study was conducted by Paces and Miller (1993), who focused on evaluating the range of ages of the main mafic intrusions comprising the Duluth and Beaver Bay complexes. Their result showed that most of the intrusions were emplaced during what would later come to be recognized as the early and main stages of the rift, and that Duluth Complex magmatism was generally 2-3 Ma older than that of the more hypabyssal Beaver Bay Complex (1099 vs. 1096 Ma). They also made the surprise discovery that, despite field evidence suggesting anorthositic rocks of the Duluth Complex were significantly older than the layered intrusions, these two dominant series of the complex were nearly synchronously emplaced.

Davis and Green (1997) reported the U-Pb zircon ages for ten volcanic and intrusive rocks from throughout the western Lake Superior region that included eight dates from northeastern Minnesota. Their ages of rhyolites and basalts from the NSVG and two Duluth Complex intrusions confirmed the presence of a hiatus in magmatism between 1107Ma and 1100 Ma, as was found in the intrusive rocks by Paces and Miller (1993). In the same Canadian Journal of Earth Science volume, Zartman et al. (1997)

found a similar hiatus in MCR volcanics on the south limb of the rift in Michigan and Wisconsin. A more recent study by Vervoort et al. (2007) of granophyric intrusions in northeastern Minnesota found similar bimodal age populations that roughly correspond to early stage and main stage magmatism.

While these geochronologic studies have provided a better understanding of MCR-related intrusive activity in northeastern Minnesota, they leave several important questions unresolved:

1) What was the full range of emplacement ages among the various intrusions comprising the Duluth Complex and Beaver Bay Complex?
2) Can the sequence of emplacement of layered intrusions (collectively termed the layered series) interpreted from field relationships and aeromagnetic data (Miller and Severson, 2002) be supported by precise geochronologic data?
3) What are the emplacement ages for some of the isolated hypabyssal intrusions within the NSVG and outside the Duluth and Beaver Bay complexes.

This study intends to address these questions using the single grain U-Pb zircon isotope dilution methods (Krogh, 1973) coupled with modified chemical abrasion (Mattinson, 2005) to acquire the most precise U-Pb ages possible on zircon and baddeleyite. These data will be acquired at the Boise State Isotope Laboratory under the direction of Professor Mark Schmitz and assisted by Jim Crowley. By sampling intrusions that field and geophysical data imply are the oldest and youngest intrusions of the Duluth Complex and the oldest intrusions of the Beaver Bay Complex, it may be possible to establish the range of emplacement ages among the two complexes and determine if any overlap of magmatic activity exists. Additionally, sampling intrusions that span the entire perceived range of layered series intrusive activity will yield the best possible chance to test the emplacement sequence proposed by Miller and Severson (2002). Finally, by sampling one of the subvolcanic sills that has an ambiguous contact relationship with the Duluth Complex in the Duluth area (Green and Miller, 2008), their specific temporal relationship may be resolved, as might the question of where these isolated intrusions fit in the overall magmatism of the MCR. Attempting to answer these unresolved questions will also add to our overall understanding of the frequency and duration of magmatism of the Midcontinent Rift.

2. Geologic Setting

2.1 The Midcontinent Rift

The Midcontinent Rift is the one of the best preserved examples of continental rifting on Earth, due to its failure to progress to a stage of ocean basin formation and to its partial structural inversion caused by compressional forces attending the 1.2-0.9 Ga Grenville orogeny (Cannon, 1992). Geologic exposure of the MCR is confined to Mesoproterozoic volcanic, intrusive and sedimentary rocks in the Lake Superior region. Geophysically, the MCR is recognized to be much more extensive and is characterized by a series of segmented linear positive gravity anomalies and strong magnetic anomalies (Van Schmus, 1985) following a 2,000 km arcuate path extending southwest from Lake Superior to Kansas, and southeast to lower Michigan (Fig. 2.1).

The MCR rifting event is inferred from geological, geophysical and geochemical evidence to have coincided with (if not to have been caused by) the sublithospheric impact of a starting mantle plume (Hutchinson et al., 1990; Nicholson and Shirey, 1990; Nicholson et al., 1997). Geological evidence comes from the thick and areally extensive flood basalts exposed along the flanks of the Lake Superior basin, locally totaling over 10 kilometers thick. Add to this the large volumes of intrusive rocks, especially comprising the Duluth Complex, and the igneous component of the MCR clearly compares with other large igneous provinces interpreted to be products of mantle plume magmatism.

Geophysical evidence comes from gravity, magnetic, and seismic data, which demonstrate the enormous volume of largely mafic magma emplaced into the crust along the MCR. Deeply-penetrating seismic reflection surveys indicate that in the Lake Superior basin, the deepest sections of rift subsidence reached depths of at least 30 km, allowing for the accommodation of at least 15 km and 10 km of rift-related volcanic and sedimentary rocks, respectively (Behrendt et al., 1988; Hinze et al., 1992). Beneath Lake Superior, the central horst, which was thrust up from the central graben by late compressional forces, displays a strong positive gravity anomaly (Fig. 2.1). The horst is bounded by segmented, asymmetric, high-angle faults, with rift-fill sedimentary basins on either side (Hinze et al., 1992, Nicholson and Shirey, 1990). The total volume of rift-related volcanic rocks is estimated by Cannon (1992) to be ~2 x 10^6 km^3, thus providing further evidence of a mantle plume origin to MCR magmatism. For a complete interpretation of the integrated gravity, magnetic and seismic data, see Hinze et al. (1992) and Allen et al. (1997).

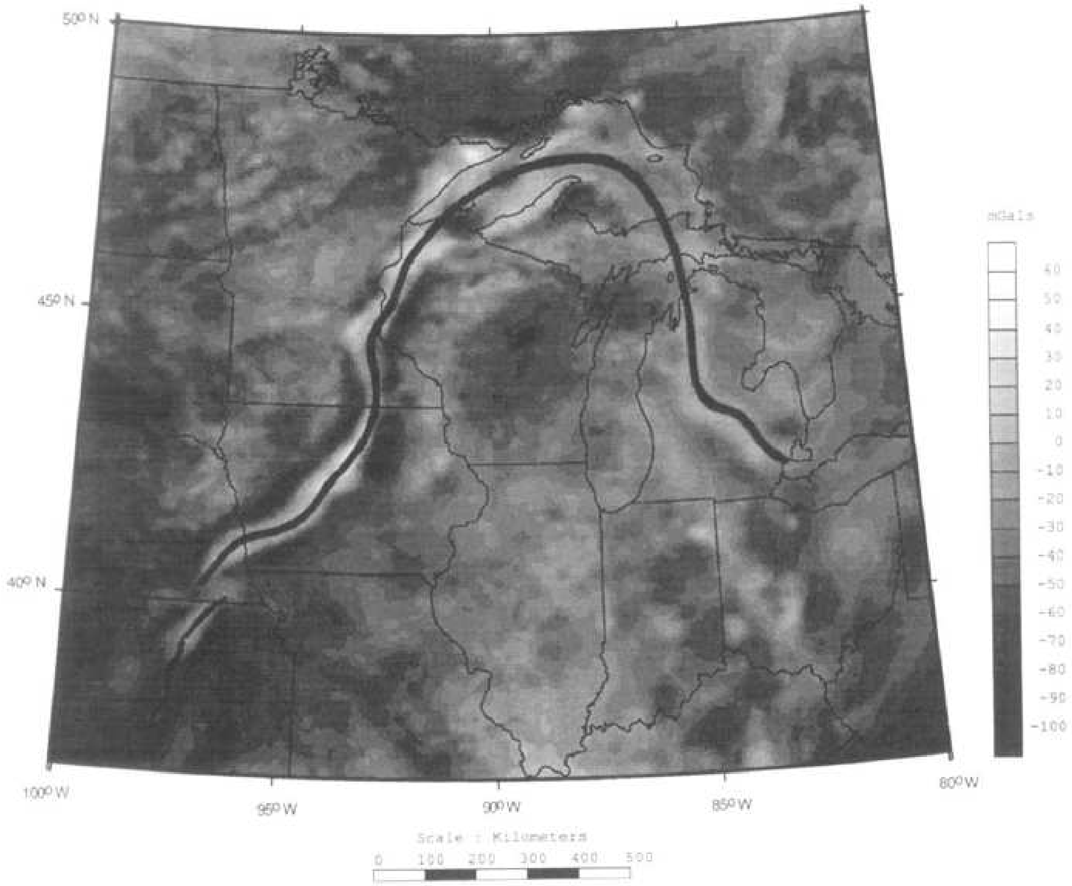

Figure 2.1. Bouger gravity map of the central United States showing the positive gravity anomaly related to the Midcontinent Rift. Taken from Hinze et al. (1992)

Geochemical evidence for the mantle plume comes from trace element and isotopic analysis on rift-related rocks (Nicholson and Shirey, 1990; Lightfoot et al., 1991; Klewin and Shirey, 1992; Shirey et al., 1994; Shirey, 1997; Nicholson et al., 1997; Hollings et al., 2007 A and B). Collectively, these studies increased our geochemical understanding of the rift. For example, in their study of the enriched tholeiitic flows of the Portage Lake Volcanics, Nicholson and Shirey (1990) found that basalts had plume-like εNd values near zero, where the more evolved rhyolites showed evidence of varying degrees of crustal contamination. Combined, these studies suggest that the onset of magmatism was initiated by an enriched mantle plume, which thermally induced extension in the crust, thereby providing accommodation space for the plume-drived magmas.

Geochronologic studies coupled with geochemical studies over the past 25 years have come to indicate that MCR-related magmatism occurred in at least four distinct stages over a span of at least 26 million years (Davis and Sutcliffe, 1985; Palmer and Davis, 1987; Davis and Paces, 1990; Paces and Miller, 1993; Davis and Green, 1997; Zartman et al., 1997, Vervoort et al 2007, Heaman et al., 2007). These stages, termed by Miller and Vervoort (1996) as the Early, Main, Latent, and Late magmatic stages, were formulated to reflect the observed temporal changes in the frequency and compositional characteristics of MCR magmatism. Based on this empirical data, along with the geophysical models of the rift, several workers have interpreted these stages to represent changes in the thermodynamic interactions between the upwelling mantle plume-derived melts, and the surrounding lithospheric mantle and continental crust through which they passed. The stages were subsequently adopted and refined by others (Nicholson et al., 1997; Miller and Severson, 2002; Vervoort et al., 2007; Heaman et al., 2007). The following description of these stages are taken from Miller and Vervoort (1996) and Miller and Severson (2002), unless otherwise noted.

The early magmatic stage (1109 – 1107 Ma) is characterized by rapid and voluminous eruption of initially primitive magmas, followed by evolved and crustally contaminated basalts and rhyolites. As the mantle derived plume impacted the lower continental lithosphere, continental crust began to thin (Fig. 2.2A). This resulted in the rapid eruption of voluminous, primitive, plume-derived magmas at first, but staging of these magmas near the Moho triggered partial melting of the lower crust. Ultimately, this resulted in more evolved and crustally contaminated mafic magmas, and the generation of felsic melts evidently by crustal anatexis.

A recent study by Heaman et al. (2007) seems to indicate that early rift magmatism could have started much earlier than the 1109 Ma date indicated by other U-Pb ages in the western Lake Superior region. Their data push the onset of early stage magmatism related to the rift back to 1115 Ma. These dates come exclusively from mafic and ultramafic intrusions in the Thunder Bay and Lake Nipigon area. The fact that the oldest volcanic ages are 1109 Ma may indicate that this earliest period of magmatism represents a period of broad doming such that volcanic products of these intrusion were not preserved (Miller, pers. comm. 2010). Heaman et al. (2007) also discovered a number of mafic, ultramafic and lamprophyric intrusions that fall in the range of 1130-1150 Ma and that overlap the 1140 Ma age of the Great Abitibi dike in eastern Ontario (Krogh et al., 1987). Heaman et al. (2007) suggested that this magmatism may also be related to the Midcontinent Rift, which if true would imply that MCR magmatism lasted over 60 million years and would seriously call into question a mantle plume origin for the rift.

The latent magmatic stage (1107 – 1102 Ma), is characterized by a hiatus in mafic volcanic and intrusive activity (Fig. 2.2B). The only magmatism evident during this period is felsic volcanism. This stage is interpreted to represent a period of significant crustal underplating of mantle plume magmas. This underplating was triggered by partial melting of the lower crust creating a rheological and density barrier that trapped mafic mantle melts in the vicinity of the Moho, but allowed for intermittent felsic magmatism to reach the surface.

Main stage magmatism (1102 – 1094 Ma) is characterized by rapid eruptions of evolved, but uncontaminated mantle-derived magmas, as well as crustally derived rhyolites (Fig. 2.2C). This stage is thought to represent the evacuation of lower crustal magma chambers following density clarifying of the trapping felsic melts. Nicholson et al. (1997) have also suggested that external (Grenvillian?) extensional forces may have been involved in triggering the onset of main stage magmatism.

Late stage magmatism (1094 – 1086 Ma) is characterized by primitive to evolved mafic to felsic lavas, commonly confined to stratovolcanic edifices, interbedded with late clastic sediments (Fig. 2.2D). This period of waning volcanic activity is thought to represent drifting of the overlying plate away from its mantle heat source, effectively ending magmatic activity in the rift basin.

Approximately 30 to 50 million years after magmatism had ceased, the rift experienced tectonic inversion due to regional compressional forces (Cannon, 1992). Originally graben-bounding normal faults were transformed into reverse faults, tectonically inverting the central graben into a horst. Continued sedimentation during compression buried the upturned volcanic flows along the faults (Cannon, 1992). The Grenville collisional event from 1030-970 Ma likely provided the compressional forces necessary to cause the observed tectonic inversion (Van Schmus, 1992).

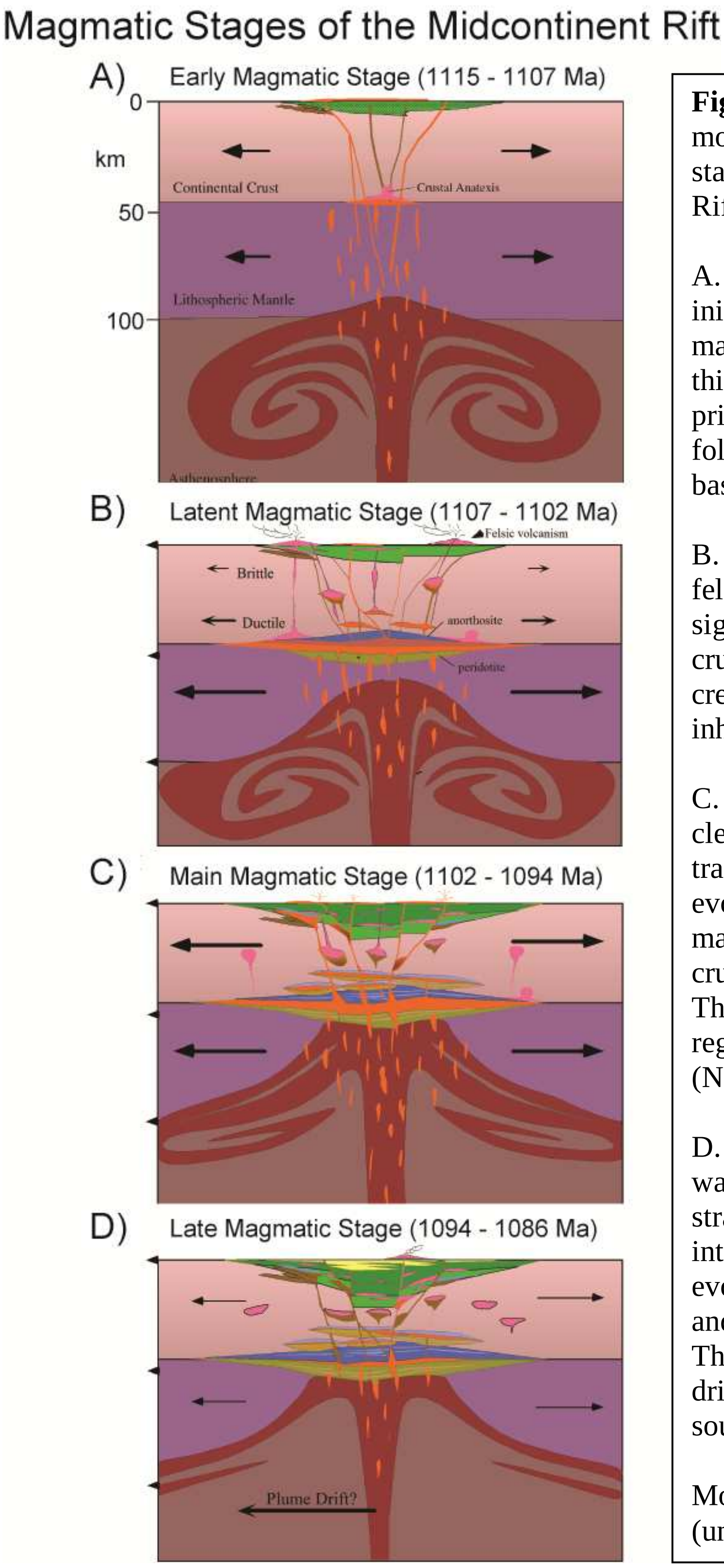

Figure 2.2. Interpretive model for the magmatic stages of the Midcontinent Rift system

A. Early Magmatic Stage - initial impact of starting mantle plume head. Crustal thinning begins and initially primitive magmas erupt, followed by more evolved basalts and rhyolites

B. Latent Magmatic Stage - felsic volcanism occurs as significant underplating and crustal anatexis. Partial melts create rheological barrier that inhibits mafic volcanism

C. Main Magmatic Stage - cleansing of the felsic melt traps. Rapid eruption of evolved and uncontaminated mantle derived magmas and crustally derived rhyolites. Thought to have initiated by regional extensional forces (Nicholson et al., 1997)

D. Late Magmatic Stage - waning volcanic activity, stratovolcanic edifices contain interbedded primitive to evolved mafic to felsic lavas and late clastic sediments. Thought to represent plate drift away from mantle heat source

Modified from Miller (unpublished figure)

2.2 Midcontinent Rift-related Geology in the Lake Superior Region

Igneous and sedimentary rocks associated with the Midcontinent Rift are exposed exclusively around the Lake Superior basin (Fig. 2.3). Stratified volcanic and sedimentary units of the MCR are grouped into the Keweenawan Supergroup, whereas intrusive rocks associated with the rift are classified as part of the Midcontinent Rift Intrusive Supersuite (Morey and Green, 1982, Miller, Green, and Severson, 2002). Traditionally, volcanic rocks of the Keweenawan Supergroup have been subdivided into upper and lower chronostratigraphic units based on a major reverse to normal paleomagnetic polarity reversal (Fig. 2.3). This polarity reversal is also recognized among the intrusive rocks and was used early on as means of discriminating early and late magmatism in the MCR. U-Pb zircon geochronology by Davis and Green (1997) constrained the timing of this reversal between 1105 Ma and 1102 Ma.

Rocks of the Midcontinent Rift are comprised of volcanic suites, intrusive complexes, and detrital sedimentary sequences. The reversed and normal-polarity volcanic suites associated with the MCR consist of dominantly mafic and minor felsic flows primarily exposed along the shoreline of Lake Superior. Volcanic packages are represented by the North Shore Volcanic Group in northeastern Minnesota, the Osler Volcanics of southern Ontario, the Mamainse Point and Michipicoten Island Formation in southeastern Ontario, and the Portage Lake Volcanics and Powder Mill Volcanic Group in northern Wisconsin and the upper peninsula of Michigan (Fig. 2.3). Intruded into these volcanic suites are the many MCR-related intrusive suites, represented by the dominantly mafic layered complexes, dikes, and sills with minor intrusions of felsic and alkaline magmas. The layered mafic intrusions of the Duluth Complex and Beaver Bay Complex intrude the NSVG in northeastern Minnesota, while the hypabyssal Logan Sills straddle the border between northeastern Minnesota and southern Ontario. In southern Ontario, the mafic Logan Sills are exposed inland of Lake Superior, while the alkaline intrusions of the Coldwell Complex are exposed further to the east. Lastly, the Mellen Intrusive Complex intrudes the Powder Mill Volcanic Group inland of the south shore of Lake Superior in northern Wisconsin (Fig. 2.3). In addition to the volcanic and intrusive suits are the interflow and late basin-fill sedimentary sequences: the pre-Keweenawan Sibley group in southern Ontario (Rogala et al., 2007), and the Bayfield and Oronto Group in northern Wisconsin and Michigan (Fig. 2.3). Several extensive, late, reverse faults are present in the basin, which represent the late compressional forces that caused the tectonic inversion in the region (Fig. 2.3)

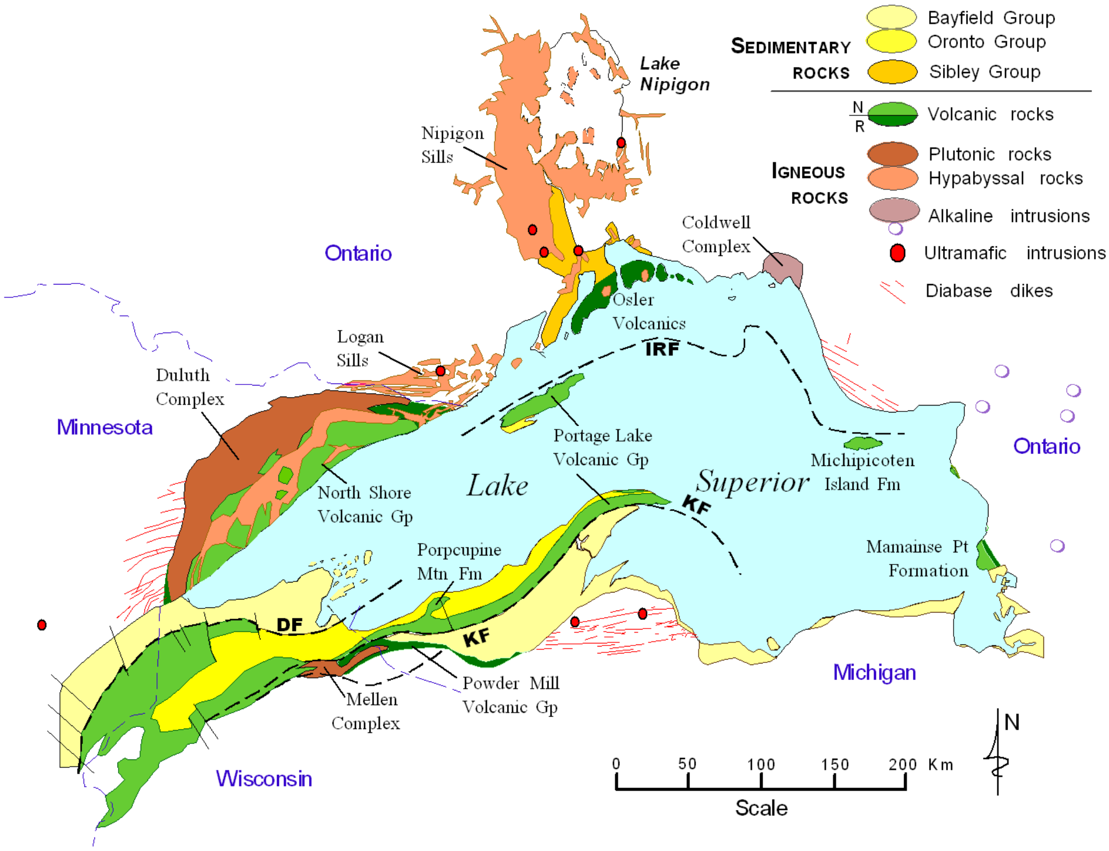

Figure 2.3. General geology of the Midcontinent Rift in the Lake Superior region. Reverse to normal polarity are distinguished within the volcanic suites. IRF – Isle Royale Fault; KF – Keweenaw Fault; DF – Douglas Fault (Modified from Paces and Miller, 1993)

2.3 North Shore Volcanic Group

In northeastern Minnesota, Midcontinent Rift volcanism is represented by a 7- to 10 kilometer-thick edifice of mafic to felsic lavas and minor interflow sediments of the North Shore Volcanic Group (NSVG) that line the shore of Lake Superior from Duluth to the Canadian border (Fig. 2.4). This volcanic edifice has been moderately tilted (10-20°) southeast to south toward the rift axis, thus exposing progressively deeper sections of the rift fill away from the central part of the Minnesota shore. Prior to intrusion of the

Duluth Complex along the basal section of the edifice, the NSVG was extruded onto a peneplained surface composed of a Paleoproterozoic sedimentary terrane of greywacke/slate and iron formation (Rove and Gunflint formations in the north and Thomson/Virginia and Biwabik formations in the southwest) and Neoarchean granite-greenstone terrane to the northwest (Peterson and Severson, 2002).

Most NSVG volcanics show a predominately tholeiitic enrichment trend, from primitive tholeiitic basalts to evolved icelandites and rhyolites (Green, 2002). NSVG flows are subdivided into four sequences along the shore of Lake Superior based on their magnetic polarity, stratigraphic position and structural orientation (Fig. 2.4). Two "limbs" are distinguished by the general tilt of the flows with the lavas of the southwestern limb tilted to the southeast and the northeastern limb tilted to the south (Fig. 2.5). The northeast limb is composed of about 6 kilometers of lavas, of which about 25% is rhyolite (Green and Fitz, 1993). This section is subdivided into a lower and upper sequence based on magnetically reversed and normal polarity, respectively. Within the southwestern limb, the magnetically reversed lower sequence is represented by a 1.5 kilometer-thick sequence of thermally metamorphosed lavas preserved beneath the Duluth Complex near Duluth. Above the Duluth Complex, the upper southwestern sequence is composed of about 8 kilometers of mixed lava flows, with less than 10% being rhyolite (Green, 2002). At the very top of the volcanic pile, a 1 kilometer-thick sequence of mostly primitive olivine tholeiite basalts, termed the Schroeder-Lutsen basalts, sit unconformably on the upper southwest and northeast sequences.

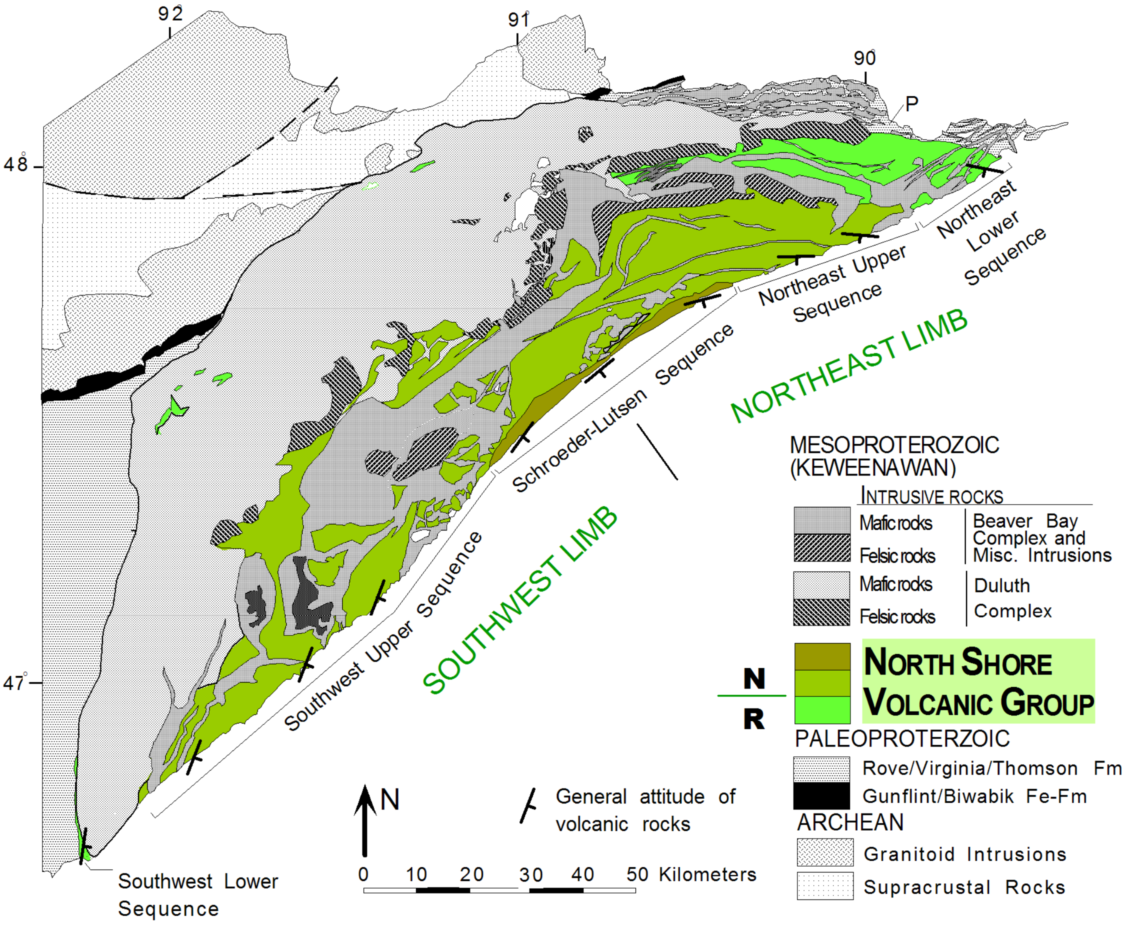

Figure 2.4. General geologic map for rocks associated with the North Shore Volcanic Group (Modified from Green, 2002)

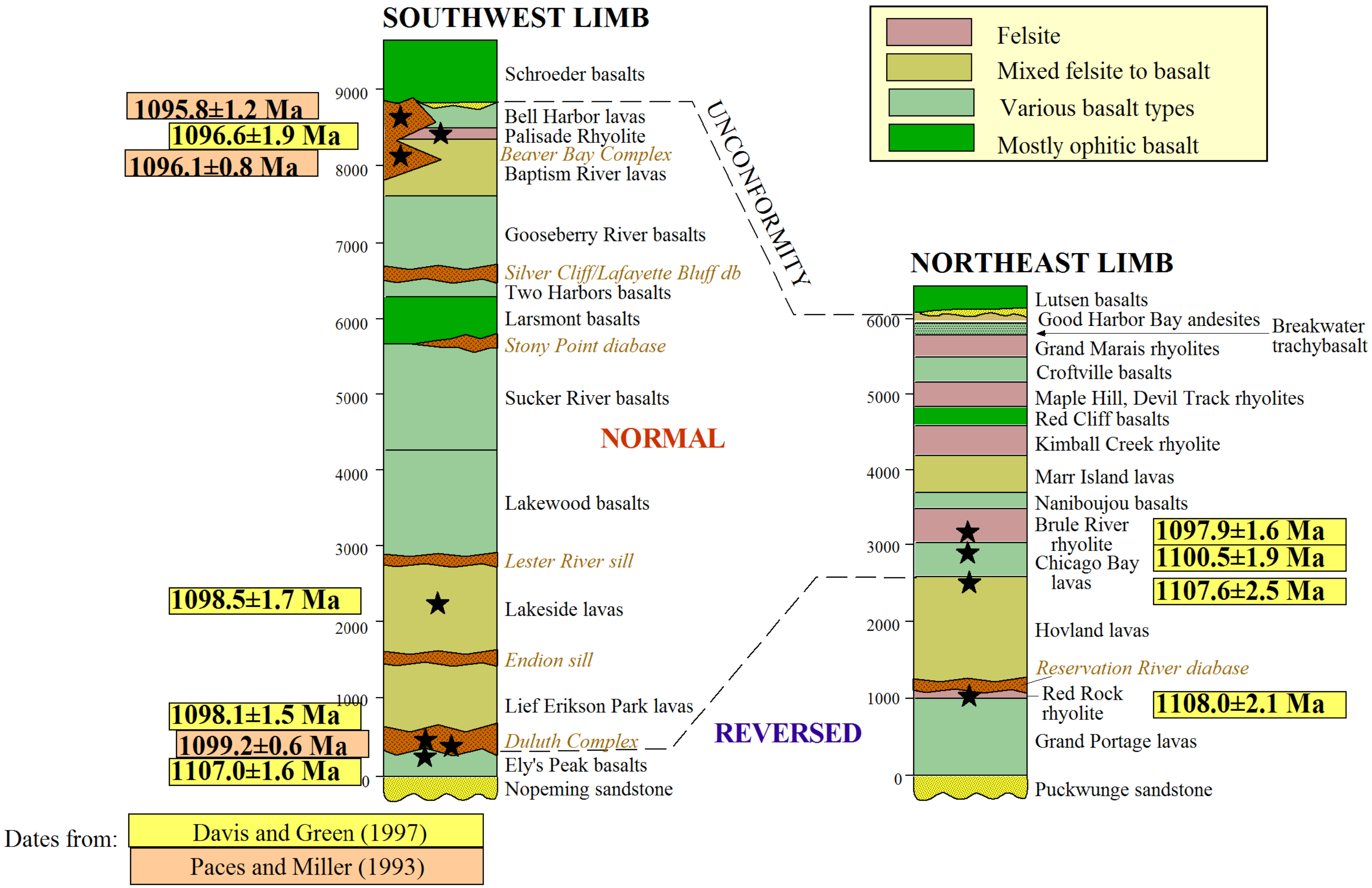

Figure 2.5. Lithostratigraphy of the southwest and northeast limb of the North Shore Volcanic Group (Modified from Davis and Green, 1997).

2.4 Duluth Complex

The multiple intrusions of the Duluth Complex, Beaver Bay Complex, and other hypabyssal intrusions of northeastern Minnesota, comprise the second largest package of mafic intrusive rocks in the world (Miller and Severson, 2002). The Duluth Complex (outlined by dashed line in Fig. 2.6) is composed of a semi-continuous assemblage of troctolitic, gabbroic, anorthositic and granitic intrusions that cover an arcuate area of over 5,000 km^2. The Duluth Complex is typically subdivided into four general rock series based on lithology, age, and internal structure: the felsic series, the early gabbro series, the anorthositic series, and the layered series.

The felsic series (1109 - 1106 Ma; Vervoort et al., 2007) and the early gabbro series (1106.9 ± 0.6 Ma; Paces and Miller, 1993) were emplaced during early stage magmatism of the Midcontinent Rift (Miller and Severson, 2002). Although U-Pb ages for felsic and early gabbro series rocks overlap, field evidence implies that the felsic series is one of the oldest rocks in the Duluth Complex. Where in contact with volcanic rocks of the NSVG, the felsic series forms a sharp contact, but has a more gradational contact with underlying rocks of the early gabbro series. The gradational relationship between the felsic series and early gabbro series is interpreted to represent partial melting of the felsic series by underplated early gabbro magmas, with the felsic series likely providing a density barrier for the rocks of the early gabbro series (Miller and Severson, 2002). In addition, felsic series rocks have a radiogenic Nd isotopic signature suggesting a source magma that incorporated partially melted, early rift related rocks, or old, near chondritic crustal rocks (Vervoort et al., 2007).

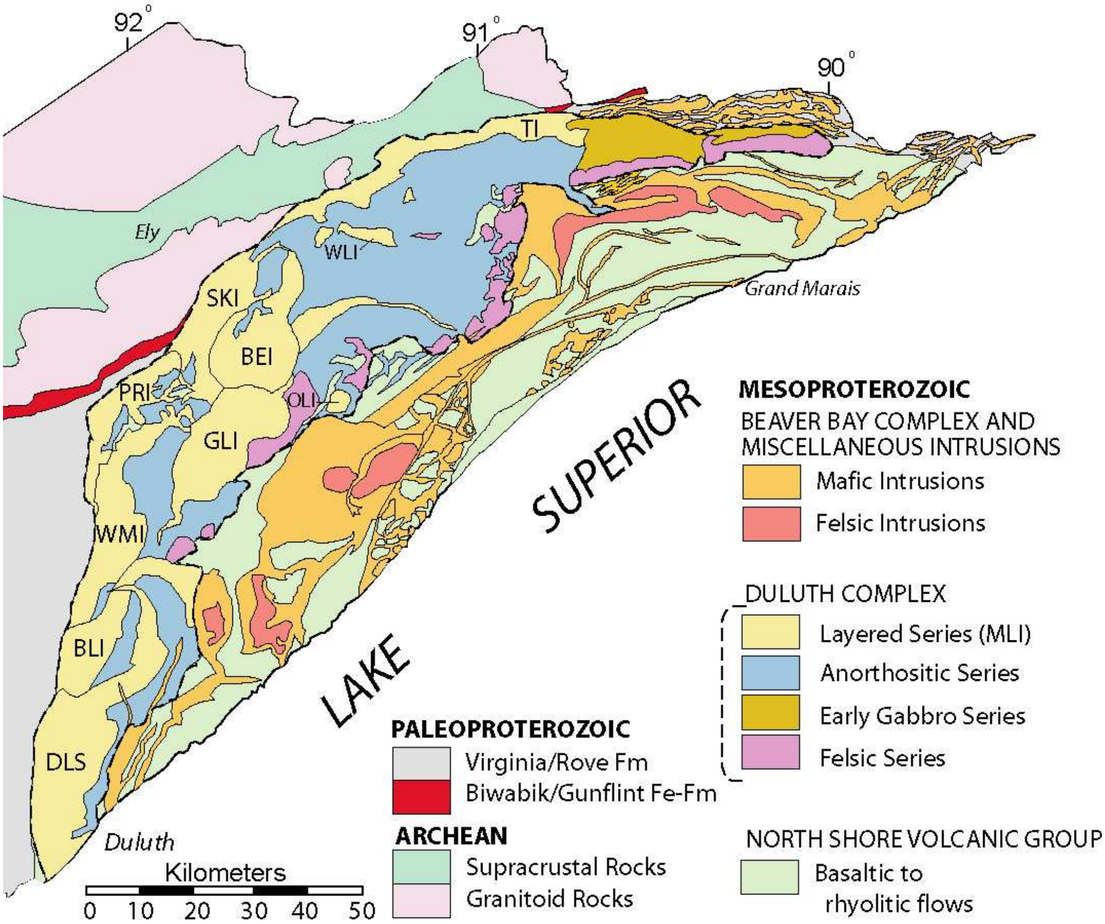

Figure 2.6. General geology of the Duluth Complex, northeastern Minnesota, with layered series intrusions highlighted to show the sequence of progression proposed by Miller and Severson (2002). TI – Tuscarora intrusion; WLI – Wilder Lake intrusion; SKI- South Kawishiwi intrusion; BEI – Bald Eagle intrusion; PRI – Partridge River intrusion; GLI – Greenwood Lake intrusion; WMI – Western Margin intrusion; BLI – Boulder Lake intrusion; DLS – Layered Series at Duluth (Modified from Miller and Severson, 2002)

The anorthositic and layered series of the Duluth Complex were emplaced during main stage magmatism of the Midcontinent Rift (~1099 Ma; Miller and Severson, 2002). The anorthositic series rocks are structurally complex plagioclase-rich cumulates (70 - 99% plagioclase) found throughout the complex (Fig. 2.6). Anorthositic series rocks are found in a direct contact with overlying volcanics of the NSVG, or with granophyre of the felsic series. The lower contact is commonly sharp to gradational with layered series rocks, even completely enveloping intrusions of the layered series in places such as the Wilder Lake intrusion (Miller and Severson, 2002). Miller and Weiblen (1990) proposed that the anorthositic series resulted from the emplacement of plagioclase crystal mushes generated from lower crustal magma chambers by buoyant plagioclase floating to the top of magma staging chambers during the latent magmatic stage. As magmatism resumed during the main stage, plagioclase crystal-rich magmas were flushed out from the lower crustal magma chambers. Subsequent evacuations evidently became progressively less crystal rich.

The layered series rocks of the Duluth Complex are a suite of at least 11 variably differentiated mafic intrusions (Fig. 2.6). The thick (2-4 km), sheet-like intrusions typically show igneous foliation and layering that gently dips southeast towards the axis of the rift basin (Miller and Severson, 2002). Internally, the layered series intrusions tend to display systematic cryptic and phase layering indicative of fractional crystallization variably interrupted by magmatic recharge and magma venting (Miller and Ripley, 1996). The common occurrence of inclusion of anorthositic series-type lithologies in all layered series intrusions has led to the conclusion that the layered series intrusions are universally younger than the anorthositic series. Layered series intrusions are typically sandwiched between a hangingwall of anorthositic series rocks and pre-Keweenawan footwall rocks. A few exceptions exist where intrusions are surrounded by earlier formed layered series intrusions and anorthositic series rocks, such as the Bald Eagle intrusion.

Interpretation of these cross-cutting relationships observed in the field and inferred from aeromagnetic data led Miller and Severson (2002) to suggest emplacement of the layered series by younger intrusions overplating older ones and thus younging upward from the northwest to the southeast. The oldest intrusions of the layered series consist of the troctolitic cumulates of the Partridge River intrusion and the crosscutting troctolitic South Kawishiwi intrusion. The next intrusion in the progression is the poorly-exposed troctolitic Western Margin intrusion, which crosscuts the Partridge River intrusion. Approximately correlative with the Western Margin intrusion are the stratigraphically isolated and poorly-mapped troctolites of the Lake One and Tuscarora intrusions along the northwestern margin of the Duluth Complex. Younger yet is the largely-unexposed, sheet-like Boulder Lake intrusion, and the time-correlative, poorly-exposed Greenwood Lake intrusion, both of which crosscut the Western Margin intrusion. The youngest intrusions of the layered series are the trough-shaped, layered cumulates of the Bald Eagle intrusion (crosscuts the Greenwood Lake intrusion), and the well-exposed, layered gabbroic cumulates of the Layered Series at Duluth (Fig. 2.6)

2.5 Beaver Bay Complex and Miscellaneous Hypabyssal Intrusions

The Beaver Bay Complex covers around 600 km^2 and generally straddles the southwest and northeast limbs of the NSVG (Fig. 2.7). It consists of at least 13 discrete hypabyssal mafic, intermediate, and felsic intrusions emplaced in the medial and upper parts of the NSVG (Miller and Chandler, 1997; Miller and Green, 2002). Most of the intrusions associated with the Beaver Bay Complex are volumetrically smaller than those of the Duluth Complex and tend to show little to no in-situ differentiation. The main exception to this is the very well differentiated Sonju Lake intrusion.

Based on field mapping and aeromagnetic interpretations from map m-119 (Miller et al., 2001), the oldest rocks of the Beaver Bay Complex seem to be the inclusion-rich diorites scattered throughout the Beaver Bay Complex. The next oldest intrusion is the differentiated ferrogabbroic xenolith, the Fourmile Lake ferrogabbro, which sits within the keel-shaped Houghtaling Creek troctolite. The plug-shaped Wilson Lake ferrogabbro (WLFG) and its dike-like extensions, is the next oldest intrusion, followed by the gabbronorite cumulates of the Dam Five, which appear to truncate the WLFG in the aeromagnetic data. The augite troctolite to olivine gabbroic cumulates of the Houghtaling Creek troctolite lie directly above the Dam Five gabbronorite, which is crosscut by the Cloquet Lake Layered Series to the southwest. The next suite of rocks is inferred to be correlative, as mapping suggests the suite was split apart by the late-intruding Beaver River Diabase. These rocks include the non-cumulate mafic to felsic Upper Manitou River gabbro, the Blesner Lake diorite, the Lax Lake gabbro; the saucer-shaped, crudely-differentiated Cloquet Lake Layered Series, and the lens-shaped Finland granophyre. Underplating the Finland granophyre is the strongly differentiated, sheet-like Sonju Lake intrusion, which is crosscut by the Beaver River Diabase. The late Beaver River Diabase intrusive activity is characterized by an extensive network of mafic dikes and sills, into which the massive and zoned ferrogabbroic Silver Bay intrusions were emplaced (Fig. 2.7)

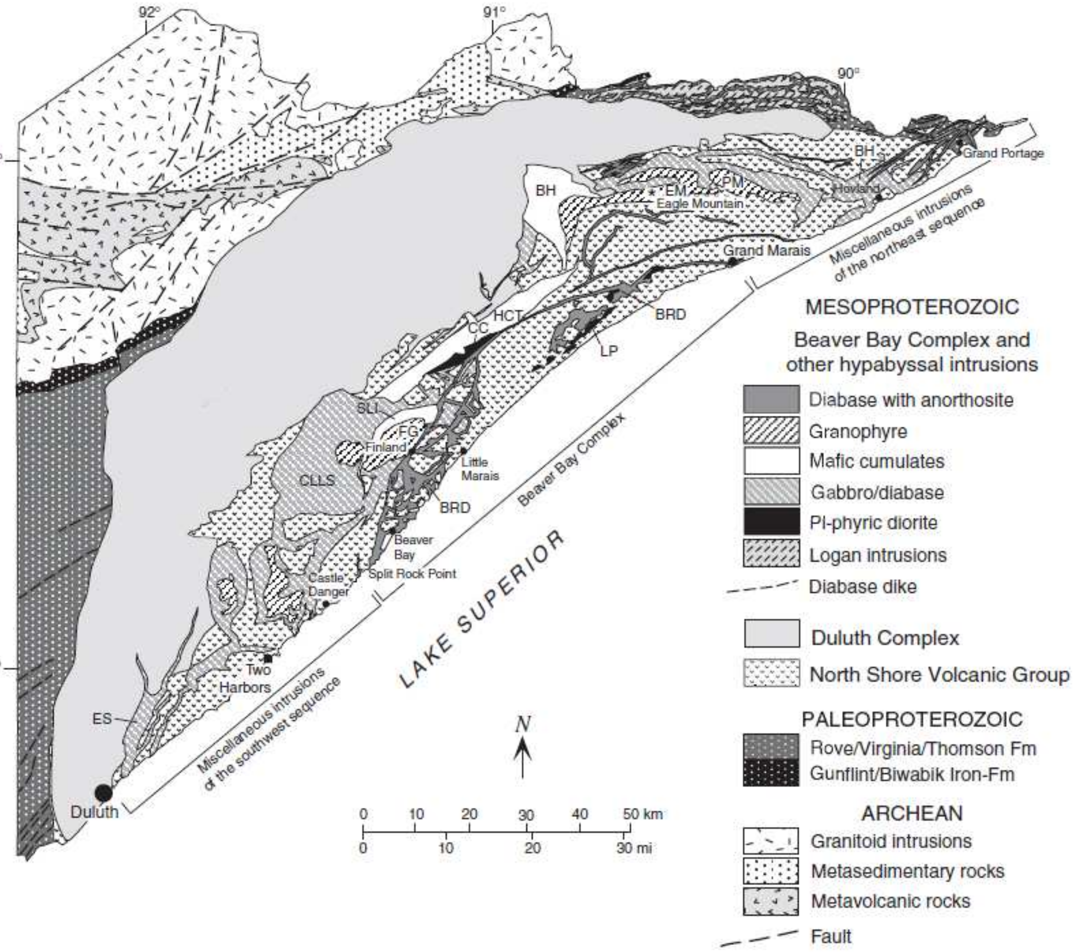

Figure 2.7. General geology of northeastern Minnesota showing the location and lithology of major Beaver Bay Complex and other hypabyssal intrusions. ES – Endion Sill; CLLS – Cloquet Lake Layered Series; BRD – Beaver River Diabase; SLI – Sonju Lake intrusion; FG – Finland Granophyre; CC – Cabin Creek porphyritic diorite; HCT – Houghtaling Creek troctolite; LP – Leveaux porphyritic diorite; BH – Brule Lake-Hovland gabbro; PM-Pine Mountain granophyre; EM – Eagle Mountain granophyre (Taken from Miller and Green, 2002)

The miscellaneous hypabyssal intrusions are isolated and thus have an uncertain correlation with other intrusive units. Based on field mapping and aeromagnetic interpretations, it appears as though the composite mafic Endion Sill appears to crosscut the Duluth Complex and could be one of the oldest hypabyssal intrusions. Other hypabyssal intrusions include the dominantly felsic Eagle Mountain and Pine Mountain granophyre, and the underlying sheet-like intrusions of the Brule Lake-Hovland gabbro (Fig. 2.7)

3. Previous Geochronologic Studies

Before the developments of single zircon dating techniques (Krogh, 1973; Krogh, 1982), the earliest geochronology studies of Midcontinent Rift were hampered by inaccuracy and imprecision associated with open system behavior. Silver and Green (1972) used a bulk U-Pb zircon analysis to show that the majority of Midcontinent Rift-related igneous activity occurred over a relatively short period of time around 1110 ± 10 Ma (Van Schmus and Hinze, 1985). Initial Rb-Sr and K-Ar studies ranged from 1200 Ma to 900 Ma (e.g. Chaudhuri and Brookins, 1969; Chaudhuri, 1972; Baragar, 1978; and others); with much of the data concordant within error of the Silver and Green (1972) dates. Several of the dates were significantly younger, e.g. 984 ± 27 Ma (Chaudhuri, 1972), and were thus treated as minimum ages due to the susceptibility of the isotopic systems to open system behavior (Van Schmus, 1982). As a result, early stratigraphic correlation studies relied on the well-preserved paleomagnetic record found in the igneous rocks of the rift.

At least one major polarity reversal is preserved in the stratigraphic record - a reversed to normal. A possible lower-normal to reverse shift may also be preserved in the Bessemer Sandstone below the Powder Mill Group in upper Michigan (Van Schmus, 1982), but this reversal is not recognized in other basal rift sandstones around the rift

(Nopeming and Puckwunge in Minnesota). An extra reversed and normal polarity interval is recognized in the Mamainse Point volcanics in eastern Lake Superior (Annels, 1973), but again is not recognized in any of the other volcanic sequences in western Lake Superior. As a consequence, early stratigraphic divisions were done based on the major reverse to normal polarity shift. Groups were initially divided into lower (reverse) and upper (normal) units as a result (Green, 1982). The 1110 ± 10 Ma date of Silver and Green (1972) included rocks of both reversed and normal polarity, so was a best estimate of the age of reversal.

With the advent of isotope dilution methods for high resolution U-Pb dating of single zircons (Krogh, 1973, 1982), early geochronologic studies in the Midcontinent Rift sought to refine the age of the major reverse to normal polarity transition, as well as better constrain the time interval of magmatic activity. The major geochronologic studies conducted over the past 25 years will be summarized below.

3.1 Davis and Sutcliffe, 1985

One of the earliest studies using the new high precision methods was conducted by Davis and Sutcliffe in 1985. They selected six lithologies related to igneous activity around the Lake Nipigon area just north of Lake Superior for zircon dating. Two of the lithologies dated were of pre-rift related igneous activity. An Archean tonalite gneiss underlying the Nipigon plate yielded a U-Pb age of 2716 ± 1.6 Ma, suggesting formation during, rather than prior to, the Kenoran event. Zircon from an anorogenic granitic pluton of the English Bay porphyry was dated at 1536.7 +10/-2.3 Ma, which they suggested might represent the age of deposition of the overlying Sibley Group.

Relative to the rift, four lithologies were dated: a Logan diabase sill, a porphyritic rhyolite near the base of the Osler Group, a rhyolite near the top of the Osler Group on Agate Point, and a felsic porphyry clast-bearing conglomerate at the base of the Osler Group (Table 3.1).

Table 3.1. $^{207}Pb/^{206}Pb$ ages of Midcontinent Rift samples reported by Davis and Sutcliffe (1985)

Rock Unit	Rock Type	Comments	Polarity	Age (Ma)
Agate Point (Osler Group)	rhyolite	upper part of the reversed sequence	R	1097.6 ± 3.7
Osler Group	rhyolite porphyry	base of the sequence	R	1107.5 +4/-2
Logan Sill	diabase	near the top of a sill	R	1108.8 +4/-2

Several interesting results arose from this study. The agreement in dates for two spatially extensive samples from the Logan Sills of 1108.8 +4/-2 indicated relatively rapid emplacement. Dates from the Logan Sills were also consistent with the dates obtained by Silver and Green (1972) for the NSVG (1110 ± 10 Ma), further indicating rapid magmatic activity around 1110 Ma. Even more surprising was the discovery that rhyolitic magmatism was apparently contemporaneous with early mafic magmatism, despite field evidence suggesting that the rhyolitic flows of the Osler Group are younger than the Logan intrusions. The date of the Agate Point rhyolite at the top of the reversed polarity section of the Osler Group suggested a minimum age of magnetic reversal at 1097.6 ± 3.7 Ma; however, the data was discordant and the authors acknowledged that the flow could be a few million years older had the zircon crystals experienced slight Pb loss (this date would later be refined by Davis and Green, 1997; see below). The conglomerate at the base of the Osler volcanics contained numerous granite porphyry clasts, which when dated, suggested the presence of pre-Keweenawan felsic intrusions in the Black Bay Peninsula between 1730 and 1600 Ma.

Another contribution from this study was the use of the mineral baddeleyite as a dating target. The authors dated baddeleyite grains in addition to zircon for the Logan sills. The agreement in the data between the two minerals for the same intrusions demonstrated the viability of baddeleyite as a geochronologic tool and laid the foundation for further age studies in the rift.

3.2 Palmer and Davis, 1987

The next pertinent U-Pb zircon study to emerge in the rift was conducted by Palmer and Davis in 1987. For their study, they targeted Michipicoten Island, located in the eastern end of Lake Superior. Their primary research goal was to precisely calibrate the polar wander track recorded in the paleomagnetic record. In addition, the normally polarized volcanic rocks exposed on Michipicoten Island provided an opportunity to bracket the upper age of the normal polarity interval. They dated zircon from a quartz feldspar porphyry that intrudes the lower Mamainse Point Formation, which is overlain unconformably by the Michipicoten Island Formation. A precise $^{207}Pb/^{206}Pb$ date of 1086.5 + 1.3/-3.0 Ma, along with the date from the Agate Point rhyolite (Davis and Sutcliffe, 1985) bracketed the age of normal interval between 1097.6 ± 3.7 Ma and 1086.5 + 1.3/-3.0 Ma. This data, along with that of the Logan Sills from Davis and

Sutcliffe (1985) put a time span of approximately 22 million years on Midcontinent Rift-related magmatism. While the range of ages for magmatism was starting to become clearer, the details of magmatic activity within the 22 million year interval had yet to be revealed and the age of the magnetic reversal had yet to be definitely established.

3.3 Davis and Paces, 1990

Aiming to further expand the regional and temporal extent of Midcontinent Rift geochronology, Davis and Paces (1990) studied three flood basalt lavas: two from the extensive Portage Lake Volcanics (PLV) on the Keweenaw Peninsula in upper Michigan, and a flow from the Lakeshore Traps located within the overlying Copper Harbor Conglomerate (Table 3.2).

Table 3.2. $^{207}Pb/^{206}Pb$ ages of Midcontinent Rift samples reported by Davis and Paces (1990)

Rock Unit	Rock Type	Comments	polarity	Age (Ma)
Lake Shore Traps	andesite	within the Copper Harbor Conglomerate, 1000 m above PLV	N	1087.2 ± 1.6
Greenstone Flow (PLV)	basalt	upper part of PLV	N	1094 ± 1.5
Copper City Flow (PLV)	basalt	near base of PLV	N	1096.2 ± 1.8

The normally polarized Copper City Flow, located near the base of the exposed Portage Lake Volcanics, provided a new minimum age of magnetic reversal in the rift. Along with the then reported age of the reversely polarized Agate Point rhyolite (Davis and Sutcliffe, 1985), Davis and Paces (1990) interpreted the age of reversal to be constrained between 1097.6 ± 3.7 Ma and 1096.2 ± 1.8 Ma.

In addition, the authors calculated rates of magma extrusion during emplacement of the Portage Lake Volcanics. They obtained a minimum volume estimation of 40,000 km^3 based on outcrop exposure and the assumption of constant thickness across the basin. Using the age data and volume estimation, Davis and Paces (1990) determined that extrusion rates were likely between 0.02-0.06 km^3/yr, consistent with other Phanerozoic continental flood basalt provinces.

3.4 Heaman and Machado, 1992

The majority of MCR-related magmatism is tholeiitic in composition, but local alkaline intrusions associated with the MCR can be found in Ontario's Coldwell Complex located along the northern shore of Lake Superior (Fig. 2.3). The Coldwell Complex is the largest of a suite of Keweenawan alkaline intrusions that occur in northwest Ontario and extend approximately 150 km north of the main rift structure. Heaman and Machado (1992) performed U-Pb, Pb-Pb, Sm-Nd, and Rb-Sr isotopic analyses to evaluate how the Coldwell Complex related geochemically and temporally to other rocks associated with the MCR.

They selected five samples for study, ranging in composition from the gabbro at the base of the intrusions, to the more evolved granites near the top. U-Pb zircon/baddeleyite ages from the samples give a $^{207}Pb/^{206}Pb$ emplacement age for the Coldwell Complex at 1108 +/- 1 Ma. This data is within error of Davis and Sutcliffe's (1985) age for the Logan sills (1108.8 +4/-2 Ma) and indicated the contemporaneous production of tholeiitic and alkaline magma. The authors also recognized two distinct mantle sources: a plume-component (εNd = +.5), which sourced the gabbroic and alkaline components of complex and an asthenospheric component (εNd = +2), which sourced the carbonatites.

3.5 Paces and Miller, 1993

The first study on the intrusive rocks of the MCR in northeastern Minnesota, including the Duluth Complex, was reported by Paces and Miller in 1993. The primary focus of their study was to evaluate the range of ages of the main mafic intrusions of the Duluth Complex and Beaver Bay Complex. They dated eight gabbroic and anorthositic intrusions that spanned both the spatial and temporal range of intrusive activity for the Duluth Complex and the Beaver Bay Complex. Results of their dating study are summarized in Table 3.3.

Table 3.3. $^{207}Pb/^{206}Pb$ ages of Midcontinent Rift samples reported by Paces and Miller (1993)

Rock Unit	Rock Type	Comments	polarity	Age (Ma)
Silver Bay ferrogabbro (BBC)	granophyric ferrogabbro	near the top of the BBC	N	1095.8 ± 1.2
Sonju Lake intrusion (BBC)	apatite ferrodiorite	middle BBC	N	1096.1 ± 0.8
Partridge River intrusion (DC)[1]	troctolite	middle DC	N	1098.6 ± 0.5
Anorthositic Series (DC)	olivine gabbroic anorthosite	northern DC	N	1099.0 ± 0.6
Anorthositic Series (DC)[2]	gabbroic anorthosite	Southern DC (Duluth area)	N	1099.1 ± 0.5
Duluth Layered series (DC)	olivine ferrogabbro	Southern DC (Duluth area)	N	1099.3 ± 0.3
Poplar Lake intrusion (DC)	olivine gabbro	base of northern DC	R	1106.9 ± 0.6

[1] The Partridge River intrusion date was later revealed to be a gabbroic phase of the anorthositic series by detailed mapping in the area (Miller and Severson, 2002).
[2] AS3 was re-dated by Schmitz et al. (2003) to assess its potential as a U-Pb geochronological standard. Their result of 1099.1 ± 0.2 Ma is in perfect agreement with the Paces and Miller (1993) date.

This study was particularly noteworthy for its highly precise results. For the first time, 1100 Ma events were precisely constrained within 0.3 million years. The data was also noteworthy for its identification of a significant hiatus (~ 7 m.y.) in intrusive activity, which would come to be recognized within MCR volcanics as well. An 1106.9 +/- 0.6 Ma age for an olivine gabbro sample from the reverse polarity Poplar Lake intrusion of the Early Gabbro Series of the Duluth Complex fell in line with the 1109-1107 ages of other reverse polarity intrusions (Logan Sills and Coldwell Complex) and volcanics (the lower Osler Group). All normal polarity intrusions of the Duluth Complex and Beaver Bay Complex had ages younger than 1099 Ma. This was the first indication of the episodic nature of MCR magmatism.

One of the most surprising results of Paces and Miller's (1993) study was that four samples from the anorthositic and layered series of the Duluth Complex[(1)] were statistically indistinguishable in age at about 1099 Ma (Table 3.3). Field evidence of consistent cross-cutting relationships have long implied that anorthositic series lithologies are older than layered series rock types and gave rise to models for the petrogenesis of the two series that inferred a considerable difference in their age and mode of formation (Weiblen and Morey, 1980; Miller and Weiblen, 1990). That the two series were essentially identical in age required a rethinking of the petrogenetic relationship between the two units (Miller and Severson, 2002).

Another interesting result was the apparent violation of the paleomagnetic record, with rocks of the Duluth Complex exhibiting normal polarity at ~1099 Ma. This appeared to be in direct contradiction of the previously-dated, reversely-polarized Agate

Point rhyolite at 1097.6 ± 3.7 Ma (Davis and Sutcliffe, 1985). Paces and Miller (1993) suggested that if the reversal age were correct, this may imply that it took over 1 million years for Duluth Complex to cool past the Currie point. A later re-dating of the Agate Point rhyolite (Davis and Green, 1997, see below) would resolve this apparent contradiction.

The samples dated from the Beaver Bay Complex were significantly younger than the intrusions dated from the Duluth Complex (Table 3.3). The younger ages for these intrusions, which reside at higher stratigraphic positions than the layered series samples, indicate that intrusions climbed higher in the volcanic pile over time. Somewhat problematic; however, was the failure to obtain ages from the oldest BBC intrusions, as indicated by mapping. This leaves the question open as to whether or not there exists a temporal overlap between BBC and DC magmatism. Moreover, only one DC age was successfully obtained from this study, so the youngest DC age remains unknown.

3.6 Zartman et al. (1997)

Looking to further constrain the interval of magmatic activity, Zartman et al. (1997) dated plutonic bodies of the Mellen Intrusive Complex (MIC) and rhyolitic rocks of the Kallander Creek Volcanics (KLV), Chengwatana Volcanics, and Porcupine Volcanics on the south shore of Lake Superior in north-central Wisconsin and the Upper Peninsula of Michigan (Table 3.4).

Table 3.4. $^{207}Pb/^{206}Pb$ ages of Midcontinent Rift samples reported by Zartman et al. (1997).

Rock Unit	Rock Type	Comments	polarity	Age (Ma)
Porcupine Volcanics	pyroclastic rhyolite		N	1093.6 ± 1.8
Chengwatana Volcanics	quartz phyric rhyolite	near base of Chengwatana volcanics, , NW WI	N	1094.6 ± 2.1
Kallander Creek Volcanics	rhyolite	Upper Kallander Creek Volcanics	N	1098.8 ±1.9
Mellen granite (MIC)	granite	late intrusion in the Mellen Complex	N	1100.9 ± 1.4
Mineral Lake intrusion (MIC)	granophyre		N	1102.0 ± 2.8

Age results from the Kallander Creek Volcanics, which occur near the Michigan-Wisconsin border area, provided additional evidence of a magmatic hiatus of several million years that straddles the magnetic reversal as interpreted from the Duluth Complex data (Paces and Miller, 1993). The Kallander Creek Volcanics, which are a mix of mafic to felsic lavas, are divided into a lower and upper member based on their reversed and normal magnetic polarity, respectively. An earlier preliminary study by Davis et al. (1995) for a rhyolite flow from the lower KCV member yielded a preliminary age of 1107.5 ± 1.6 Ma, in line with other reversed polarity rocks in the western Lake Superior region. However, Zartman et al. (1997) acquired an age of, 1098.8 ± 1.9 Ma for a rhyolite flow from the upper KCV.

The stratigraphic separation between the two Kallander Creek flows, which differ in age by at least 5 Ma, is at most 1.5 km. Zartman et al. (1997) interpret the lack of sedimentary units at the hiatus as evidence that subsidence after eruption of the lower KCV was minimal. Moreover, they suggest that one or more significant time breaks in basaltic volcanism was due to non-deposition in a topographically high area, rather than the 5 Ma hiatus in volcanism proposed by Miller (Miller et al.,1995; Miller and Vervoort, 1996).

The normally polarized rhyolitic flow of the upper KCV also placed a new lower boundary on the magnetic reversal at no less than 1098.8± 1.9 Ma within the MCR volcanics, which is in line with the 1099 Ma ages of normal polarity Duluth Complex rocks. The age results from felsic intrusive rocks from the Mellen Complex pushed the youngest age for the reversal even further back to approximately 1102 Ma (Table 3.4).

The Chengwatana Volcanics, located in the Ashland syncline, were long thought to be the equivalent to the Portage Lake Volcanics due to their stratigraphic position right below the Oronto Group. The U-Pb zircon age of 1094.6 ± 2.1 is statistically indistinguishable from dates for the Portage Lake Volcanics determined by Davis and Paces (1990) and further corroborated the correlation of these two units.

Another interesting aspect of this study was the age of the Porcupine Volcanics, which is a composite volcanic sequence occurring stratigraphically above the Portage Lake Volcanics and below the Copper Harbor Conglomerate of the Oronto group. The 1093.6 ± 1.8 Ma age for the Porcupine Volcanics give an upper limit for the significant volcanic activity in the area.

3.7 Davis and Green (1997)

Reporting on a collection of ages from the MCR that had been acquired over several years, Davis and Green's (1997) publication established the current geochronologic framework of MCR igneous rocks in the western Lake Superior region, especially the presence of a magmatic hiatus between 1107 and 1102 Ma. They reported on the U-Pb ages of eight samples from volcanic and intrusive bodies in northeastern Minnesota. They also reported a revised date for the lower Kallander Creek Volcanics previously reported in an abstract (Davis et al., 1995) and re-dated zircons from the Agate Point rhyolite of the Osler Group. They were primarily looking to accurately constrain the age of the magnetic reversal, as well as gain further insight into the geodynamic evolution of MCR magmatism (Table 3.5).

Table 3.5. $^{207}Pb/^{206}Pb$ ages of Midcontinent Rift samples reported by Davis and Green (1997).

Rock Unit	Rock Type	Comments	Polarity	Age (Ma)
Kallander Creek (Powder Mill Group)	rhyolite	near the base of the exposed KCV	R	1107.3 ± 1.6
Palisade rhyolite (NSVG)	rhyolite	stratigraphically highest sample collected	N	1096.6 ± 1.7
Devil's Kettle porphyry (NSVG)	porphyritic rhyolite	800 m above Big Bay rhyolite	N	1097.7 ± 1.7
Kenwood Av. Granite (Duluth Complex)	granite	few 100 m's above roof zone of DC	N	1098.2 ± 1.4
Lakeside Lavas (NSVG)	icelandite	1600 m above base of sw limb of NSVG in Duluth	N	1098.4 ± 1.9
Big Bay (NSVG)	rhyolite	near the base of normal NSVG section	N	1100.2 ± 2.2
Swamper Lake (Duluth Complex)	monzogabbro	adjacent to the Poplar Lake intrusion	R	1107.0 ± 1.1
Hovland lavas/Tom Lake (NSVG)	rhyolite	near the top of reverse NSVG section	R	1107.7 ± 1.9
Red Rock rhyolite (NSVG)	rhyolite	stratigraphically lowest in reverse NSVG sequence	R	1107.9 ± 1.8
Agate Point rhyolite (Osler Group)	rhyolite	re-date of Davis and Sutcliffe (1985)	R	1105.3 ± 2.1

The re-date of the reversely magnetized Agate Point rhyolite confirmed the suspicions of Davis and Sutcliffe (1985), as it ended up several million years older than previously thought (1105.3 ± 2.1 Ma). This date, along with the average age of the normally magnetized Mellen Intrusive Complex (Zartman et al. 1997) has now constrained the age of the field reversal to between 1105 ± 2 Ma and 1102 ± 2 Ma, a major accomplishment that was over 20 years in the making. In addition, based on latitude variations in the paleomagnetic data, they determined that the drift rate for the North American plate during the early part of the rift was approximately 22 cm/yr, but slowed to approximately 8 cm/yr as rifting started to wane around 1095 Ma.

A major result from this paper was the confirmation of an approximate seven million year hiatus in magmatic activity, the latent magmatic stage, which was suggested by Miller and Vervoort (1996) as an explanation for the time gap observed in the plutonic bodies of the Duluth Complex (Paces and Miller, 1993). A new age from a rhyolite sampled near the exposed base of the Kallander Creek volcanics of the Powder Mill Group was distinctly older than the upper Kallander Creek age of Zartman et al. (1997) (Tables 3.4, 3.5). In addition, ages from the Red Rock rhyolite and Hovland lavas from the northeast limb of the NSVG were dated at 1107.7 ± 1.9 Ma and 1107.9 ± 1.8 Ma, respectively; with similar results on the southwest limb (Table 3.5). By finding similar time gaps between 1107 and 1100 Ma on both the south and north shore of Lake Superior, Davis and Green (1997) were able to prove unequivocally the existence of the latent magmatic stage. This result proved that the observed magmatic hiatus was not a function of non-deposition due to topographic highs as proposed by Zartman et al. (1997). Moreover, the dates from the Kenwood Av. granite at 1098.2 ± 1.4 Ma and the Palisade rhyolite at 1096.6 ± 1.7 Ma constrained approximately seven kilometers of normally polarized lavas over an interval of approximately two million years. This was the first indication of the extent and duration of the voluminous volcanism associated with the MCR.

3.8 Vervoort et al. 2007

Vervoort et al. (2007) reported on the ages and geochemistry of a suite of granophyres from the Duluth Complex and Beaver Bay Complex in order to investigate and constrain the genesis of the rhyolitic magmas in an otherwise mafic-dominated system. Secondary to this objective was to address several other questions: (1) What were the mechanisms of felsic magma formation? (2) How do the felsic magmas and mafic magmas relate temporally? (3) What do these relationships imply about the overall magmatic and chemical evolution of the MCR? Using U-Pb zircon geochronology coupled with Nd isotope and trace-element analysis, Vervoort et al. (2007) were able to provide some compelling answers to their main research objectives.

Although the U-Pb zircon ($^{207}Pb/^{206}Pb$) ages of the granophyres proved to have significantly large errors (2.8-5.5 Ma), the results from seven granophyre bodies clearly showed two distinct age groupings: an early group from 1109 Ma to 1106 Ma, and a late group from 1099 Ma to 1095 Ma (Fig. 3.1).

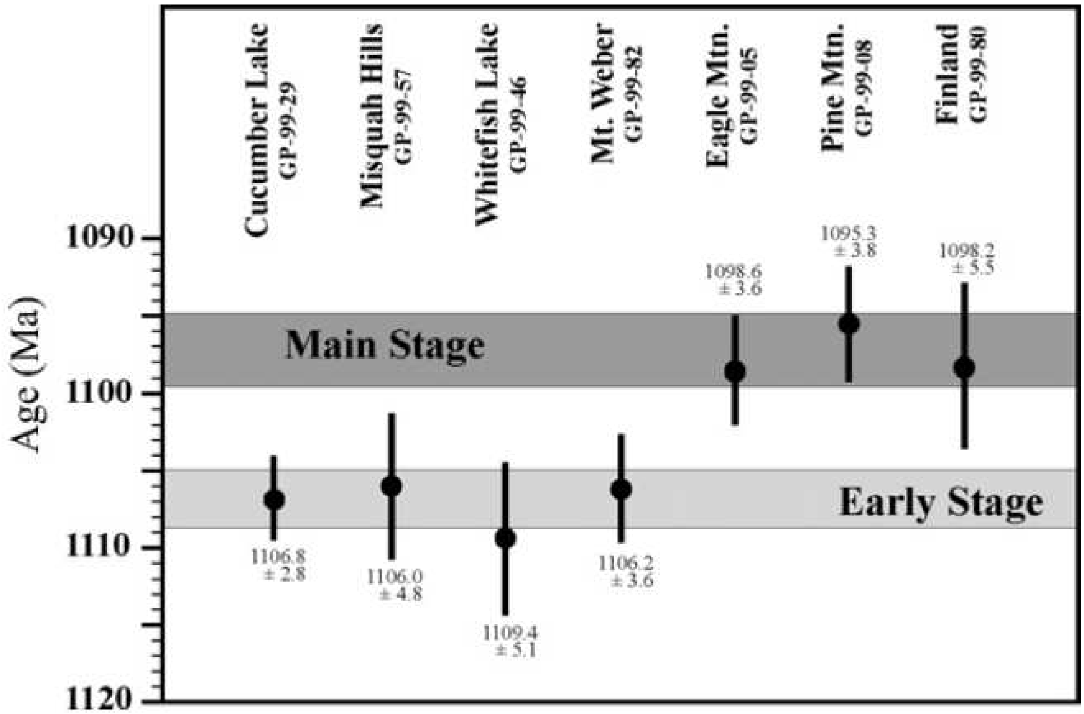

Figure 3.1. Summary plot of U-Pb zircon ages from granophyre complexes. The bands labeled “early” and “main” magmatic stages are based on the weighted mean of the reported granophyre ages (from Vervoort et al., 2007).

The early and main stage granophyres observed in the data are consistent with the evolutionary stages of the MCR proposed by Miller and Vervoort (1996). Main stage granophyres are also consistent with the main stage plutons dated by Paces and Miller (1993), Green et al. (2001), and Schmitz et al. (2003), further confirming the episodic nature of rift magmatism and providing additional evidence for the existence of a latent magmatic stage (Fig. 3.2). Moreover, Nd and trace-element characteristics supported the notion of significant crustal underplating causing partial melting of the lower crust.

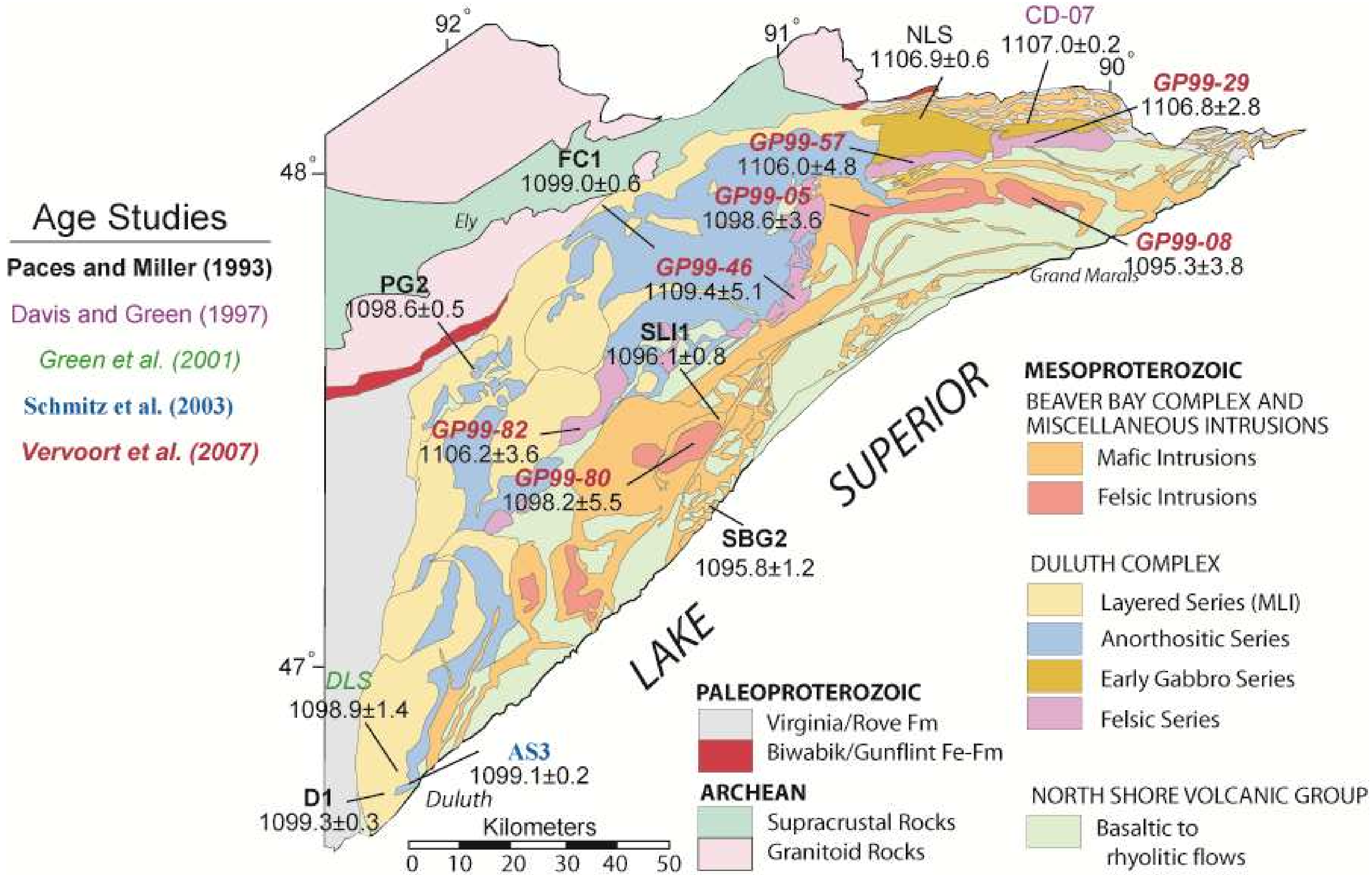

Figure 3.2. Summary of studies pertaining to the Duluth Complex and related intrusions, northeastern Minnesota (modified from Miller and Severson,

Major and trace-element compositions for both early and main stage granophyres were nearly indistinguishable; however, the Nd isotopic compositions were distinctly different. Early stage granophyres exhibited non-radiogenic εNd values ranging from -3.7 to -0, whereas main stage granophyres had much more radiogenic isotopic compositions with εNd values ranging from -7.6 to -3.1. While the values for the younger granophyres are consistent with their source being partial melting of Paleoproterozoic and Archean crust, the moderately negative εNd values for the early granophyres suggest either fractionation of MCR mafic magmas or remelting of a Keweenawan to Paleoproterozoic source. The large volume of the granophyre bodies argues against their formation by fractionation. This study was significant to supporting the hypothesis that significant magmatic underplating caused varying degrees of crustal anatexis throughout the evolution of the MCR.

3.9 Heaman et al. (2007)

Heaman et al. (2007) dated 29 samples of mafic to ultramafic intrusions, dike swarms, and alkaline complexes from the Ontario portion of the MCR. Prior to this study, a vast majority of MCR geochronologic studies focused on the main volcanic packages found throughout the rift (e.g. Davis and Sutcliffe, 1985; Palmer and Davis, 1987; Davis and Paces, 1990; Zartman et al., 1997; Davis and Green, 1997); with little study given to the many subvolcanic intrusive complexes (save Paces and Miller (1993). Heaman et al. (2007) therefore sought to expand the understanding of the timing of subvolcanic intrusive activity, particularly in the Lake Nipigon region of Ontario.

Table 3.6. $^{207}Pb/^{206}Pb$ ages of Midcontinent Rift samples reported by Heaman et al. (2007).

Rock Unit	Rock Type	Comments	Age (Ma)
Pigeon River	diabase	sample collected from dyke	1141.0 ± 20.0
Kitto	olivine gabbro	drill core from Kitto intrus., (98.3-98.6m)	1117.5 ± 3.7
Seagull	peridotite	drill core sample, ultramafic intrusion	1112.8 ± 1.4
Jackfish sill	gabbro	Jackfish Island near English Bay	1112.4 ± 2.8
Disraeli	olivine gabbro	drill core from Disraeli intrusion	1109.0 ± 1.5
Kitto	diabase	drill core from Kitto intrus., (24.7-24.9m)	1110.8 ± 4.3
Hele	olivine gabbro	drill core sample, ultramafic intrusion	1106.6 ± 1.5
Inspiration	diabase	from McLaurin Lake area	1159.0 ± 33.0
Logan, Mt. McKay	diabase	upper Logan Sill	1114.7 ± 1.1
Muskrat Lake	diabase	drill core near Muskrat Lake	1112.7 ± 2.4
Grand Bay	diabase	drill core from Grand Bay drill hole	1114.4 ± 8.3
Havoc	diabase	drill core near Havoc Lake	1110.1 ± 2.5
Nipigon, North Bay	diabase	outcrop on west side of North Bay	1110.1 ± 2.1
Nipigon, Gull River	troctolite	530 m depth of Gull River drill hole	1111.0 ± 15.0
Nipigon, South Bay	diabase	from South Bay of Lake Nipigon	1106.8 ± 1.9
McIntyre	diabase	western end of Lake Nipigon	1100.8 ± 4.4
Crystal Lake	gabbro	sample collected near Crystal Lake	1099.6 ± 1.2
Moss Lake	gabbro	sample collected near Moss Lake	1094.7 ± 3.1
Arrow River dyke	diabase	sample collected from diabase dyke	1078.0 ± 3.0
Blake Twp.	gabbro	two pieces of drill core	1091.1 ± 4.5
Nemegosenda	carbonatite	sample taken east of Lake Superior	1105.4 ± 2.6
Lackner Lake	carbonatite	sample taken east of Lake Superior	1100.6 ± 1.5

The Heaman et al. (2007) study calls into question some of the current thoughts on the plume-generated, episodic nature of rift magmatism and suggests that perhaps there were earlier episodes of rift-related magmatism. Previous studies indicate that magmatic activity was concentrated in two stages that abruptly began around 1109 Ma (i.e. early and main stage magmatism). However, Heaman et al. (2007) reported ages for several diabase and gabbro sills in the Lake Nipigon area that may push the onset of early stage magmatism back at least 5 Ma to around 1115 Ma. In addition, the authors recognized an even earlier stage of magmatism that they suggest may also be related to the MCR between 1150 and 1130 Ma. Ages by Queen et al. (1996) from lamprophyre dikes located along the shore of Lake Superior, Krogh et al. (1987) on the Great Abitibi dykes (1140.6 ± 2.0 Ma), and Heaman et al. (2007) on the Pigeon River Dike Swarm at (1141 ± 20 Ma) and Inspiration diabase (1159.0 ± 33.0) all suggest the existence of this period of early magmatism. Heaman et al. (2007) speculates that these ancient mafic-ultramafic dykes are possibly feeder systems to older undiscovered basaltic flows.

Issues with these older ages, specifically the Pigeon River Dike Swarm, arise when the ages are compared to the field relationships. The Pigeon River Dike Swarm appears to crosscut the younger Logan Sills in some locations; whereas, the field relationships are not so clear in others (Hollings et al., 2010). In addition, geochemical evidence collected by Hollings et al. (in press) suggest that the Arrow River dike (1078 Ma – Heaman et al., 2007) and Rita Bolduc dike (1141 Ma – Heaman et al., 2007), both of the Pigeon River Dike Swarm, are geochemically consistent, which would seem improbable if they were indeed emplaced some 60 million years apart. The date of 1141 Ma reported by Heaman et al. (2007) defines an upper intercept age, and although the baddeleyite grains analyzed are collinear, they are significantly discordant (4-12%), calling the overall accuracy of this age into question (Hollings et al., in press).

If the assertion from Heaman et al. (2007) is correct and the ~1140 Ma dike swarms are indeed related to the Midcontinent Rift, then this requires a re-examination of rift initiation and development by a starting mantle plume (Hutchinson et al., 1990; Miller and Vervoort, 1996; Nicholson et al., 1997). It would require the presence of a long-lived mantle plume (for which evidence of significant crustal doming is lacking), or two consecutive mantle plumes (an early one at 1140 Ma and a later one at 1115 Ma), or the interaction between the arrival of an early mantle plume around 1140 and subsequent upwelling of asthenosphere (Heaman et al., 2007). More work is needed to evaluate this possible relationship. It also suggests that a plume may not be involved at all, but rather that MCR magmatism may be a passive response to periodic dilation of the lithosphere and diapirism of the asthenospheric mantle.

3.10 Summary

It is clear from the combined data (Fig. 3.3) that rift-related magmatism occurred in distinct stages. The latent magmatic stage is clearly observed in the all of the mafic data for the rift. The onset of early stage magmatism is more problematic as shown by the Ontario data of Heaman et al. (2007). The discovery of pre-1110 Ma ages among mafic and ultramafic intrusions by Heaman et al. (2007) may push the onset of rifting back to 1115 Ma, or even earlier if the pre-1115 Ma ages prove to be related. Miller (pers. comm., 2010) suggested that these early intrusions without correlative volcanics may indicate an early episode of crustal doming that preceded the impact of the plume into the base of the lithosphere and the onset of active rifting. It is unclear if and how the pre-1115 Ma dyke swarms relate to MCR magmatism, but if true it would require a significant paradigm shift for the formation of the Midcontinent Rift.

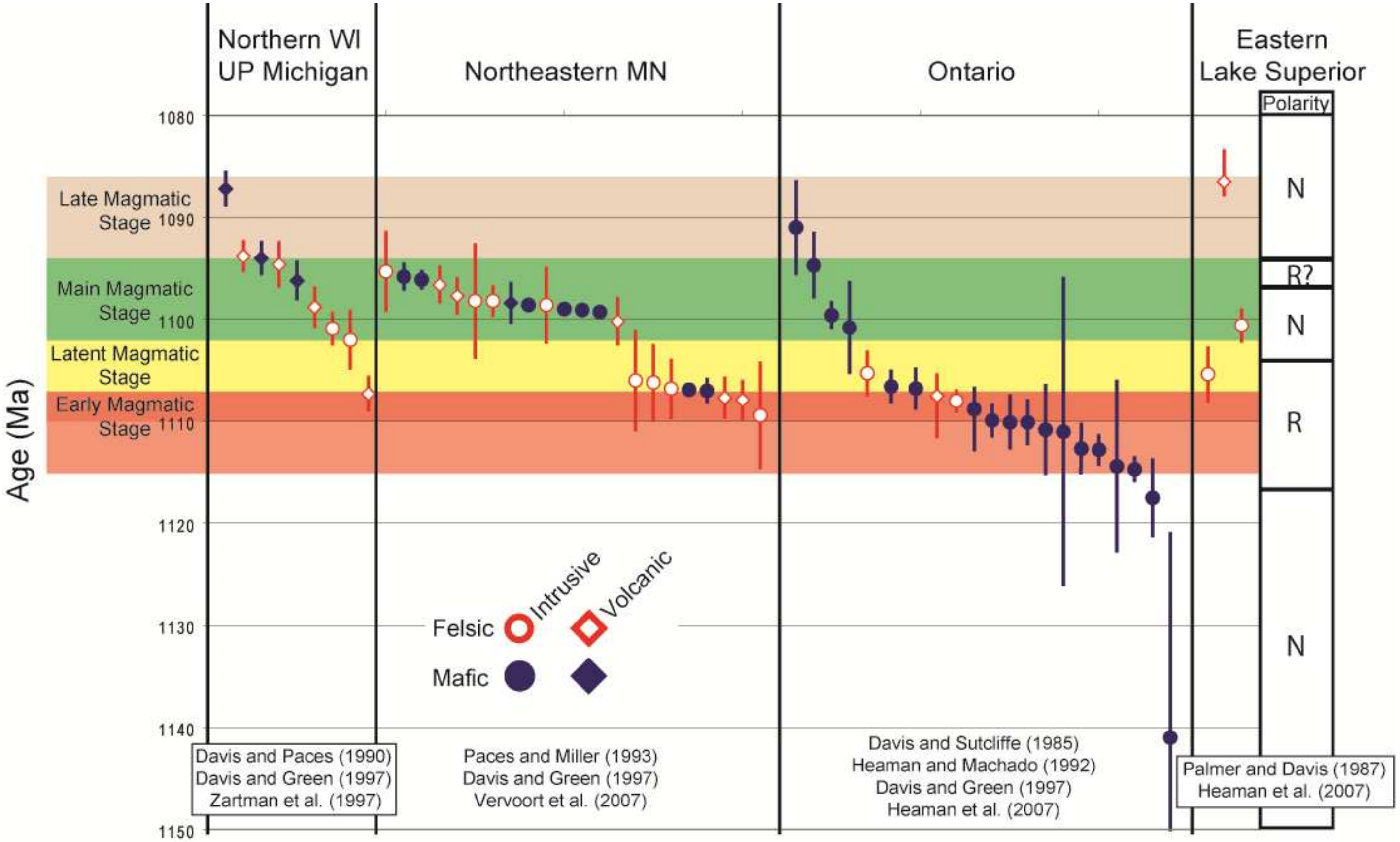

Figure 3.3. Summary of U-Pb weighted mean $^{207}Pb/^{206}Pb$ studies on rocks related to the Midcontinent Rift. The magmatic stages of Miller and Vervoort (1996) are highlighted by color. The lighter shade of red reflects the extension of the early stage to 1115 Ma as suggest by Heaman et al. (2007). Shape of each point illustrates intrusive or extrusive, with color and line illustrating felsic or mafic. Data is from Davis and Sutcliffe (1985); Palmer and Davis (1987); Davis and Paces (1990); Paces and Miller (1993); Zartman et al. (1997); Davis and Green (1997); Vervoort et al. (2007); and Heaman et al. (2007).

4. Purpose of Study

Several problems remain unresolved following the work of previous geochronologic studies on MCR rocks in northeastern Minnesota. Studies focused primarily on establishing the temporal relationship between the four main series of the Duluth Complex and the span of intrusive activity within the Duluth and Beaver Bay complexes (Paces and Miller, 1993; Davis and Green, 1997; Vervoort et al., 2007). The purpose of this study is to address several unresolved questions about the timing of intrusive magmatism in northeastern Minnesota.

1) <u>Relative Ages of Layered Series Intrusions</u> – Paces and Miller (1993) attempted to test an interpretation of the aeromagnetic data that layered series intrusions were emplaced by successive overplating from the northwest to the southeast (Miller and Severson, 2002; Fig. 4.1). Accordingly, they selected samples from what they perceived to be the oldest layered series intrusion, the Partridge River intrusion (PRI), and one of the youngest layered series intrusions - the Duluth Layered Series (DLS), to test the range of layered series emplacement. The ages for both intrusions were irresolvable within error. Moreover, later mapping (Severson and Miller, 1999) revealed that their Partridge River intrusion sample was actually a gabbroic phase of the anorthositic series. Therefore, the question still remains: can precise U-Pb zircon ages be used to support the aeromagnetic interpretation of layered series emplacement? Resolution of this question requires dating several layered series intrusions that span sequentially from oldest to youngest.

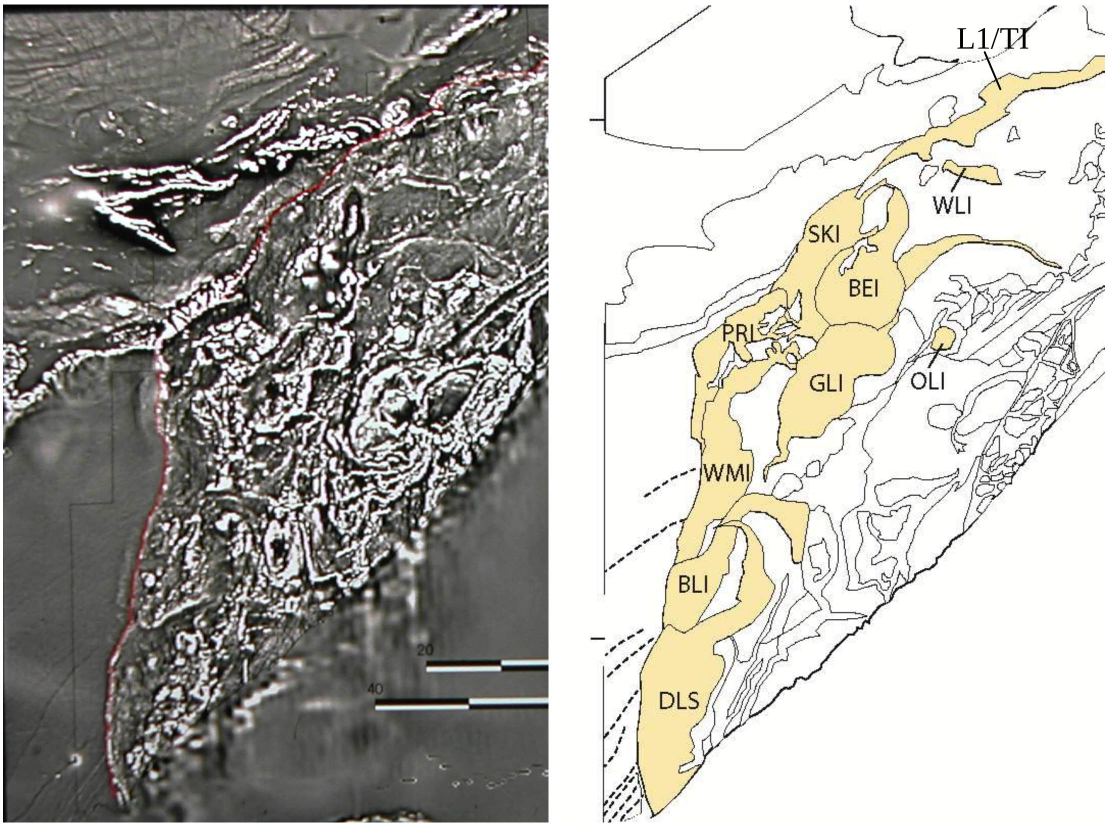

Figure 4.1. 1st vertical derivative of the aeromagnetic data and geologic interpretation of layered series intrusions for the western part of the Duluth Complex (interpreteation based on Miller et al., 2001). Crosscutting relationships implied by the aeromagnetic data serves for the basis of the sequential emplacement model suggested by Miller and Severson (2002). They suggest the following intrusive sequence: Partridge River intrusion (PRI) → South Kawishiwi intrusion (SKI), Western Margin intrusion (WMI), Lake One troctolite (L1), Tuscarora intrusion (TI) → Boulder Lake intrusion (BLI), Greenwood Lake intrusion (GLI) → Bald Eagle intrusion (BEI), Layered Series at Duluth (DLS)

2) Time-span of Duluth Complex and Beaver Bay Complex Emplacement – Paces and Miller (1993) attempted to date one of the oldest BBC intrusions based on field relationships, the Lax Lake gabbro, and the youngest BBC intrusion, the Silver Bay gabbro, to determine the relative timing between Duluth Complex and Beaver Bay Complex magmatism. They were unable to extract useable data from the small

inclusion filled zircons from the Lax Lake gabbro so they sampled baddeleyites from a differentiated phase of the Sonju Lake intrusion, which, according to field relationships, is younger than the Lax Lake gabbro and older than the Silver Bay gabbro. The Sonju and Silver Bay ages are irresolvable within error (1096.1 ± 0.8 Ma and 1095.8 ± 1.2 Ma, respectively), and were approximately 2-3 Ma younger than the oldest dates from the layered series. As a result, the question remains: is the apparent 2-3 Ma time-gap between Duluth Complex and Beaver Bay Complex magmatism real, or just a function of insufficient data? Resolution of this question requires dating the latest Duluth Complex intrusions and the earliest Beaver Bay intrusions.

3) <u>Age of Miscellaneous Hypabyssal Intrusions not Spatially Associated with the Duluth Complex or Beaver Bay Complex</u> - Many intrusions that are not spatially associated with the Duluth or Beaver Bay complexes are classified as miscellaneous intrusions on the regional geologic map of northeastern Minnesota (M-119; Miller et al., 2001). These intrusions span a large compositional range (from primitive olivine tholeiitic diabase to granophyre) and occur as subconcordant sheet-like intrusions in the volcanic edifice of the NSVG (Miller and Green, 2002). While they are generally interpreted to be younger than intrusions of the Duluth Complex (see correlation diagram for M-119; Miller et al., 2001), it is unclear when they intruded. To determine the age relationships of these miscellaneous intrusions to the Duluth and Beaver Bay complexes, the lowest hypabyssal intrusion in the southeastern sequence,

the Endion Sill, was chosen for dating. Green and Miller's (2008) map of the Duluth Quadrangle shows the Endion Sill as intrusive into the underlying Duluth Complex, based on ambiguous field and aeromagnetic data. This interpretation is very speculative, however (Miller, 2010, pers. comm.).

5. Methods

5.1 Sampling Strategy

Based on the work of Paces and Miller (1993), it appears that mafic rocks with the highest probability of containing zircon or baddeleyite are coarse-grained, poorly foliated, and more gabbroic in modal composition (i.e. augite- and oxide-rich). Greater abundances of pyroxene and oxide, as well as biotite, in the largely troctolitic intrusions of the Duluth Complex were used as an indicator of a greater trapped liquid component, which would facilitate the crystallization of zircon in a mafic plutonic rock.

The 1:100,000 scale geologic map of northeastern Minnesota (M119, Miller et al., 2001) is not only the most comprehensive compilation of the bedrock geology of the Duluth Complex and Beaver Bay Complex to date, but also summarily portrays the age relationships of the numerous units comprising these intrusive complexes. Most of these age relationships are inferred from field relationships or interpreted from aeromagnetic data (Miller et al, 2001). The temporal relationships shown on this map serves as the model to be tested by this study and the basis for the sample selection. Eight sample sites were selected for this study in order to test the three basic problems put forth in the previous chapter (Fig. 5.1, Table 5.1).

Five samples were selected to address the age span of Layered Series intrusive activity. Based on interpretations of aeromagnetic data, and to a lesser extent field relationships, Miller et al. (2001) deduced that the Partridge River intrusion was likely the oldest intrusion of the layered series. Although Paces and Miller (1993) thought they had sampled the Partridge River intrusion (PG2, Fig. 3.2), later mapping (Severson and Miller, 1999) revealed that this gabbro (the Powerline Gabbro of Bonnichsen, 1971) is actually a phase of the anorthositic series.

Table 5.1. Summary of sample locations for this study. Unit abbreviations as in Figure 5.1

		UTM (NAD 1983, 15N)			T, R, S	
Unit	Rock Type	E	N	Section	Township	Range
PRI	augite troctolite	567165	5266451	SW 34	T59N	R14W
TI	melatroctolite	653325	5324622	NE 3	T64N	R5W
DLS	olivine gabbro	557786	5171911	SE 28	T49N	R15W
GLI	oxide gabbro	602351	5268421	SW 29	T59N	R10W
BEI	olivine gabbro	607331	5289687	SW 23	T61N	R10W
WLFG	ferrogabbro	645515	5280554	SE 22	T60N	R6W
HCT	augite troctolite	639083	5273599	NW 18	T59N	R6W
ES	oxide gabbro	570062	5185705	NE 14	T50N	R14W

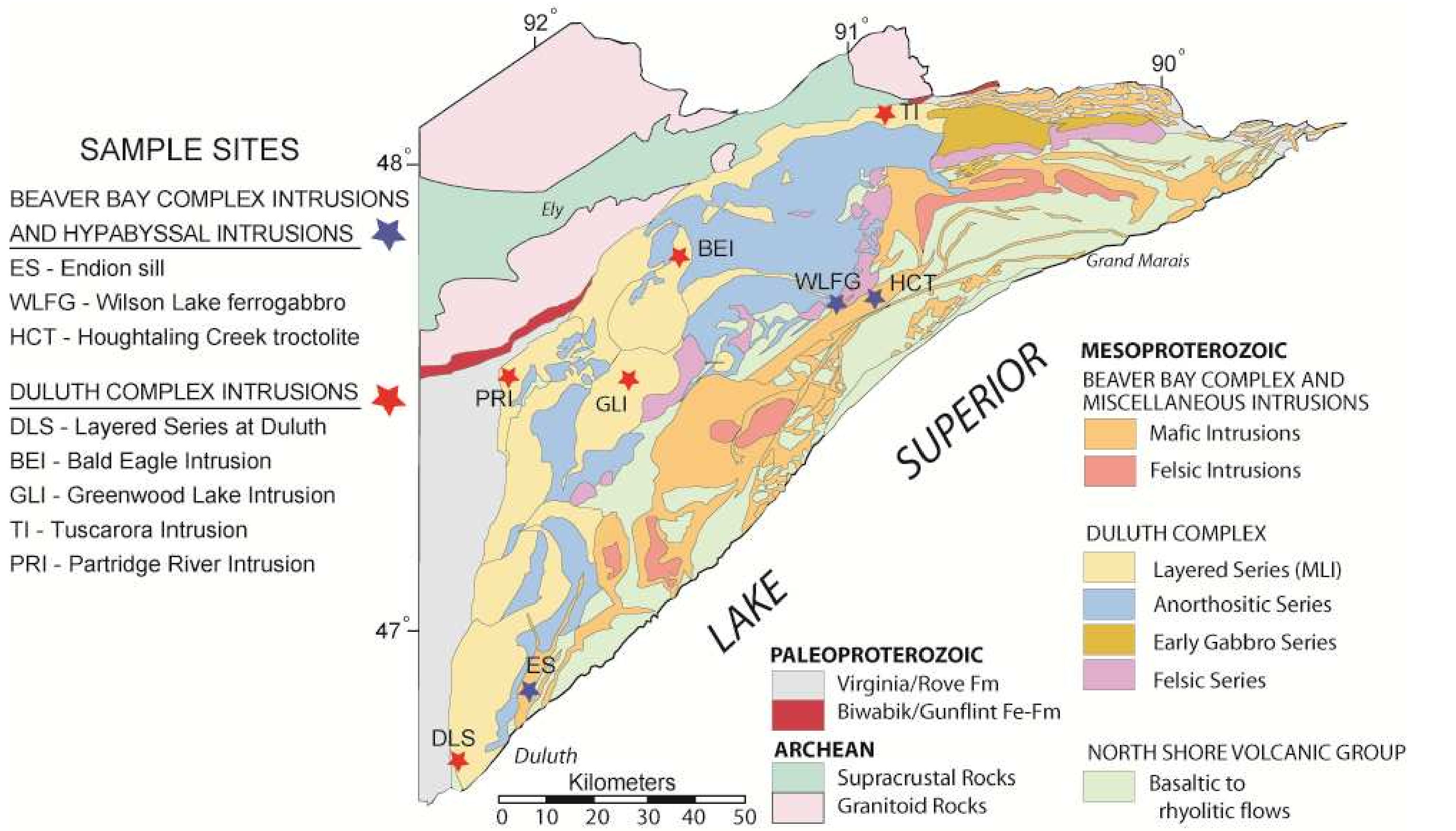

Figure 5.1. Summary of sample locations for this study in the context of the general geologic setting (modified from Miller, 2008, unpublished figure)

The Partridge River intrusion forms the northwestern margin of the Duluth Complex and is described by Miller and Severson (2002) as a southeast dipping, mafic layered intrusion, consisting predominately of troctolitic cumulates. It is in contact with Paleoproterozoic metasedimentary rocks of the footwall and locally contains inclusions of various anorthositic series rocks and volcanic hornfels. Bulk sample collected for this study was taken from the Ppct unit near the base of the Partridge River intrusion from a pavement outcrop off of Forest 117 Rd. north of Hoyt Lakes, MN. Severson and Miller (1999) describe the Ppct unit as a homogeneous coarse to very coarse-grained, poorly laminated to decussate, ophitic leucocratic troctolite to augite troctolite. In hand sample, the rock for this study consisted of coarse-grained, moderately foliated, subophitic augite troctolite (Fig. 5.1, Table 5.1).

The Tuscarora intrusion is one of the least understood layered series intrusions because of its remote location in the Boundary Waters Canoe Area Wilderness. Miller and Severson (2002) speculated that given its predominately troctolitic composition, it may be comparable in age to older layered series intrusions such as the Partridge River intrusion and the South Kawishiwi intrusion. Like the PRI and SKI, the Tuscarora is situated along the margin of the Duluth Complex and is in contact with a footwall of Paleoproterozoic metasedimentary rocks and Neoarchean granite-greenstone terrane. However, the lack of detailed mapping along the northern margin of the Duluth Complex makes it difficult to ascertain its temporal relationship with other intrusions to the west. Recent mapping by Costello (unpublished M.S. thesis, 2010) in the Gillis Lake and Gabimichigami Lake 7.5' quadrangles shows the Tuscarora intrusion to be composed of two distinct zone – a lower zone dominated by basalt inclusion-rich augite troctolite to olivine gabbro, and an upper zone of augite-poor troctolite, melatroctolite and leucotroctolite, with an abundance of anorthositic series inclusions. To steer clear of possible footwall contamination, a melatroctolite from the upper zone of the intrusion was sampled on the northern shore of Fern Lake in the Boundary Waters Canoe Area Wilderness (Costello, unpublished M.S. thesis, 2010). The sample was taken from the Mtum unit, which Costello (M.S. thesis) describes as coarse to medium-grained melatroctolite with local modal layering of olivine, ranging in content from 15-30%. In hand sample, rock from this unit appears as coarse to medium-grained melatroctolite (Fig. 5.1, Table 5.1).

The Layered Series at Duluth is a 3.5 to 5 kilometer thick, sheet-like, layered mafic intrusion that forms the southern margin of the Duluth Complex. It is subdivided into five stratiform units based on lithology, cumulus mineralogy, texture and large-scale layering (Miller and Green, 2008). Paces and Miller (1993) selected a ferrogabbro sample (D1) from the upper portion of the Layered Series at Duluth to determine its age. Green et al. (2001) speculated that the precise zircon age of 1099.3 ± 0.3 Ma from Paces and Miller (1993) may represent inherited zircon from the anorthositic series rocks hanging wall, which gave an identical age of 1099.1± 0.5 Ma. Green et al. (2001) were unable to substantiate this with their less precise date of 1098.9 ± 1.4 Ma from a monzodiorite, also collected near the top of the Layered Series at Duluth. Miller and Severson (2002) hypothesized, based on aeromagnetic crosscutting relationships, that the Duluth Layered Series may be the youngest layered series intrusion. However, questions about inheritance and the imprecision of the Green et al. (2001) age make it difficult to evaluate this interpretation. To try and resolve this issue, the sample collected for this study was from the troctolitic Mdt zone of Miller and Green (2008), which is described as a 1,000 to 1,800 meter thick zone of massive, medium-grained, poorly to moderately-foliated, ophitic augite-bearing troctolite to augite troctolite. It was collected north of W. Skyline Parkway on the northern bank of Sargent Creek. In hand sample, it is a coarse-grained to pegmatitic, ophitic olivine gabbro (Fig. 5.1, Table 5.1).

The poorly exposed Greenwood Lake intrusion, a layered series body in the central Duluth Complex (Fig. 5.1), is also interpreted to be one of the younger intrusions of the Duluth Complex (Miller and Severson, 2002). Its geophysical signature appears to truncate underlying intrusions, such as the South Kawishiwi and Western Margin intrusions (Figs. 2.6, 4.1). Based on a traverse of shallow drill hole and limited outcrop along the former LTV Mining railroad grade, the Greenwood Lake intrusion is a 2 kilometer thick, poorly exposed, well-differentiated, sheet-like layered intrusion with a lower leucotroctolite zone and an upper olivine oxide gabbro zone (Miller, 2004; Jirsa and Miller, 2004). The bulk of exposed Greenwood Lake intrusion is a well foliated, four-phase (Pl-Cpx-Ox-Ol) cumulate rock with little to no trapped liquid component or coarse segregations. In addition to possibly being one of the youngest intrusions of the layered series, the aeromagnetic anomaly associated with Greenwood Lake appears to arc through the anorthositic series rocks and merge with the Wilson Lake ferrogabbro of the Beaver Bay Complex (Figs. 2.6, 4.1) implying a possible genetic link between these two intrusions. For this study, a medium-grained, well-foliated, olivine oxide gabbro was collected from the Mgg unit of the Greenwood Lake intrusion on the north side of the former Erie railroad grade about 1 kilometer east of Highway 2 (Jirsa and Miller, 2004; Fig. 5.1, Table 5.1).

In the central Duluth Complex, the Bald Eagle intrusion (BEI) appears to be the youngest layered series intrusion as its aeromagnetic signature appears to truncate the central body of the Greenwood Lake intrusion (Figs. 2.6, 4.1; Miller and Severson, 2002). Weiblen's (1965; Green et al., 1966) mapping of the tear drop-shaped Bald Eagle intrusion showed it to be a concentrically zoned intrusion with an outer zone of troctolite to melatroctolite (Pl+Ol) cumulates and an inner core of olivine gabbro (Pl+Ol+Aug) cumulates, partially emplaced into rocks of the anorthositic series, and the South Kawishiwi and Greenwood Lake intrusions (Jirsa and Miller, 2004; Green et al., 1966). For this study, sample BEI was taken from unit bg, which is described by Green et al. (1966) as a medium-grained, foliated, olivine-bearing gabbro. The sample outcrop is a coarse-grained, moderately foliated, intergranular, olivine gabbro and was collected one kilometer south of Tonic Lake off of US Forest Service Road 387A, north of Isabella, Minnesota (Fig. 5.1, Table 5.1).

To address the issue of temporal overlap between Duluth Complex and Beaver Bay Complex magmatism, BBC intrusions were sought out that field mapping indicates (Miller and Chandler, 1997) may represent the oldest intrusive activity. Accordingly, two intrusions from the northern part of the Beaver Bay Complex were selected for study: the plug-shaped Wilson Lake ferrogabbro and the keel-shaped macrodike intrusion termed the Houghtaling Creek troctolite (Fig. 5.1, Table 5.1). Geologic mapping by

Boerboom and Miller (1994) inferred from field relations and aeromagnetic data that the Wilson Lake ferrogabbro, a plug-shaped intrusion composed of well-foliated olivine oxide gabbro to ferromonzodiorite, is cross-cut by the Houghtaling Creek troctolite. Miller and Chandler (1997) interpret the Wilson Lake ferrogabbro to be the oldest intrusion of the Beaver Bay Complex. In addition, they noted that the aeromagnetic signature of the Greenwood Lake intrusion of the Duluth Complex appears to funnel into the Wilson Lake ferrogabbro and could provide a genetic link between Duluth Complex and Beaver Bay Complex magmatism. For this study, a coarse-grained, granophyric ferrogabbro with interstitial biotite was collected from a somewhat weathered outcrop along the southwestern shoreline of Wilson Lake (Boerboom and Miller, 1994). The sample was collected from the wlmg unit, which is composed of medium to very coarse-grained, pink to black monzogabbro with local patches of coarsely pegmatitic gabbro (Boerboom and Miller, 1994; Fig. 5.1, Table 5.1).

The Houghtaling Creek troctolite was mapped and described by Miller et al. (1994), as a keel-shaped macrodike composed of moderately differentiated olivine plagioclase cumulates. Aeromagnetic signatures indicate the HCT is approximately two to four kilometers wide, and strikes for a distance of approximately 40 kilometers, separating the bulk of overlying Beaver Bay Complex magmatism from the underlying anorthositic cumulates. Paces and Miller (1993) dated the Sonju Lake intrusion at 1096.1 ± 0.8 Ma. The aeromagnetic anomaly associated with the Sonju Lake clearly crosscuts the Cloquet Lake layered series, which in turn, appears to crosscut the Houghtaling Creek troctolite (Chandler and Miller, 1997; Miller and Green, 2002). The Houghtaling Creek troctolite should provide a reasonable age for intrusive activity between early BBC magmatism (WLFG) and late (~1096Ma) BBC magmatism (SLI1 and SBG2 from Paces and Miller, 1993). For this study, a sample of medium-grained, ophitic augite troctolite was collected from a glacially polished pavement outcrop on the west side of USFR 359 (Little Manitou Rd) from the hct unit of Miller et al. (1994). The bulk unit is described by Miller et al. (1994) as a medium to medium coarse-grained, poorly to well-laminated, locally layered, ophitic augite troctolite to olivine gabbro (Fig. 5.1, Table 5.1).

Lastly, the Endion Sill near Duluth is classified by Miller et al. (2001) as a miscellaneous intrusion because it is not clear that it is associated with Duluth Complex or Beaver Bay Complex magmatism. Green and Miller (2008), in their geologic map of the Duluth quadrangle, describe the sill as a lithologically complex mafic to intermediate sill, approximately 425 meters thick, that sits stratigraphically above the roof zone of the Duluth complex, emplaced within volcanics of the North Shore Volcanic Group, in contact with overlying granophyre. They interpret the Endion Sill to be younger than the Duluth Complex based on aeromagnetic crosscutting relationships, but state on the map that this conclusion is very speculative. Determining the age of the hypabyssal Endion Sill will provide important constraints on the estimated depth of emplacement of the Duluth Complex (Miller and Severson, 2002). For this study, the outcrop sampled (unit Mes – Green and Miller, 2008) was from the middle section of Endion Sill near the intersection of Woodland Ave and Norton St. in the city of Duluth, MN. The outcrop consisted of weathered, coarse-grained, poorly foliated augite troctolite. In hand sample, it was medium-grained, intergranular, oxide gabbro (Fig. 5.1, Table 5.1).

5.2 Mineral Separations and Analytical Procedure

The protocols for zircon and baddeleyite separation follow a standard series of well developed techniques (Fig. 5.2). Roughly 30 – 40 kilograms of rock from each sample site was collected (equivalent of four 5 liter sample bags full of fragmented rock) and crushed using a steel jaw crusher and ceramic disc mills. For each sample, a 64 oz split of milled material (ground to less than 500 microns) was processed through a series of density and magnetic separations.

Bulk density separations were performed on a Rogers table, 64 oz at a time. The heaviest grains, which come off the Rogers table at the far end, were collected in small plastic tubs, poured into baking pans, and dried in a furnace for about twenty minutes. Iron filaments picked-up during the crushing process are pulled out of the heavy grain fraction using a hand-magnet. The non-magnetic heavy grains are then run through an initial Frantz magnetic separation (0.3 Amps, 20 degrees tilt). The non-magnetic fraction is then subjected to heavy liquid density separation using metheleyne iodide (specific gravity = 3.33). The heavy grains from this fraction are then subjected to another Frantz magnetic separation (1.0 Amps, 20 degrees tilt), prior to grain picking under microscope. Grains are picked with tweezers in methanol (to cut down static charge) from Petri dishes. Zircon and baddeleyite were selected and put into clean dishes for analysis. A complete description of separation techniques can be found in the BSU Isotope Geology Laboratory Mineral Separations Guidebook (available for download from the Boise State Isotope Geology Laboratory LABSHARE website: <http://earth.boisestate.edu/isotope/labshare.html>)

Zircon was chemically abraded using a modified method of Mattinson (2005). Grains of zircon were hand separated from other minerals, transferred to a quartz beaker, and placed in a muffle furnace for bulk annealing at 900 ºC for 60 hrs (Mattinson, 2005).

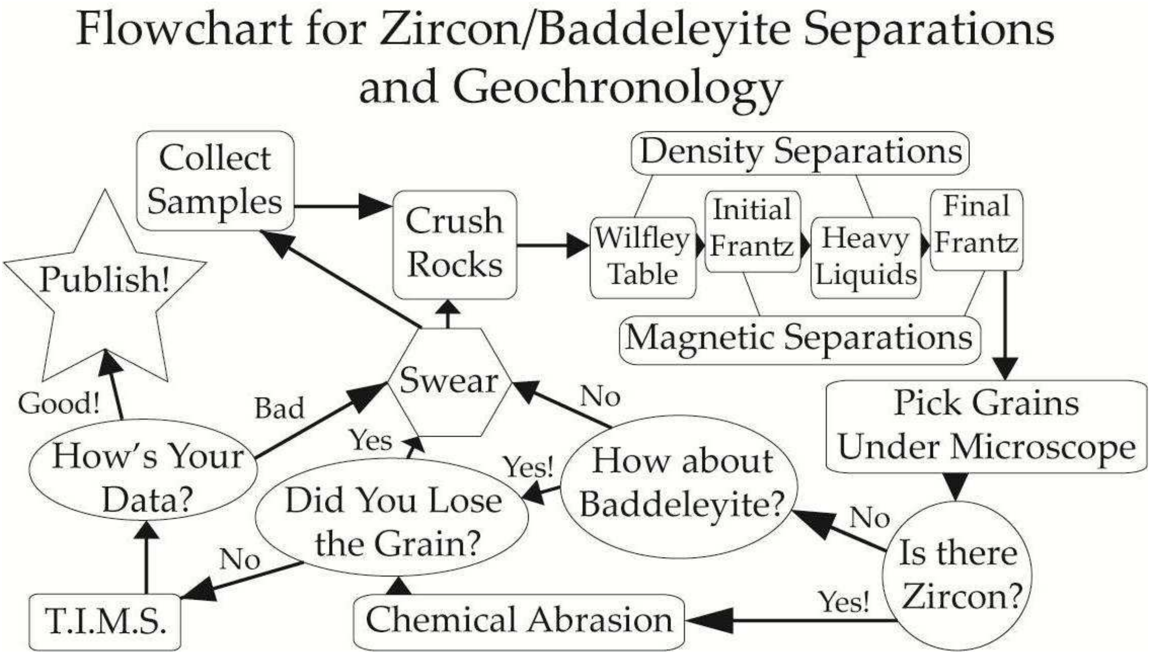

Figure 5.2. Generalized flow chart for zircon/baddeleyite separations and CA-TIMS

Zircon selected for analysis was generally chosen based on the absence of cracks, inclusions, and other surface imperfections. Selected grains were transferred into 300 μl Teflon PFA microcapsules, placed in an acid digestion bomb, and leached in 29 M HF for 12 hours at 180 ºC. The leached solution was removed and the grains were washed using ultra pure H_2O, ultrasonically cleaned in 3.5 M HNO_3 for 30 minutes, and fluxed on a hot plate for ~30 min. Baddeleyite grains do not receive the chemical abrasion treatment as they are less resistant to the treatment than zircon.

Both zircon and baddeleyite grains were then dissolved using methods outlined by Davydov and others (2010). Grains were loaded into 300 μl Teflon PFA microcapsules for total dissolution and spiked using Earthtime (ET-535) ^{205}Pb - ^{233}U - ^{235}U tracer, with ratios of $^{235}U/^{205}Pb = 100.206$, and $^{233}U/^{235}U = 0.9946$ (Condon et al., 2007). Zircon and baddeleyite grains are dissolved in 29 M HF and 3.5 M HNO_3 at 220 ºC for 48 hrs, and dried down to fluoride salts on a hot plate. The fluorides are redisolved using 6 M HCl at 180 ºC overnight, and fluxed on a hot plate for 10 min. U and Pb were separated using the anion-exchange chromatographic procedure developed by Krogh (1973).

Grains were loaded onto single Re filaments using silica gel/phosphoric acid mixture (Gerstenberger and Haase, 1997) and analyzed on an Isotopx IsoProbe-T Thermal Ionization Mass Spectrometer equipped with a Daly detector and Faraday cups. The Daly detector is used for smaller ion beams, as the weak beam is passed through a photomultiplier to amplify the signal. Larger beams are fun on a dynamic Faraday-Daly routine, as the signal jumps from the Faraday collectors to the Daly detector to establish real-time gain correction. Both routines were checked against each other using the same ET-535 spike, and were revealed to be statistically equivalent. U-Pb ages and associated uncertainties were calculated using the algorithms and data reduction of Schmitz and Schoene (2007), the ET-535 ratios of Condon and others (2007), and the U decay constants of Jaffey and others (1971).

6. Results

Of the eight intrusions sampled, six yielded dateable materials (Fig. 6.1). U-Pb data from 38 zircon and baddeleyite analyses are presented in Table 6.1, with best estimate crystallization ages represented in Table 6.2. $^{207}Pb/^{206}Pb$ and $^{206}Pb/^{238}U$ ages were calculated using Isoplot 3.0 (Ludwig, 2003) using the data reduction of Schmitz and Schoene (2007) and all errors are at the 95% confidence interval.

Table 6.1. Summary of isotopic data calculated for this study. Calculations performed using Isoplot 3.0 (Ludwig, 2003) and the data reduction of Schmitz and Schoene (2007).

		Compositional Parameters							Radiogenic Isotope Ratios				Isotopic Ages			
Sample	Fraction	Wt. mg	U ppm	Th/U	Pb ppm	Pb*/Pb_c	Pb_c (pg)	$^{206}Pb/^{204}Pb$	$^{208}Pb/^{206}Pb$	$^{207}Pb/^{206}Pb$	$^{207}Pb/^{235}U$	$^{206}Pb/^{238}U$	$^{207}Pb/^{206}Pb$	±	$^{206}Pb/^{238}U$	±
		Duluth Complex: Partridge River intrusion														
PRI	z1	0.010	275.45	0.714	56.92	414.41	1.37	23778.8	0.2163	0.076092	1.94424	0.185314	1097.50	0.88	1095.94	0.46
	z2	0.010	265.71	0.665	54.24	597.71	0.91	34687.5	0.2015	0.076125	1.94528	0.185333	1098.35	0.84	1096.05	0.45
	z3	0.010	58.70	0.669	12.04	191.44	0.63	11111.4	0.2027	0.076183	1.94652	0.185310	1099.89	1.12	1095.92	0.48
	z4	0.010	141.27	0.609	28.50	271.29	1.05	15965.4	0.1847	0.076126	1.94481	0.185287	1098.38	0.92	1095.79	0.47
	z5	0.010	196.93	0.795	41.47	469.08	0.88	26405.6	0.2409	0.076104	1.94474	0.185334	1097.80	0.84	1096.05	0.45
	z6	0.010	159.99	0.624	32.36	391.28	0.82	22937.1	0.1892	0.076108	1.94433	0.185284	1097.91	0.79	1095.78	0.45
		Duluth Complex: Tuscarora intrusion														
TI	b2	0.010	211.08	0.013	36.30	481.30	0.75	33086.5	0.0040	0.076166	1.94145	0.184869	1099.43	1.07	1093.52	0.46
	b3	0.010	389.98	0.009	66.81	544.05	1.23	37445.5	0.0026	0.076144	1.93651	0.184452	1098.86	0.84	1091.25	0.45
	b4	0.010	248.03	0.010	42.70	242.47	1.75	16691.7	0.0031	0.076135	1.94053	0.184856	1098.62	0.79	1093.45	0.45
	b5	0.010	161.22	0.013	27.65	199.88	1.38	13752.0	0.0040	0.076129	1.93017	0.183883	1098.47	0.84	1088.15	0.46
	b6	0.010	335.17	0.011	57.62	707.02	0.81	48626.3	0.0033	0.076135	1.94259	0.185053	1098.62	0.78	1094.52	0.45
	b7	0.010	131.74	0.009	22.76	109.60	2.06	7546.3	0.0027	0.076169	1.93945	0.184672	1099.51	1.07	1092.45	0.49
	b8	0.010	223.38	0.009	38.66	108.66	3.53	7319.3	0.0026	0.076139	1.94201	0.184988	1098.72	0.94	1094.17	0.46
		Duluth Complex: Bald Eagle intrusion														
BEI	z1	0.010	76.67	0.522	15.17	158.79	0.95	9552.6	0.1584	0.076157	1.944317	0.185164	1099.20	1.10	1095.12	0.50
	z3	0.010	86.23	0.575	17.29	177.97	0.97	10566.6	0.1744	0.076139	1.944865	0.185259	1098.74	1.06	1095.64	0.46
	z4	0.010	207.16	0.680	42.49	341.29	1.24	19742.2	0.2061	0.076109	1.944515	0.185300	1097.93	0.88	1095.87	0.44
	z5	0.010	60.91	0.652	12.44	185.86	0.67	10833.1	0.1975	0.076107	1.944305	0.185285	1097.88	1.01	1095.78	0.46
	z6a	0.010	385.96	0.649	78.40	911.36	0.86	53088.7	0.1965	0.076088	1.943671	0.185271	1097.37	0.91	1095.71	0.45
	z6b	0.010	319.23	0.841	67.85	801.29	0.85	44619.6	0.2548	0.076091	1.943613	0.185258	1097.45	0.79	1095.64	0.48

		Compositional Parameters							Radiogenic Isotope Ratios				Isotopic Ages			
Sample	Fraction	Wt. mg	U ppm	Th ppm	Pb ppm	$\frac{Pb^*}{Pb_c}$	Pb_c (pg)	$\frac{^{206}Pb}{^{204}Pb}$	$\frac{^{208}Pb}{^{206}Pb}$	$\frac{^{207}Pb}{^{206}Pb}$	$\frac{^{207}Pb}{^{235}U}$	$\frac{^{206}Pb}{^{238}U}$	$\frac{^{207}Pb}{^{206}Pb}$	±	$\frac{^{206}Pb}{^{238}U}$	±
			Beaver Bay Complex: Wilson Lake ferrogabbro													
WLFG	z2	0.010	46.89	1.224	10.88	110.91	0.97	5693.0	0.3711	0.075970	1.933044	0.184543	1094.29	1.40	1091.74	0.49
	z9	0.010	15.46	1.236	3.76	18.40	1.94	957.5	0.3750	0.076097	1.937508	0.184660	1097.63	6.82	1092.38	1.38
	z16	0.010	9.93	1.209	2.36	27.89	0.82	1449.8	0.3667	0.076014	1.935578	0.184678	1095.45	4.45	1092.48	1.21
	z19	0.010	5.13	2.350	1.56	15.31	0.95	651.6	0.7128	0.076090	1.938477	0.184770	1097.44	9.25	1092.98	1.73
	z26	0.010	16.98	1.115	3.90	45.43	0.84	2397.5	0.3381	0.075950	1.932335	0.184523	1093.77	2.83	1091.64	0.68
	z27	0.010	9.18	2.406	2.74	24.21	1.09	1009.3	0.7305	0.076033	1.929104	0.184013	1095.95	6.35	1088.86	1.17
	z28	0.010	6.04	1.613	1.57	21.39	0.70	1030.0	0.4893	0.075899	1.923580	0.183811	1092.41	6.48	1087.76	2.03
	b1	0.010	50.38	0.091	8.88	103.86	0.85	7000.7	0.0277	0.076078	1.929663	0.183959	1097.12	1.30	1088.57	0.48
	b4	0.010	28.17	1.394	6.68	117.88	0.56	5829.6	0.4255	0.076063	1.904999	0.181643	1096.73	1.51	1075.94	0.68
	b5	0.010	14.23	0.057	2.56	22.21	1.10	1525.6	0.0175	0.076004	1.921371	0.183347	1095.18	4.39	1085.23	1.05
	b6	0.010	18.94	0.080	3.34	59.27	0.55	4015.7	0.0242	0.076003	1.922758	0.183483	1095.14	1.85	1085.97	0.65
			Beaver Bay Complex: Houghtaling Creek troctolit													
HCT	z1	0.010	47.48	0.396	9.21	54.19	1.67	3378.0	0.1200	0.076071	1.942381	0.185188	1096.95	2.12	1095.26	0.61
	z5	0.010	35.60	1.078	8.16	38.50	2.07	2050.8	0.3269	0.076095	1.939192	0.184827	1097.56	3.28	1093.29	0.68
	z6	0.010	61.05	0.666	12.56	100.85	1.23	5866.1	0.2019	0.076141	1.944670	0.185235	1098.79	1.40	1095.51	0.52
	z7	0.010	149.92	0.764	31.47	148.42	2.11	8426.7	0.2317	0.076171	1.945218	0.185216	1099.57	1.14	1095.41	0.46
	z9	0.010	62.52	1.052	13.97	172.79	0.80	9190.3	0.3191	0.076121	1.941280	0.184961	1098.27	1.10	1094.02	0.48
	z10	0.010	44.97	0.719	9.37	93.49	0.99	5371.5	0.2179	0.076165	1.944308	0.185145	1099.40	1.46	1095.02	0.51
	z11	0.010	28.07	0.687	5.83	60.88	0.94	3530.5	0.2084	0.076130	1.941209	0.184934	1098.49	2.05	1093.87	0.58
	z12	0.010	61.61	1.397	14.81	166.36	0.88	8229.1	0.4237	0.076114	1.940484	0.184903	1098.08	1.18	1093.70	0.50
			Miscellaneous intrusion: Endion sill													
ES	z1	0.010	20.83	0.408	3.94	22.96	1.64	1438.8	0.1241	0.074290	1.80024	0.175751	1049.36	5.36	1043.72	1.02
	z2	0.010	33.43	0.280	7.03	20.36	3.29	1287.7	0.0845	0.079393	2.19307	0.200341	1181.95	3.06	1177.15	1.50
	z6	0.010	7.87	1.030	5.17	47.11	1.07	2400.7	0.2853	0.179268	12.59540	0.509575	2646.11	2.03	2654.82	15.56
	z7	0.010	26.99	0.397	5.48	37.77	1.41	2357.2	0.1200	0.077592	2.05505	0.192090	1136.44	3.73	1132.69	1.74

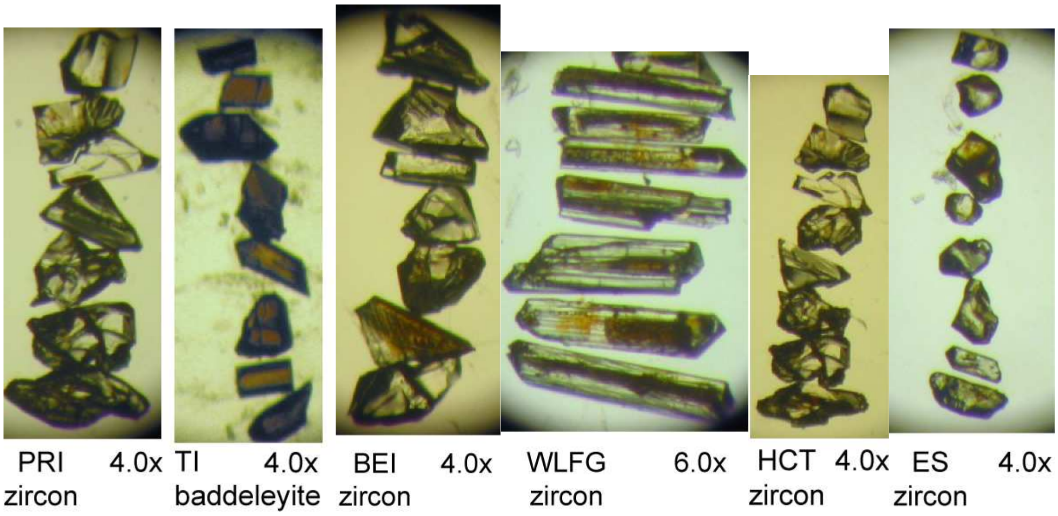

Figure 6.1. Photomicrographs of zircon and baddeleyite grains selected for U/Pb TIMS analysis. The elongate, euhedral, brown-cored Wilson Lake ferrogabbro zircons were especially susceptible to dissolving during the chemical abrasion process. Endion Sill zircon yielded discordant results.

Table 6.2. Summary of the U/Pb ages obtained from this study. All dates presented are weighted mean averages at the 95% confidence interval.

Sample Name	Intrusive Unit	Rock Type	Grain Type	$^{207}Pb/^{206}Pb$ age (Ma)	$^{206}Pb/^{238}U$ age (Ma)
PRI	Early Phase (DC-LS)	augite troctolite	zircon	1097.98 ± 0.37	1095.94 ± 0.18
TI	Early Phase? (DC-LS)	Troctolite	baddeleyite	1098.81 ± 0.32	not defined
DLS	Late Phase (DC-LS)	Gabbro	no material	not defined	not defined
GLI	Middle Phase (DC-LS)	olivine oxide gabbro	no material	not defined	not defined
BEI	Late Phase (DC-LS)	olivine gabbro	zircon	1097.97 ± 0.72	1095.64 ± 0.19
WLFG	Early Phase (BBC)	Ferrogabbro	zrc./badd.	1095.75 ± 0.92	1091.88 ± 0.35
HCT	Early Phase (BBC)	augite troctolite	zircon	1098.62 ± 0.50	1095.31 ± 0.25
ES	Miscellaneous Intrusion	augite troctolite	zircon	not defined	not defined

6.1 Duluth Complex: Partridge River intrusion - *Sample PRI*.

Petrographic observations of sample PRI found it to be a coarse-grained, poorly foliated, ophitic biotitic augite leucotroctolite with 75-80% plagioclase commonly containing inclusions of olivine. Mineral separation resulted in a population of ~20-40 large zircon grains, of which seven were selected for analysis (Fig. 6.1). Six grains yielded concordant results with a weighted mean $^{207}Pb/^{206}Pb$ age of 1097.98 ± 0.37 Ma, and a $^{206}Pb/^{238}U$ age of 1095.94 ± 0.18 Ma (Fig. 6.2, Table 6.2).

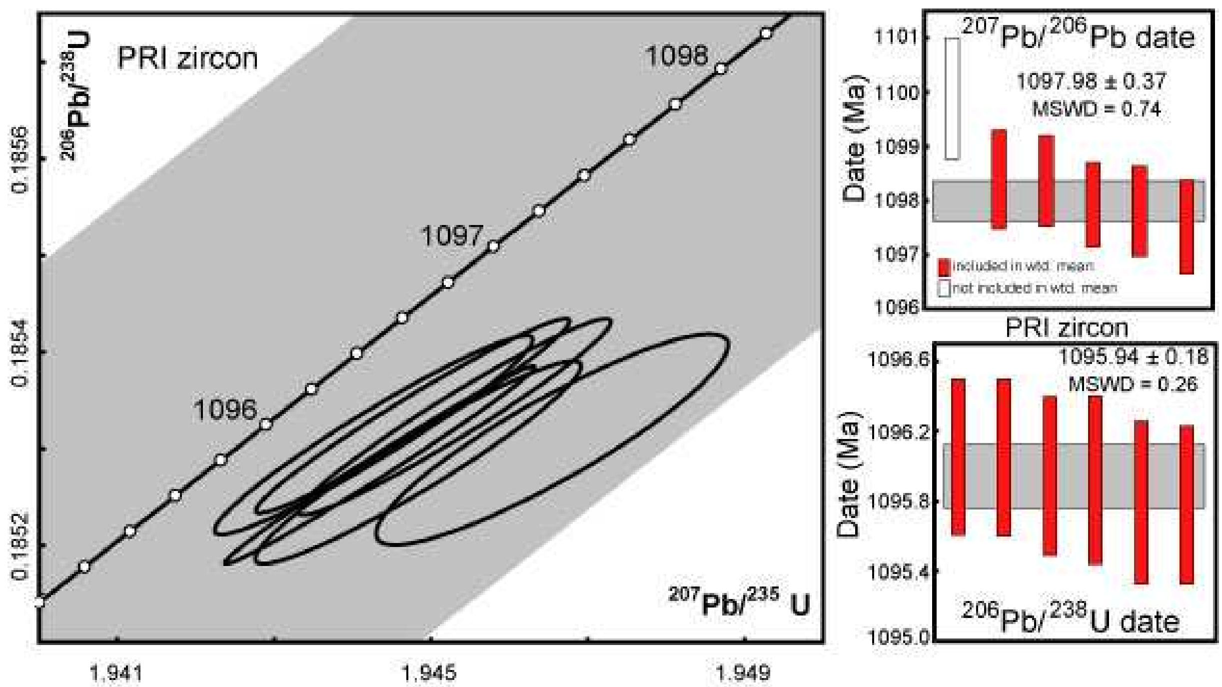

Figure 6.2. Concordia plot of Partridge River intrusion with age data. Weighted mean ages are presented at the 95% confidence interval

6.2 Duluth Complex: Tuscarora intrusion - *Sample TI*

Petrographically, the TI sample consists of a coarse-grained, moderately foliated, ophitic, augite-bearing troctolite. Mineral separation yielded no zircon, but abundant subhedral to euhedral baddeleyite grains (Fig. 6.1). Eight baddeleyite grains were selected for analysis, of which seven yielded concordant results. The seven grains yielded a weighted mean $^{207}Pb/^{206}Pb$ age of 1098.81 ± 0.32 Ma (Table 6.2). As seen on the concordia plot (Fig. 6.3), the baddeleyite grains experienced noticeable Pb loss. As a result, the $^{206}Pb/^{238}U$ crystallization ages are unreliable and cannot be used.

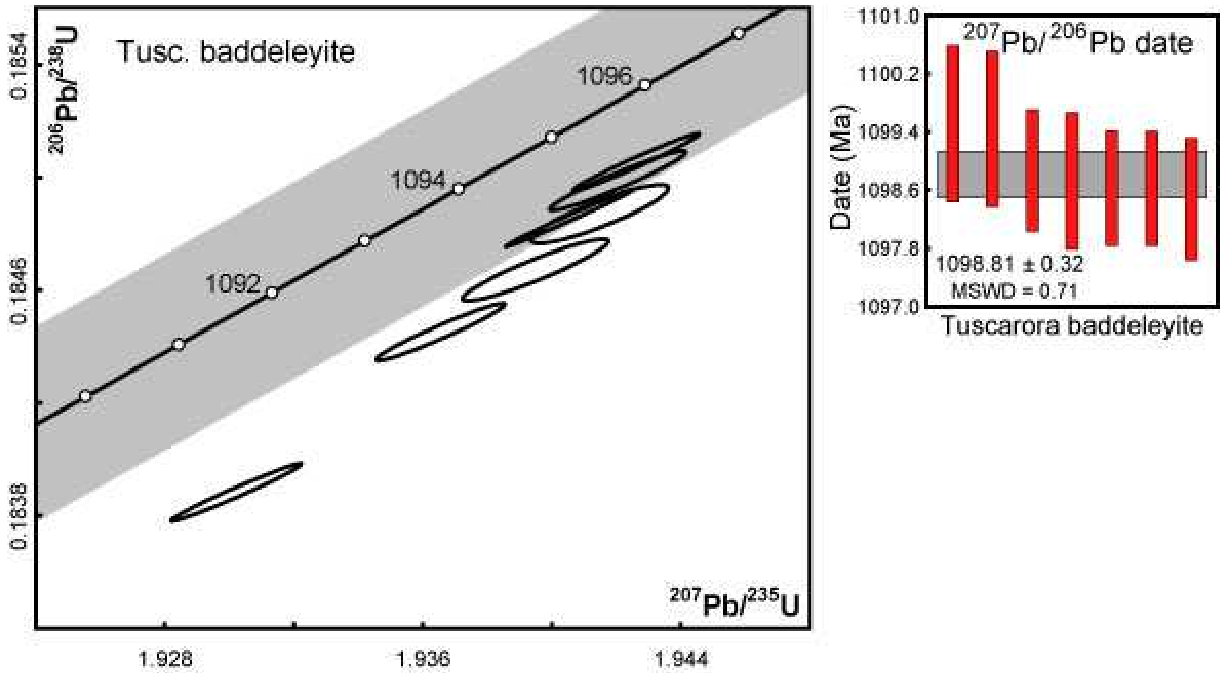

Figure 6.3. Concordia plot of Tuscarora intrusion with age data. Weighted mean ages are presented at the 95% confidence interval

6.3 Duluth Complex: Duluth Layered Series - *Sample DLS.*

Petrographically, the sample DLS is a coarse-grained, moderately foliated, ophitic olivine gabbro with minor amounts of biotite. Unfortunately, this sample was processed on an uncalibrated Wilfley Table at the University of Minnesota Duluth and thus failed to yield any dateable material. This was one of the motivating factors for performing the remainder of analysis under the supervision of Professor Mark Schmitz and Jim Crowley at the Boise State Isotope Geology Laboratory. Because the processing, and not necessarily the sample selection, led to the absence of dateable material, this sample site still remains a viable option for U-Pb zircon study.

6.4 Duluth Complex: Greenwood Lake intrusion - *Sample GLI*

Although processed correctly, this sample of medium-grained, moderately foliated, intergranular olivine oxide gabbro did not yield any dateable material. Given that its textural characteristics imply that it is an adcumulate with little trapped liquid component, this is perhaps not surprising.

6.5 Duluth Complex: Bald Eagle intrusion - *Sample BEI*.

A thin section of this sample, which in the field was observed to be a coarse-grained, moderately foliated, intergranular olivine gabbro was not made as all the sample was processed for zircon/baddeleyite separation. Despite its seemingly adcumulate character, mineral separation resulted in approximately ten large, angular zircon grains. Of these ten grains, six were selected for analysis (Fig. 6.1). One of the larger grains was split in half using the tip of a sharp metal tool, and each fragment was analyzed separately. All six analysis yielded concordant results, with a weighted mean $^{207}Pb/^{206}Pb$ age of 1097.97 ± 0.72 Ma, and a $^{206}Pb/^{238}U$ age of 1095.64 ± 0.19 Ma (Fig. 6.4, Table 6.2).

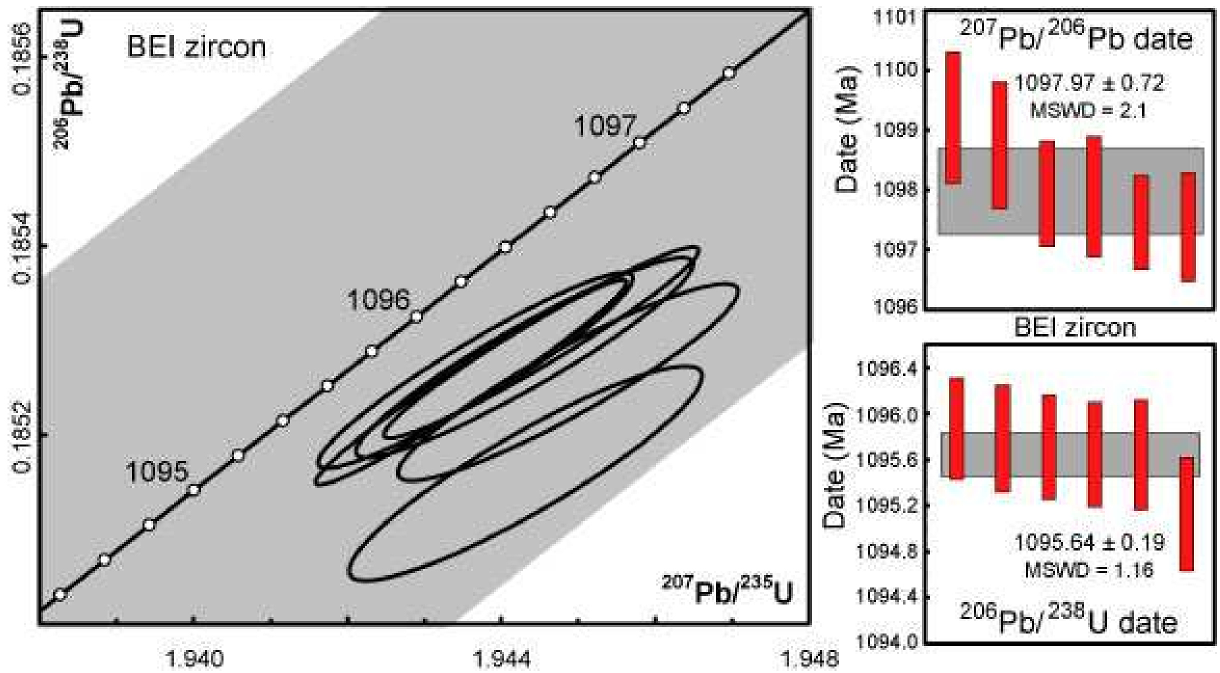

Figure 6.4. Concordia plot of Bald Eagle intrusion with age data. Weighted mean ages are presented at the 95% confidence interval

6.6 Beaver Bay Complex: Wilson Lake ferrogabbro - *Sample WLFG*

The petrography of a hand sample collected by Boerboom and Miller (1994) from the same outcrop as the bulk sample area (K052.05C) is a coarse-grained, non-foliated, subprismatic granular, oxide ferrodiorite with moderate deuteric alteration.

Initial mineral separation yielded a population of approximately forty zircon grains, with subsequent separations yielding seven baddeleyite grains. Seventeen of the clearest euhedral zircon grains were selected for chemical abrasion and four baddeleyite grains were selected for analysis. Zircon grains had visible cores (Fig. 6.1), with the population containing a mix of high-U grains and low-U grains. Grains that had higher U content were nearly all dissolved during the chemical abrasion process. Subsequent chemical abrasion was modified to approximately 3 hours to prevent the grains from dissolving.

High-U grains that survived chemical abrasion were generally discordant and not included in weighted mean calculations.

Seven zircon grains and four baddeleyite grains are nearly concordant and yield a $^{207}Pb/^{206}Pb$ age of 1095.75 ± 0.92 Ma (Fig. 6.1, Table 6.2). Several of the $^{206}Pb/^{238}U$ ages showed signs of obvious Pb loss and were not included in the weighted mean $^{206}Pb/^{238}U$ age calculation (Fig. 6.5). As a result, the weighted mean $^{206}Pb/^{238}U$ age from five concordant zircon grains yielded a crystallization age of 1091.88 ± 0.35 Ma (Table 6.2).

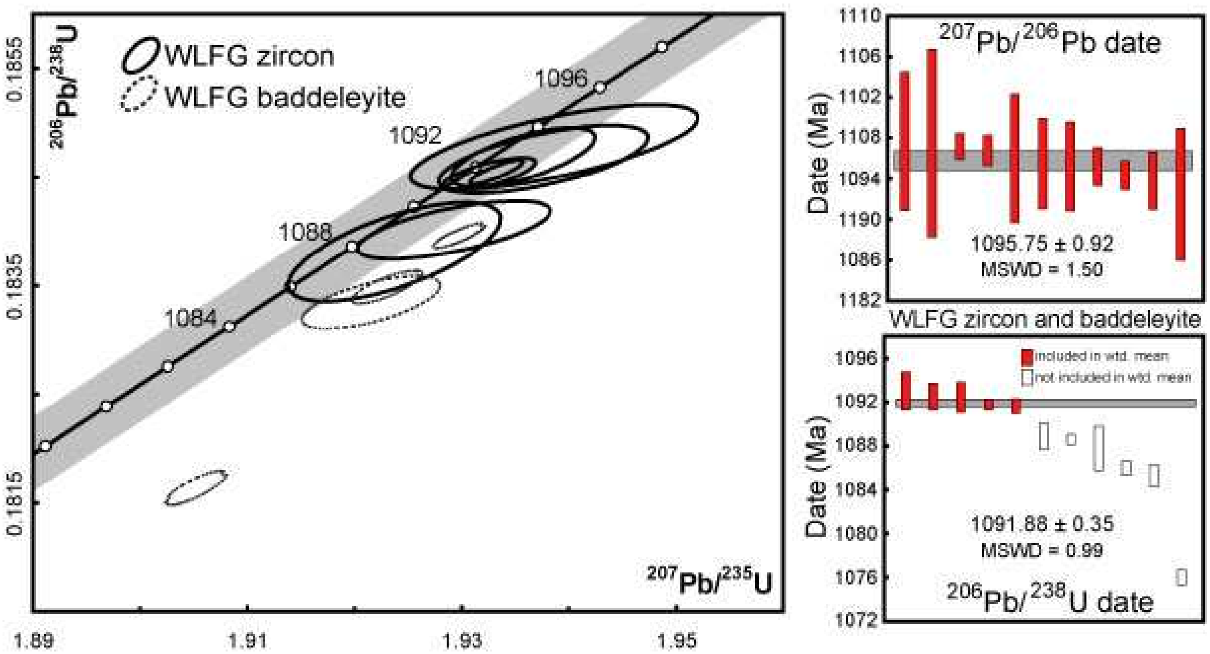

Figure 6.5. Concordia plot of Wilson Lake ferrogabbro with age data. Weighted mean ages are presented at the 95% confidence interval

6.7 Beaver Bay Complex: Houghtaling Creek troctolite - *Sample HCT*

The petrography of the HCT sample shows it to be a coarse-grained, poorly-foliated, coarsely ophitic, leucocratic augite troctolite, with weak to moderate amounts of deuteric alteration. The mineral separation process yielded a small population (< 20) of clear, fractured zircon grains and no baddeleyite. Eleven of the clearest grains were selected for chemical abrasion and analysis.

Of the eleven grains, eight yielded a concordant $^{207}Pb/^{206}Pb$ age of 1098.62 ± 0.50 Ma (Fig. 6.1, Table 6.2). In the $^{206}Pb/^{238}U$ data, four of the grains experienced obvious Pb loss and were not included in the weighted mean age. Four concordant zircon grains thus yielded a weighted mean $^{206}Pb/^{238}U$ age of 1095.31 ± 0.25 Ma (Fig. 6.6, Table 6.2).

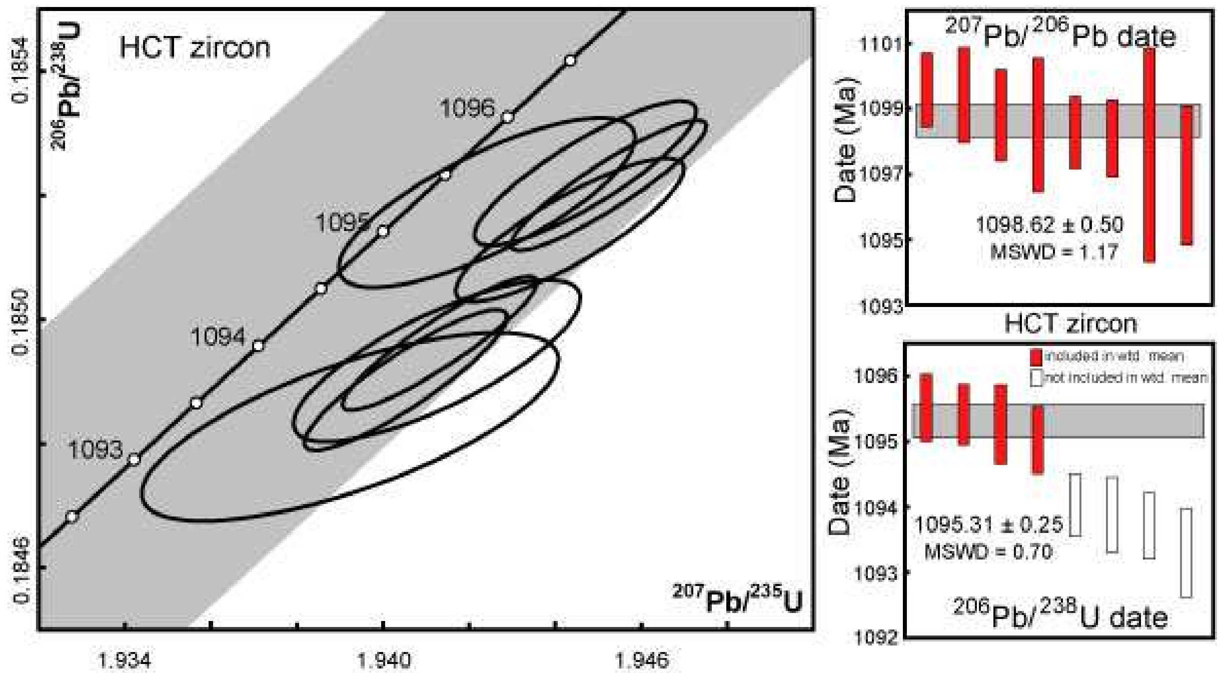

Figure 6.6. Concordia plot of Houghtaling Creek troctolite with age data. Weighted mean ages are presented at the 95% confidence interval

6.8 Miscellaneous Intrusion: Endion Sill - *Sample ES*

Petrographically, the ES sample appears as a medium-grained, poorly foliated, apatitic, granophyric intergranular oxide gabbro with moderate degrees of deuteric alteration. Bulk separation yielded a small population of variably shaped zircon grains.

The clearest grains were selected for chemical abrasion, with some grains being rounded and others euhedral (Fig. 6.1). Four grains yielded discordant U-Pb ages at 1049 Ma, 1182 Ma, 1136 Ma, and 2646 Ma. No weighted mean ages were calculated.

These nonsensical results are likely indicative of incomplete mixing and assimilation between of the Endion Sill and the older, overlying Tischer Creek Rhyolite. Field relations show variable degrees of mixing between the partially melted base of the rhyolite (now a granophyre) and the mafic rock of the sill (Green and Miller, 2008). Whole rock and radioisotope geochemistry data also point to variable degrees of mixing and assimilation of the rhyolite and mafic sill (Ernst, 1960; Gardener, 1987; Jerde, 1991)

7. Discussion

7.1 Differences in $^{207}Pb/^{206}Pb$ and $^{206}Pb/^{238}U$ ages

Before delving into an interpretation of the age results from this study, it is important to discuss the current state of radiometric dating. Comparing age results from this study to previous studies is problematic, mostly due to improvements in analytical methods and recent questions regarding the accuracy of decay constants. As analytical uncertainties began to approach the uncertainty of the decay constants, workers sought to reassess the uranium decay constants. Schoene et al. (2006) tested a large volume of samples ranging in age from 0.1 to 3.3 Ga to evaluate this problem. To check for internal bias in the U-Pb system, high-n statistically equivalent datasets were analyzed from eleven different zircon populations. U-Pb ages of zircon from the eleven different samples consistently plotted below concordia (Fig. 7.1). It is highly unlikely that all the zircons experienced the same Pb-loss or intermediate daughter product disequilibria; therefore, Schoene et al. (2006) concluded the likely cause of the discordance is error within the decay constants determined by Jaffey et al. (1971).

In the Jaffey et al. (1971) experiments, four alpha-counting experiments on two separate batches of high-purity ^{238}U and two alpha-counting experiments on one batch of high-purity ^{235}U were conducted. While the experiments on ^{238}U were less precise than the ^{235}U experiments, the results agreed within error and exhibited no signs of drift or systematic errors. The ^{235}U experiments were different in that they exhibited an unknown source of systematic drift in the measurements. As a result, the ^{235}U values did not agree within error and a correction coefficient had to be applied. Schoene et al. (2006) proposed that the ^{235}U decay constant is likely inaccurate for these reasons, which is why $^{206}Pb/^{238}U$ ages do not agree with $^{207}Pb/^{206}Pb$ ages and cannot be accurately compared against each other.

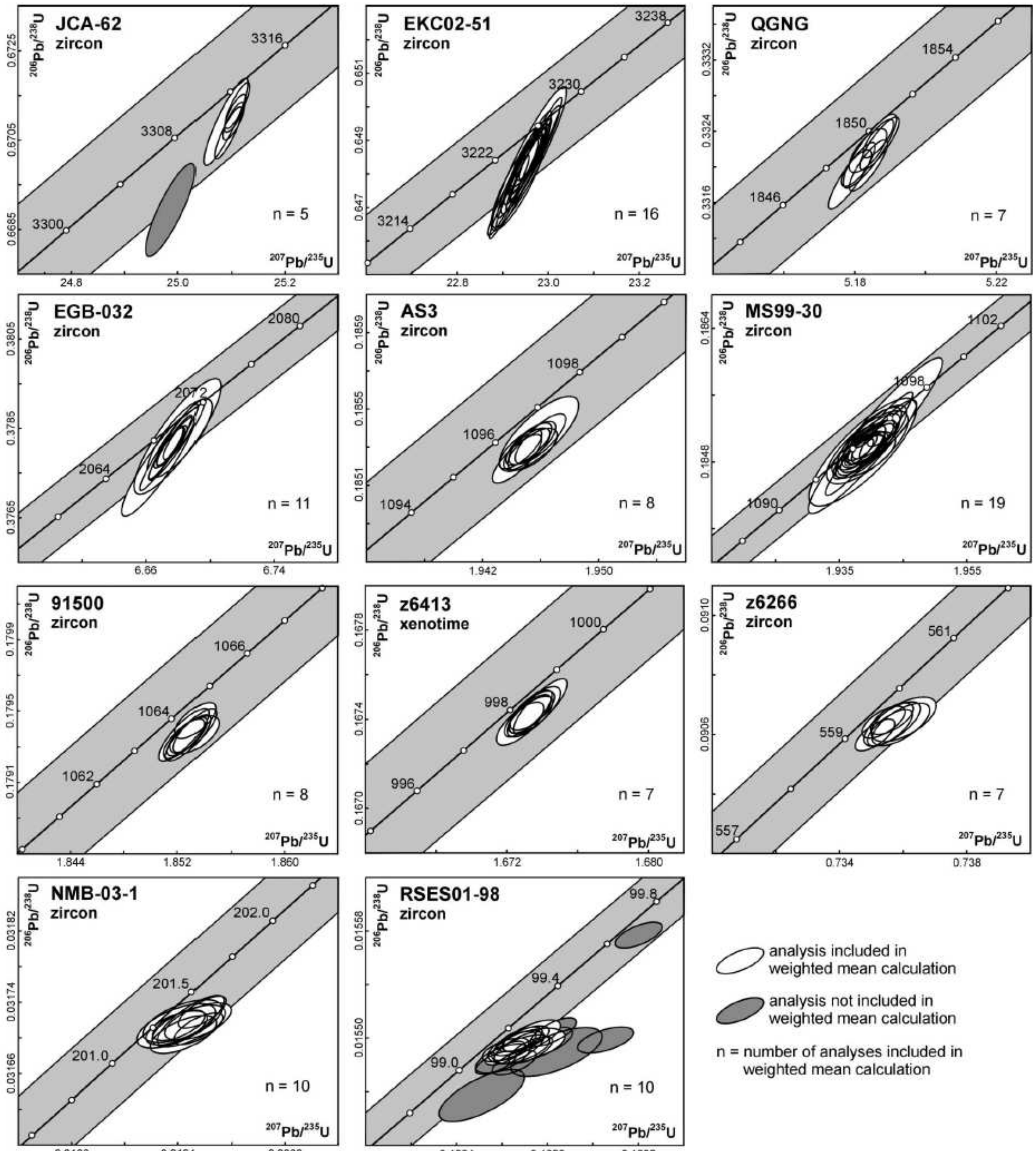

Figure 7.1. Figure of zircon concordia plots from grains ranging in age from 0.3 to 3.3 Ga. From Schoene et al. (2006)

The inaccuracy of the ^{235}U decay constant is the crux of the problem when comparing ages from this study to previous studies. Previous geochronologic studies of MCR samples used weighted mean $^{207}Pb/^{206}Pb$ ages in their analyses, since Pb-loss issues are minimized by using the upper-intercept of concordia as the crystallization age. As methods developed (specifically the annealing/chemical abrasion method of Mattinson (2005)), it has become possible to obtain very precise $^{206}Pb/^{238}U$ ages (.01% versus .04% for $^{207}Pb/^{206}Pb$ from the same sample), which are better for determining relative crystallization age. Absolute age is less important than relative age, thus the more precise weighted mean $^{206}Pb/^{238}U$ ages are desirable for comparing the ages of intrusions within this study. When comparing dates from intrusions from this study to intrusions of previous studies the less precise weighted mean $^{207}Pb/^{206}Pb$ ages are used in order to remain consistent with the reported dates.

7.2 Baddeleyite vs. Zircon

Since Davis and Sutcliffe (1985) successfully dated baddeleyite from the Logan diabase sills, workers have treated baddeleyite as an analogue to zircon. As more precise data sets have become available for zircon and baddeleyite from the same samples, it appears as though baddeleyite dates are not in direct agreement with those obtained from zircon. In baddeleyite analyses from some of the more precise studies of MCR rocks (e.g. Paces and Miller, 1993; Heaman et al., 2007), there appears to be a consistent discordance problem shifting baddeleyite data off concordia towards younger $^{207}Pb/^{235}U$ and $^{206}Pb/^{238}U$ ages. In addition, this has been recognized in the Tuscarora results from this study (Fig. 6.4), as well as an unpublished date from anorthositic series rocks (M. Schmitz, pers. comm., 2009; Fig. 7.2). The consistent discordance problem associated with baddeleyite could result from 1) Pb-loss on the outside of the grain that cannot be removed using annealing and abrasion because baddeleyite is too fragile; or 2) intermediate daughter product disequilibria (M. Schmitz, pers. comm., 2009). Schoene et al. (2006) suggested intermediate daughter product disequilibria, specifically ^{230}Th and ^{231}Pa, as a possible reason for the disagreement in $^{207}Pb/^{235}U$ and $^{206}Pb/^{238}U$ ages in zircon; however, they dismissed this as a possibility when datasets from zircon spanning ages from 0.1 to 3.3 Ga showed the same systematic errors. While it appears that intermediate daughter product disequilibria is not a problem in zircon, it could be an issue in baddeleyite.

One possibility for the apparent older $^{207}Pb/^{235}U$ ages in baddeleyite proposed by Schmitz and Crowley (personal correspondence, 2009) could be the preferential incorporation of pentavalent ^{231}Pa in the baddeleyite crystal lattice. Since ^{231}Pa is in the ^{235}U decay chain, it would ultimately decay to ^{207}Pb and create an apparent older $^{207}Pb/^{235}U$ age. While Pb-loss is clearly an issue in baddeleyite analyses, the issue of intermediate daughter product disequilibria has not yet been adequately evaluated and more work is needed to address this possibility.

Regardless of the reason, it is clear that precise baddeleyite and zircon analyses do not give consistent results. Zircon and baddeleyite from the same sample, FC-4b (Fig. 7.2), have different relative crystallization ages. The weighted mean $^{207}Pb/^{206}Pb$ age from the baddeleyite is nearly one million years older than the zircon age, which suggests that perhaps either an excess of ^{207}Pb exists in the system, or the grain experienced some amount of Pb-loss. In addition, the ^{206}Pb/^{238}U age for baddeleyite is younger outside of error than the zircon age, which would be expected if the grain experienced some minor Pb-loss. It is for these reasons that caution must be taken when comparing baddeleyite ages to zircon ages.

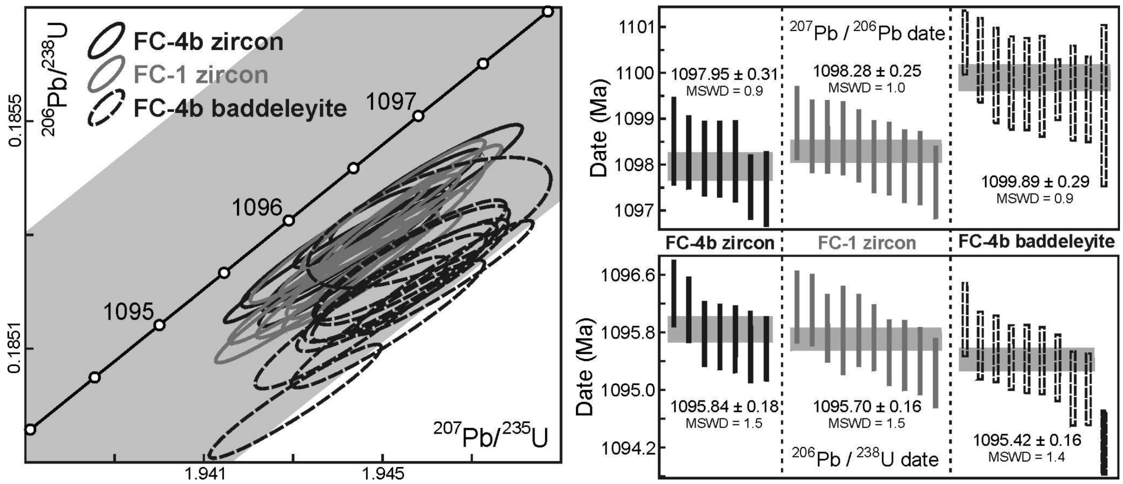

Figure 7.2. Concordia plot for zircon FC1, FC4b, and baddeleyite FC4b. Sample FC-1 and FC-4b are from the same general location of gabbroic anorthosite as FC-1 from Paces and Miller (1993). Plot from by J. Crowley, Boise State Isotope Geology laboratory.

7.3 Relative Ages of Layered Series Intrusions

One of the principle objectives of this study is to determine whether the sequence of emplacement of layered series intrusions implied by field and geophysical evidence can be verified by precise dating. Comparing the ^{207}Pb/^{206}Pb ages from Paces and Miller (1993) and this study (Fig. 7.3, Table 7.1), it appears as though most intrusions from the layered series are indistinguishable within error. The Bald Eagle intrusion (BEI), which appears to be one of the youngest layered series intrusions, has a ^{207}Pb/^{206}Pb age of 1097.97 ± 0.72 Ma, which is indistinguishable from both the Partridge River intrusion

(PRI-1097.98 ± 0.37 Ma) and the Tuscarora intrusion (TI-1098.81 ± 0.32 Ma) (Fig. 7.4). The more precise $^{206}Pb/^{238}U$ dates from BEI and PRI are similarly indistinguishable within a narrow range of maximum error from 1096.12 Ma to 1095.45 Ma, respectively (Fig.7.5, Table 7.1). The extremely narrow time interval of overlap for these two intrusions and others implies that the bulk of layered series intrusive activity occurred over a 670 thousand year period.

The slightly older $^{207}Pb/^{206}Pb$ age for the Tuscarora intrusion (TI) from the northwestern margin of the Duluth Complex compared to the Partridge River intrusion from the central Duluth Complex margin (1098.81 ± 0.32 vs. 1097.98 ± 0.37 Ma, respectively) is suspect given that the Tuscarora age comes from baddeleyite, whereas the Partridge River age is from zircon. Because of the potential differences in the zircon and baddeleyite U-Pb geochronology systematics discussed above, it is difficult to directly compare the two results. The approximately 1 Ma age difference is similar to that observed for baddeleyite and zircon from the FC-4b sample analyzed by Schmitz (unpublished data). While it would be hard to definitively say that the Tuscarora intrusion was emplaced prior to the Partridge River intrusion in light of new information regarding the differences in zircon and baddeleyite ages, it is reasonable to assume that the two intrusions were emplaced at approximately the same time. Direct geochronologic support cannot be given; however, until the differences in the zircon and baddeleyite systems are more fully understood.

The Duluth Layered Series dated by Paces and Miller (1993) and Green et al., (2001) has a significantly older $^{207}Pb/^{206}Pb$ age (D-1=1099.3 ± 0.3 Ma; DLS=1098.9± 1.4

Ma, respectively) than both the Partridge River intrusion and the Bald Eagle intrusion (1097.98 ± 0.37 and 1097.97 ± 0.72 Ma, respectively). This seems to contradict the emplacement model which predicts that the DLS should be relatively young and approximately equivalent to the Bald Eagle in the sequence of emplacement. However, the two DLS samples are from the upper part of the well differentiated intrusion, which is rich in gabbroic anorthosite inclusions that were evidently derived from the overlying anorthositic series (Miller and Green, 2008). It therefore seems plausible, as suggested by Green (2001), that the DLS samples may have inherited zircons from the anorthositic series, which has a similar age of 1099.1 ± 0.2 Ma (AS-3 revised, Schmitz et al., 2003). It was this possibility that motivated sampling of the lower section of the DLS for this study. Unfortunately, no dateable material was recovered from the sample taken.

Weighted mean $^{207}Pb/^{206}Pb$ zircon ages imply that both the Partridge River and Bald Eagle intrusions are generally younger than anorthositic series samples dated by Paces and Miller (1993) - FC1, AS3, and PG2 (Fig. 7.4); however, re-dating of sample FC-1 and a nearby sample FC-4 by the Boise State Isotope Lab (Schmitz, unpublished data) imply more coeval ages. Furthermore, precise $^{206}Pb/^{238}U$ dates (Fig. 7.5) show a clear contemporaneity between layered series and anorthositic series ages. These results provide further evidence for the near synchronous emplacement of not only individual layered series intrusions, but also formation of the extensive anorthositic series and the layered series.

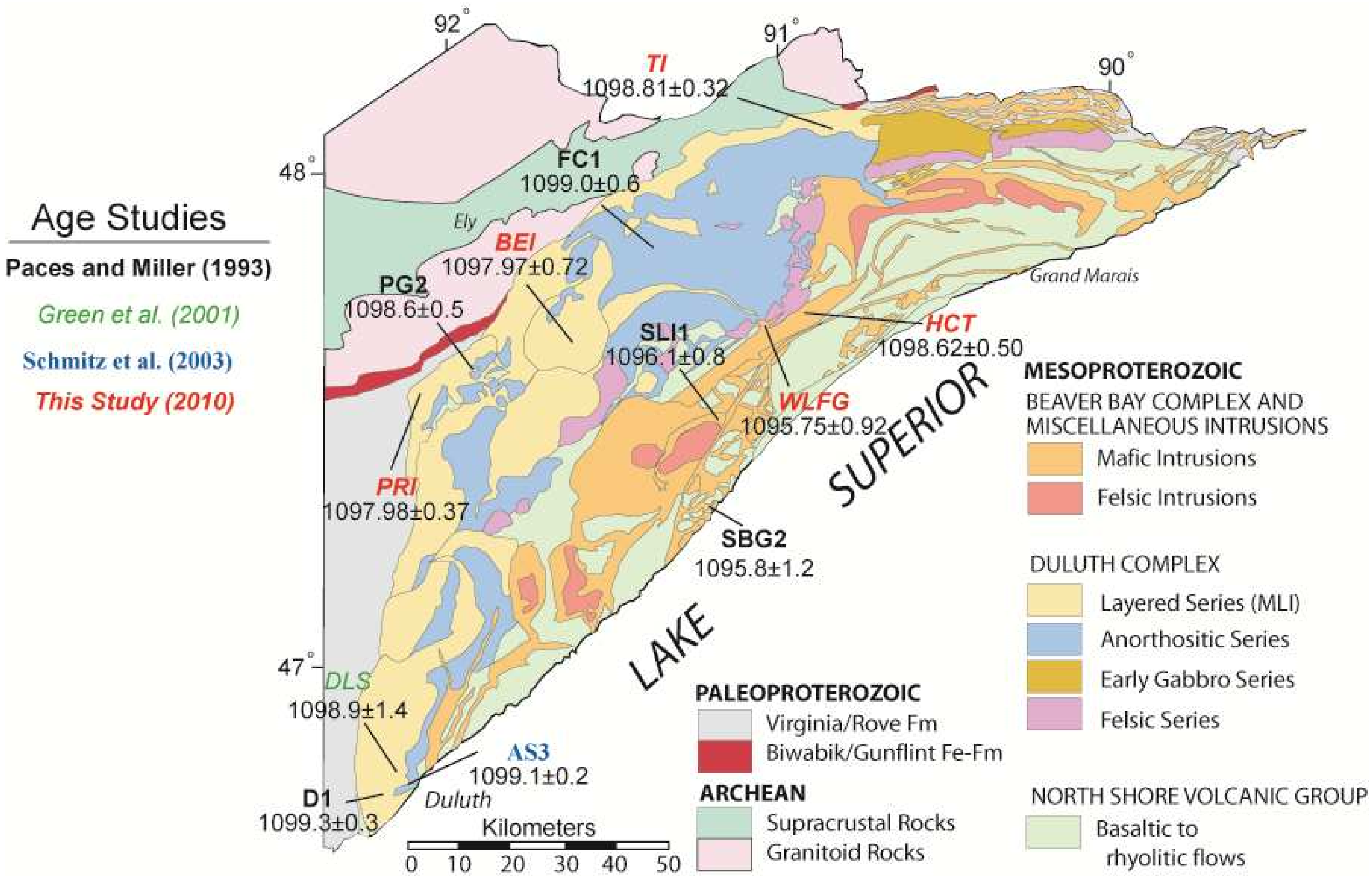

Figure 7.3. Summary of $^{207}Pb/^{206}Pb$ ages for intrusions related to the Duluth Complex and Beaver Bay Complex (modified from Miller and Severson, 2002)

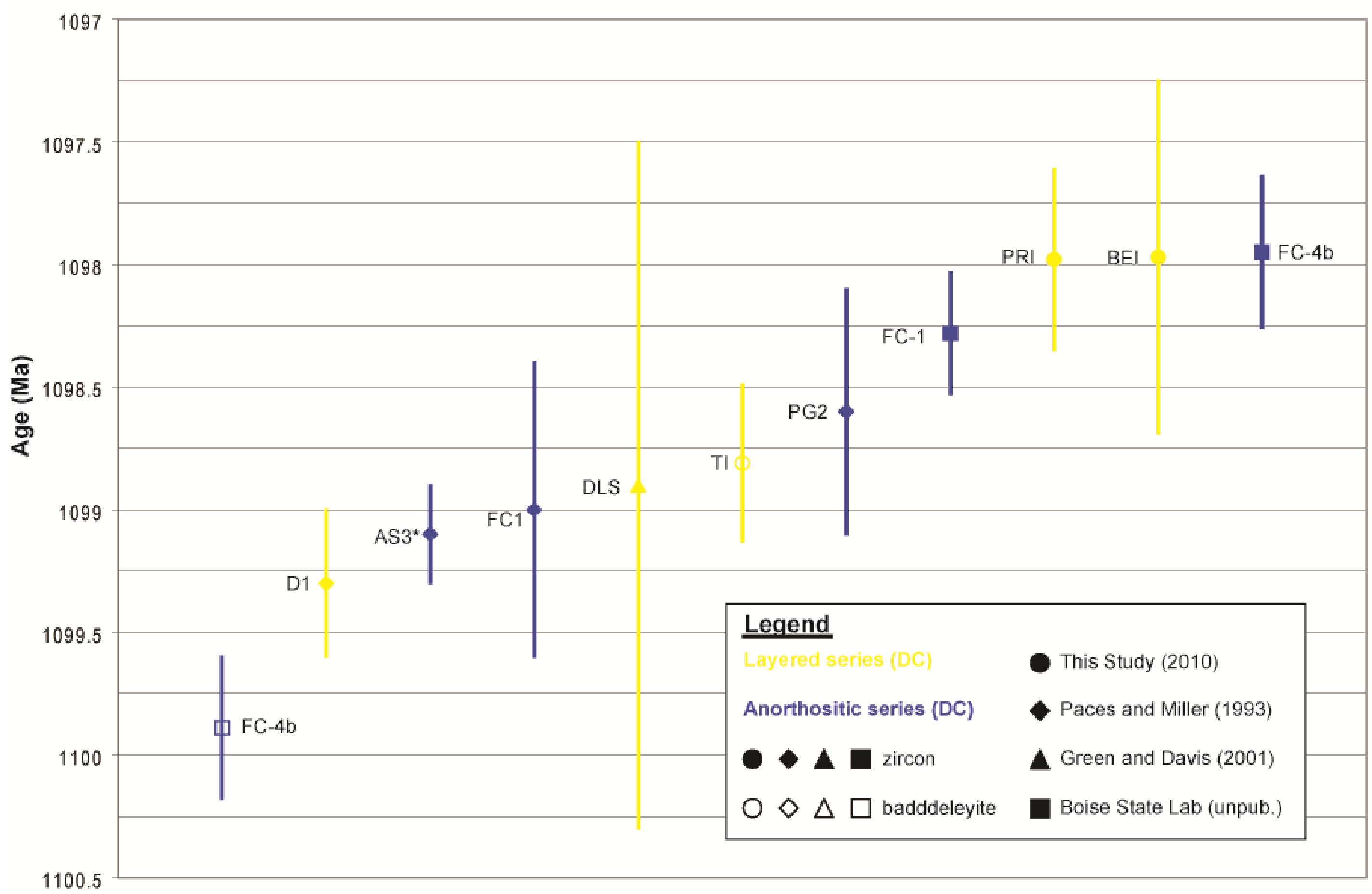

Figure 7.4. $^{207}Pb/^{206}Pb$ weighted mean ages for layered series and anorthositic series intrusions dated for this study. Boise State Isotope Geology Laboratory Anorthositic Series ages are unpublished. *revised date from Schmitz et al. (2003)

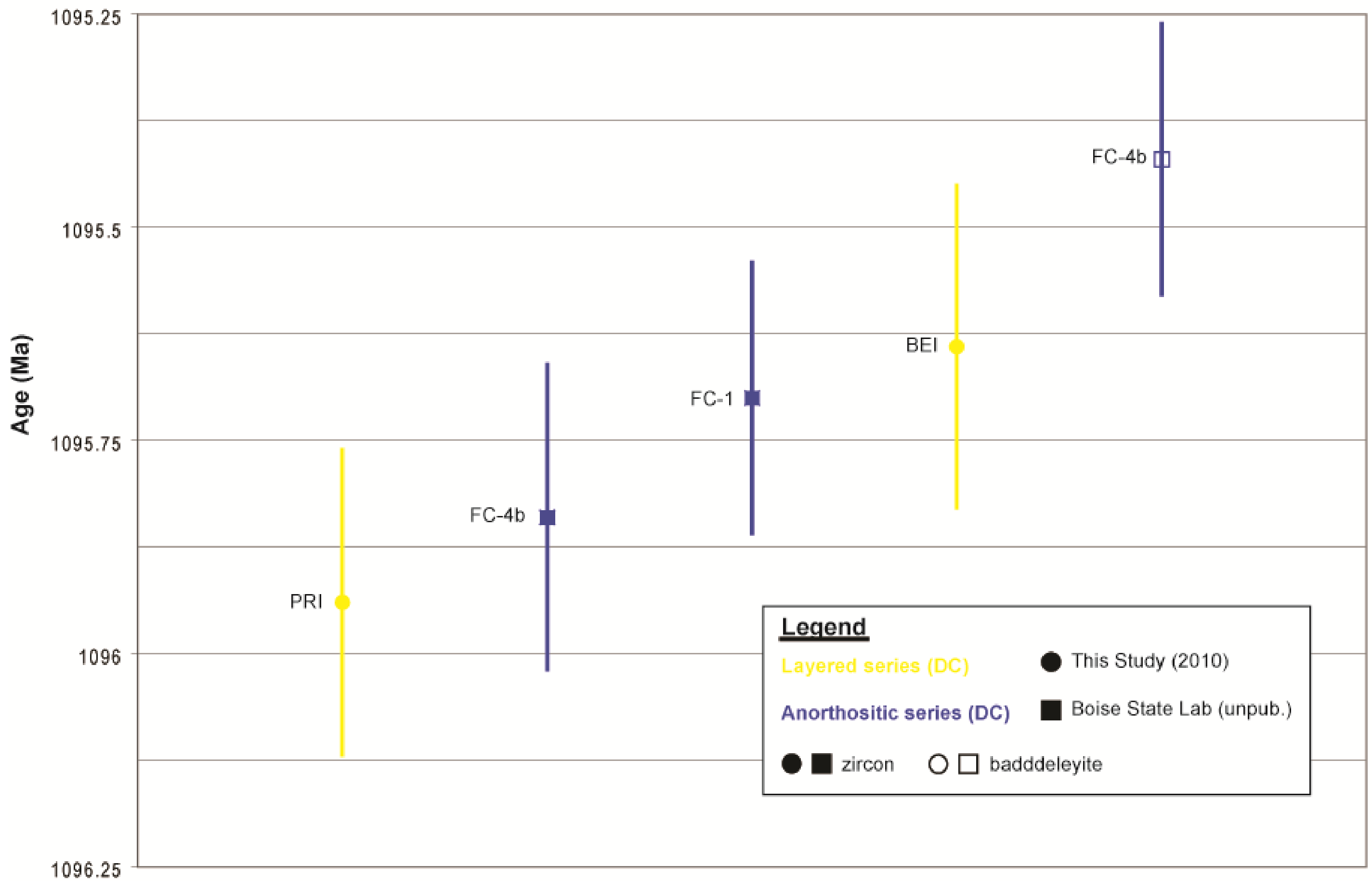

Figure 7.5. $^{206}Pb/^{238}U$ weighted mean ages for layered series and anorthositic series intrusions dated for this study. Anorthositic series ages are unpublished dates from the Boise State Isotope Geology Laboratory.

Table 7.1. Summary of U-Pb ages obtained for samples from the layered series and anorthositic series of the Duluth Complex (DC) and from the Beaver Bay Complex (BBC)

Sample Name	Intrusive Unit	Rock Type	Grains	$^{207}Pb/^{206}Pb$ age	$^{206}Pb/^{238}U$ age
$WLFG_a$	late BBC	ferrogabbro	zrc./badd.	1095.75 ± 0.92	1091.88 ± 0.35
$SBG2_c$	late BBC	granophyric ferrogabbro	zircon	1095.8 ± 1.2	not defined
$SLI1_c$	middle BBC	apatite ferrodiorite	baddeleyite	1096.1 ± 0.8	not defined
FC-4b_b	anorthositic series (DC)	olivine gabbroic anorthosite	zircon	1097.95 ± 0.31	1095.84 ± 0.18
BEI_a	late layered series (DC)	olivine gabbro	zircon	1097.97 ± 0.72	1095.64 ± 0.19
PRI_a	early layered series (DC)	augite troctolite	zircon	1097.98 ± 0.37	1095.94 ± 0.18
FC-1_b	anorthositic series (DC)	olivine gabbroic anorthosite	zircon	1098.28 ± 0.25	1095.70 ± 0.16
$PG2_c$	anorthositic series (DC)	troctolite	zircon	1098.6 ± 0.5	not defined
HCT_a	early BBC	augite troctolite	zircon	1098.62 ± 0.50	1095.31 ± 0.25
TI_a	early layered series (DC)	troctolite	baddeleyite	1098.81 ± 0.32	not defined
$FC1_c$	anorthositic series (DC)	olivine gabbroic anorthosite	zircon	1099.0 ± 0.6	not defined
AS3*$_e$	anorthositic series (DC)	gabbroic anorthosite	zircon	1099.1 ± 0.2	not defined
$D1_c$	late layered series (DC)	olivine ferrogabbro	zircon	1099.3 ± 0.3	not defined
FC-4b_b	anorthositic series (DC)	olivine gabbroic anorthosite	baddeleyite	1099.89 ± 0.29	1095.42 ± 0.16

a-this study; b-Boise State Isotope Geology Lab; c-Paces and Miller (1993); d-Green et al. (2001), e-Schmitz et al. (2003)

7.4 Overlap of Duluth Complex and Beaver Bay Complex Magmatism

One of the unrealized objectives of the Paces and Miller (1993) study was to determine the oldest emplacement age of the multiply-intruded Beaver Bay Complex. In attempt to establish this lower limit, samples were collected from the Houghtaling Creek troctolite and the Wilson Lake ferrogabbro intrusions in the northern Beaver Bay Complex (Miller and Chandler, 1997). Detailed geologic mapping in the area (Miller et al. 1994; Boerboom and Miller, 1994) interpreted the Wilson Lake ferrogabbro to be one of the earliest intrusions and the Houghtaling Creek troctolite to be somewhat younger, but still an early Beaver Bay event. Therefore, one of the surprises of this study is that the Houghtaling Creek troctolite has a very Duluth Complex-like $^{207}Pb/^{206}Pb$ age of 1098.62 ± 0.50 Ma (Fig. 7.6). Even more surprising, the Wilson Lake ferrogabbro, which based on aeromagnetic and sparse outcrop data appears to be truncated and overlain by the Houghtaling Creek troctolite, is significantly younger with a $^{207}Pb/^{206}Pb$ age of 1095.75 ± 0.92 Ma (Fig. 7.7). This age falls in line with other Beaver Bay ages determined by Paces and Miller (1993; Sonju Lake intrusion - 1096.1 ± 0.8; Silver Bay intrusions - 1095.8 ± 1.2Ma). More precise $^{206}Pb/^{238}U$ ages also support these conclusions, as the Houghtaling Creek troctolite is notably older than the Wilson Lake ferrogabbro and indistinguishable in age from the layered series and anorthositic series intrusions of the Duluth Complex (Fig. 7.8). These results have important implications for the overlap and periodicity of intrusive magmatism that formed the Beaver Bay Complex. While they answer some questions about the overlap of magmatism between Duluth and Beaver Bay complexes, they disprove several previous interpretations about the relative ages of specific BBC intrusions, and leave questions about the periodicity of Beaver Bay magmatism unresolved.

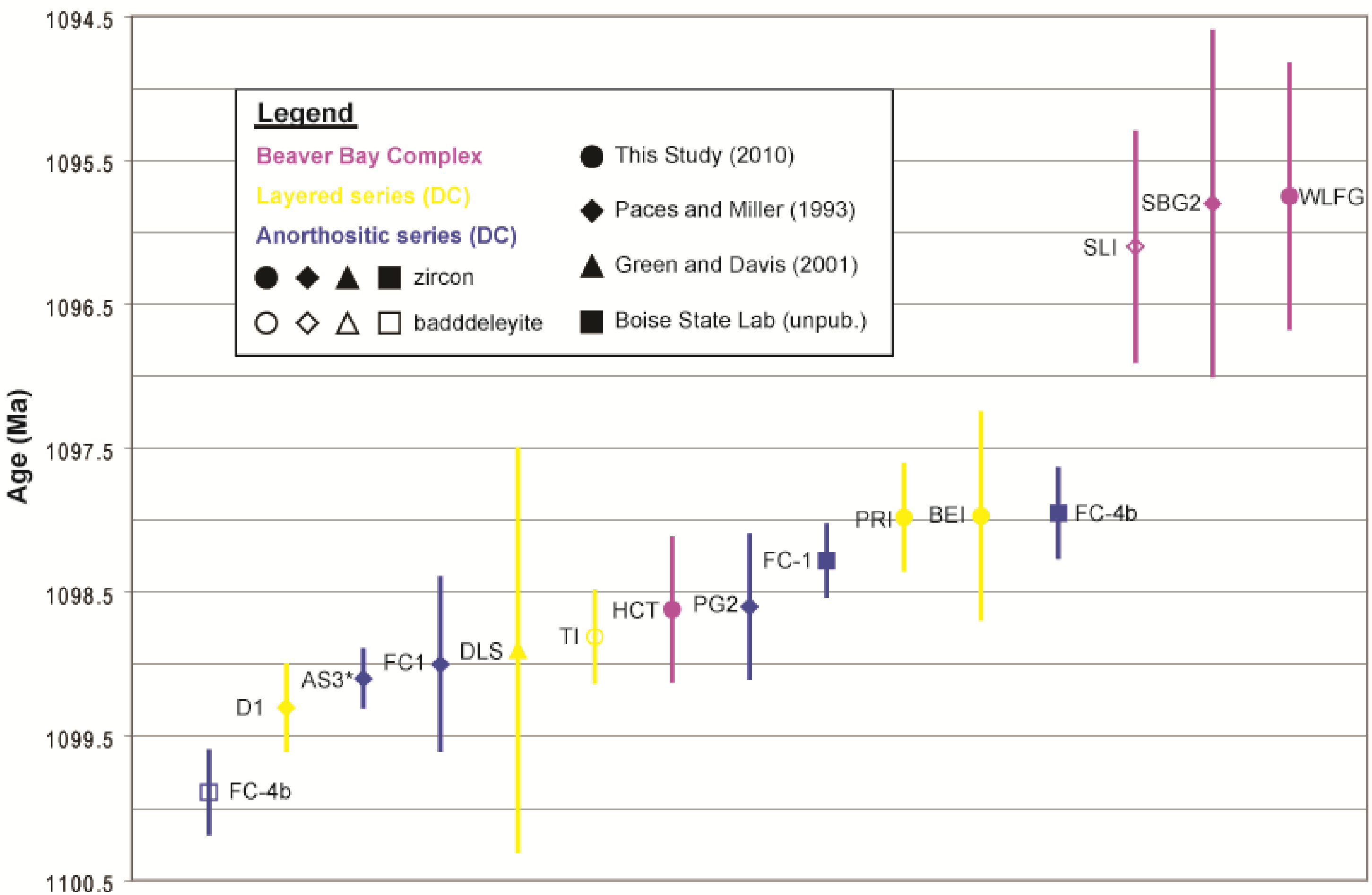

Figure 7.6. $^{207}Pb/^{206}Pb$ weighted mean ages for samples from layered series and anorthositic series intrusions of the Duluth Complex and Beaver Bay Complex intrusions dated for this study. Anorthositic series ages are unpublished dates from the Boise State Isotope Geology Laboratory.

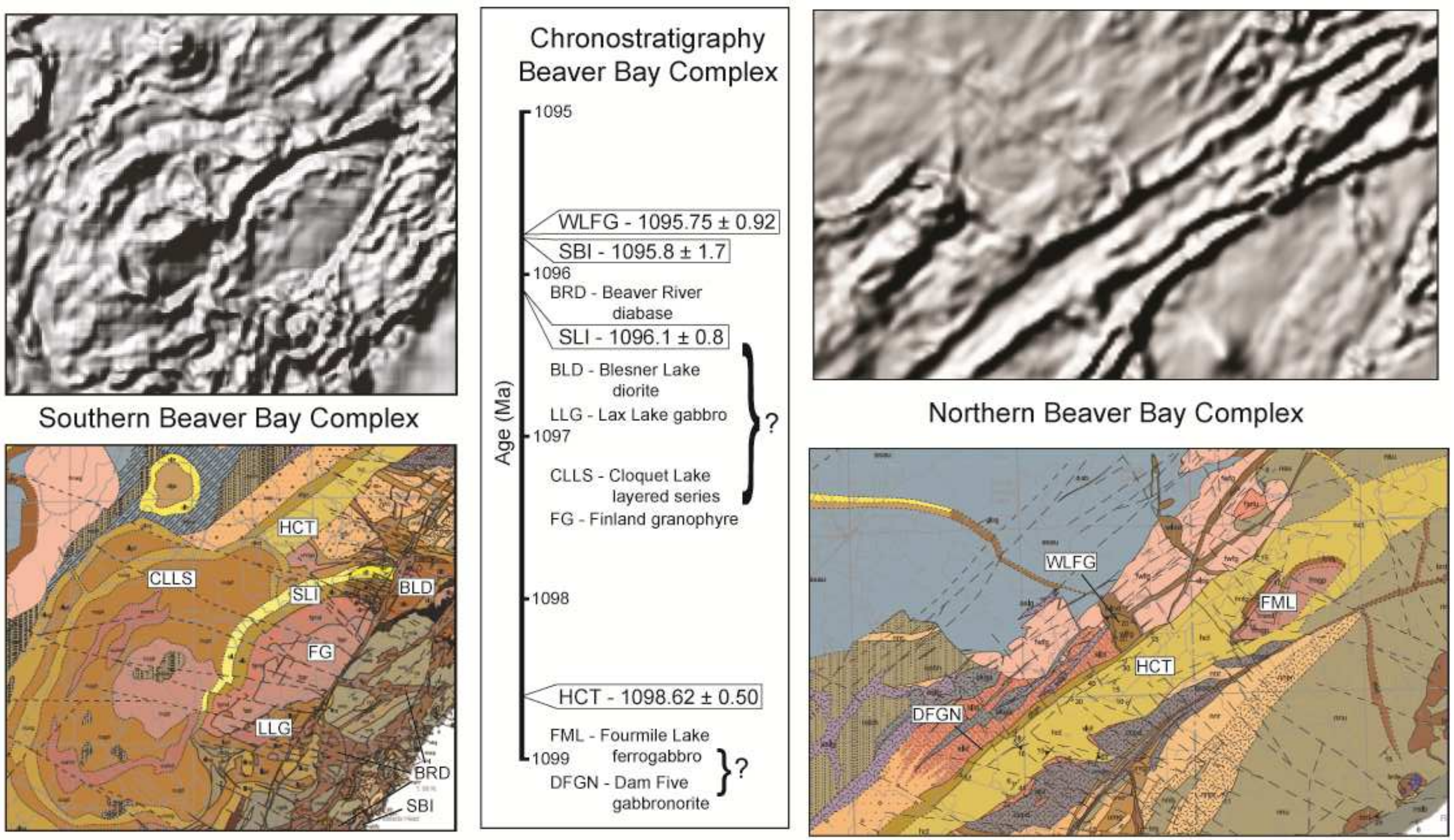

Figure 7.7. Shaded-relief total magnetic field images along with corresponding geologic maps of the southern and northern Beaver Bay Complex as portrayed on map M-119(Miller et al., 2001). Also shown is a chronostratigraphic column for intrusions of the BBC. Each pair of magnetic field data and geologic map is presented at approximately the same scale. The aeromagnetic image of the southern Beaver Bay Complex is modified from Miller and Green (2002) and the image of the northern Beaver Bay Complex was provided by Dean Peterson.

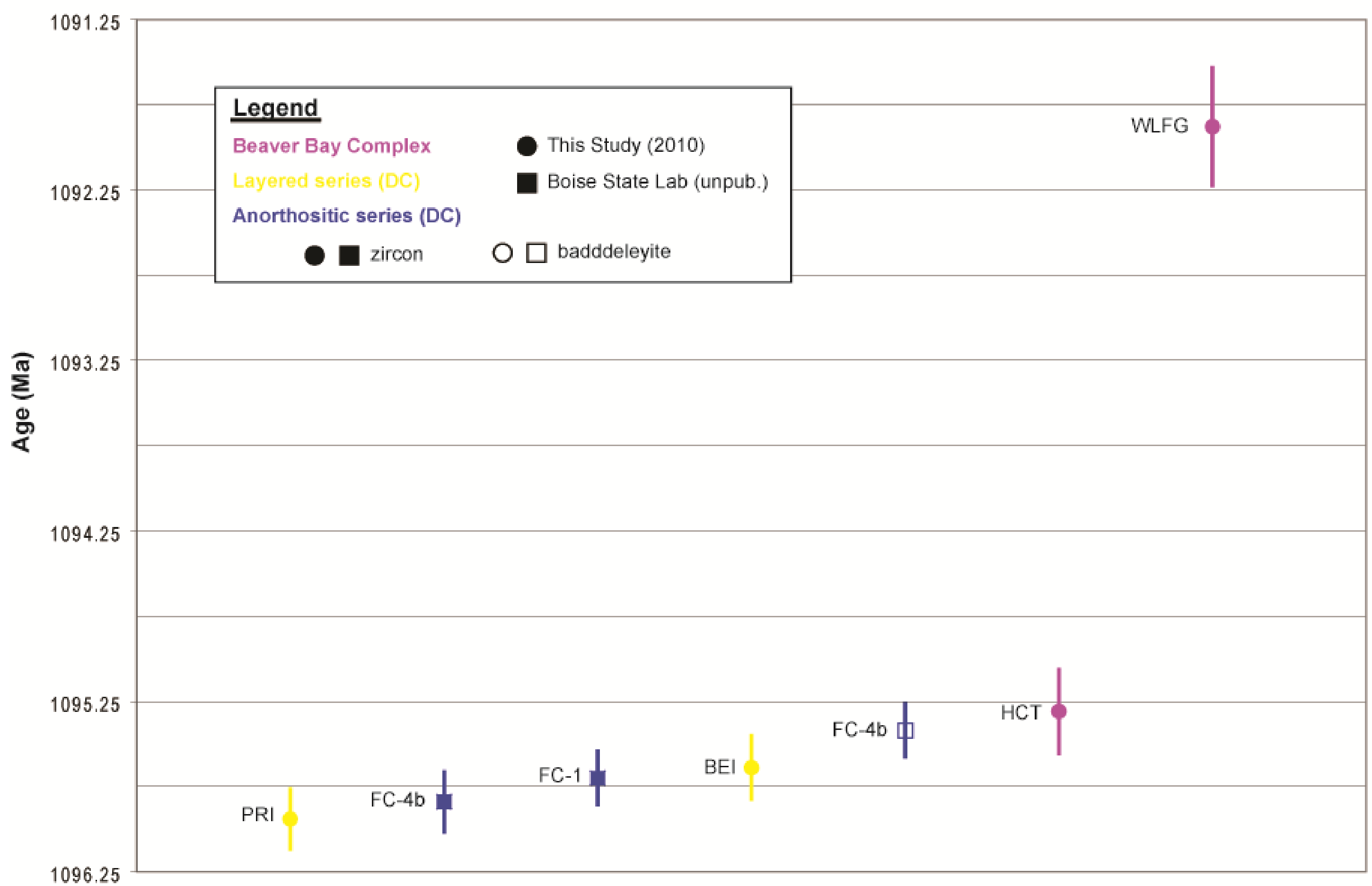

Figure 7.8. $^{206}Pb/^{238}U$ weighted mean ages for layered series and anorthositic series intrusions, and Beaver Bay Complex intrusions dated for this study. Anorthositic Series ages are unpublished dates from the Boise State Isotope Geology Laboratory.

The realization that the Wilson Lake ferrogabbro is substantially younger than the Houghtaling Creek troctolite would seem to contradict the field relationships inferred from mapping by Boerboom and Miller (1994). In the Wilson Lake area (Fig. 7.9), they show the Dam Five gabbronorite and the Houghtaling Creek troctolite as cross-cutting the Wilson Lake ferrogabbro. They interpret the gabbronorite as an earlier intrusion into the same northeast-trending conduit that was later intruded by the troctolite. Although not seen in contact, the northeasterly strike of the well foliated Dam Five gabbronorite appears to continue unabated across the contact with the Wilson Lake ferrogabbro, which has foliation and layering trending to the northwest. According to Miller (pers. communication), this apparent discordancy and the very prominent and linear aeromagnetic anomaly pattern of the northwestern margin of the Houghtaling Creek troctolite (Fig. 7.7) led to the conclusion that Dam Five gabbronorite and the Houghtaling Creek troctolite cross-cut the Wilson Lake ferrogabbro. The unequivocal ages now show that interpretation is incorrect.

Given the U-Pb ages, a more likely scenario is that the Houghtaling Creek troctolite and perhaps the Dam Five gabbronorite contact, which dips moderately (15-45°) to the southeast based on foliation and layering, served as the hanging wall to the later intrusion of the Wilson Lake ferrogabbro. Also, given that there is no outcrop of the Dam Five gabbronorite in the contact zone, it is possible that the Wilson Lake ferrogabbro actually cuts out part of the gabbronorite as shown in Figure 7.9. Although the young age for the Wilson Lake ferrogabbro has compelled a major reinterpretation of its relationship to adjacent units, its age actually makes sense, given its evolved composition. The $^{207}Pb/^{206}Pb$ age of 1095.75 ± 0.92 Ma of the Wilson Lake ferrogabbro is remarkably similar to the 1095.8 ± 1.2 Ma age of a Silver Bay gabbro intrusion dated by Paces and Miller (1993). The Silver Bay intrusions, which are known from well-exposed field relationships near the Lake Superior shoreline (e.g., Miller, 1988; Miller et al., 1989) to be the youngest intrusions in the Beaver Bay Complex, are a collection of small zoned intrusions emplaced into Beaver River diabase.

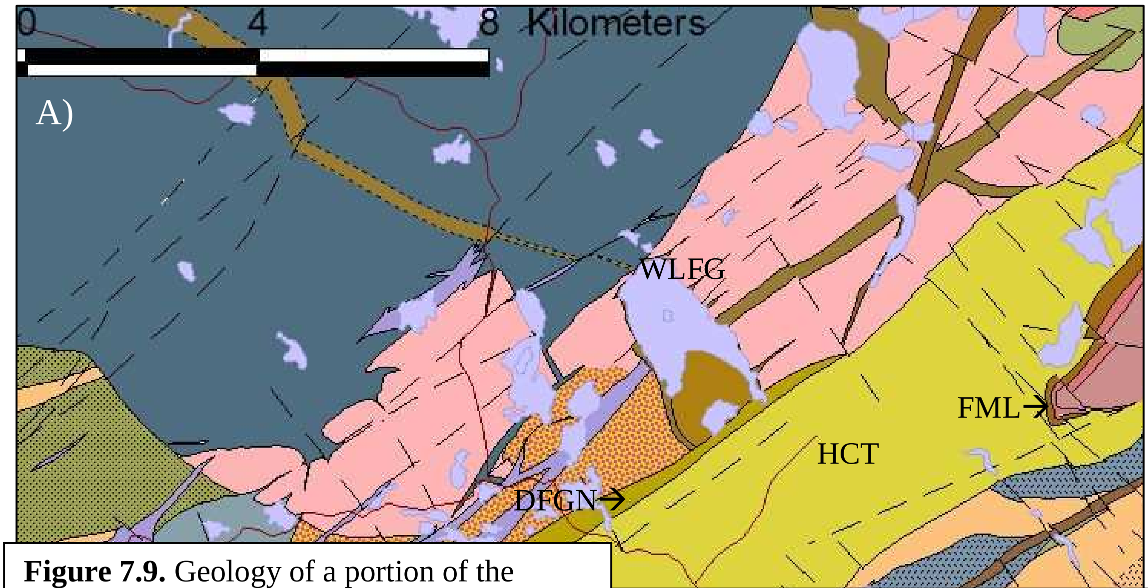

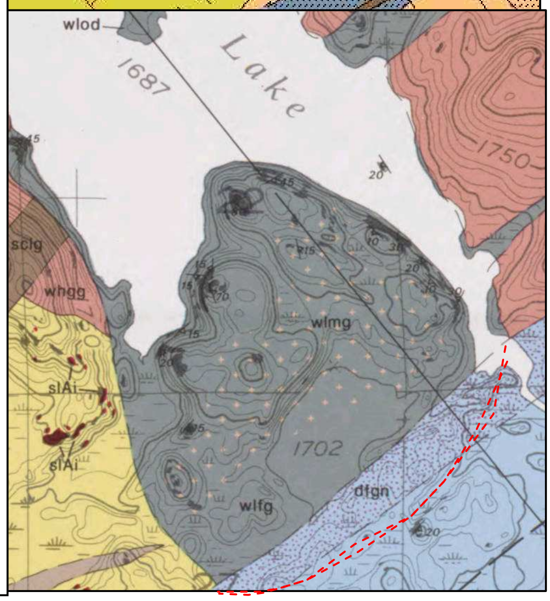

Figure 7.9. Geology of a portion of the Wilson Lake area showing the Houghtaling Creek troctolite (HCT), Wilson Lake ferrogabbro (WLFG), Dam Five gabbronorite (DFGN), and Fourmile Lake gabbro (FML). A) Portion of the regional 1:100,000) M-119 map (Miller et al., 2001). B) Part of the 1:24,000 scale map of the Silver Island, Wilson Lake, and Toohey Lake quadrangles (Boerboom and Miller, 1994). The red dashed line shows a permissible dfgn-wlfg contact that is more consistent with the younger age of the WLFG

The Silver Bay intrusions are typically cored by foliated ferrogabbroic to ferromonzodioritic cumulates with coarse-grained ferromonzonitic to melanogranophyric lithologies at the margins (Miller and Chandler, 1997). This is exactly the distribution of lithologies found in the Wilson Lake ferrogabbro intrusion (Boerboom and Miller, 1994), and suggests a possible genetic link.

Another implication of the young age for the Wilson Lake ferrogabbro is that it discounts the speculation by Miller and Severson (2002, p. 139) of a genetic link between the WLFG and the Greenwood Lake intrusion of the Duluth Complex. They interpreted a narrow aeromagnetic anomaly pattern than can be traced from the northwestern margin of the Wilson Lake ferrogabbro (Figs. 7.7, 4.1) to the west, where it widens and seems to project into the northeastern extent of the anomaly associated with the Greenwood Lake intrusion. With the Greenwood Lake intrusion evidently cut by the 1098 Ma (^{207}Pb/^{206}Pb age) Bald Eagle intrusion (again an interpretation of aeromagnetic anomaly patterns, Miller and Severson, 2002), the Greenwood Lake is by implication, significantly older than the Wilson Lake and therefore cannot be genetically linked.

Yet another geologic interpretation disproven by the results of this study pertains to the Fourmile Lake gabbro, which occurs as a large inclusion of strongly differentiated layered gabbro to ferromonzonite within the Houghtaling Creek troctolite (Figs. 7.7, 7.9). Boerboom and Miller (1994) note a sharp compositional break between the troctolite and the least differentiated portions of the Fourmile Lake gabbro, and conclude that it did not differentiate in situ. They propose that the Fourmile Lake gabbro is a detached portion of either the Wilson Lake ferrogabbro, or the Dam Five gabbronorite. The result of this study now reveals that the Fourmile Lake gabbro is not related to the Wilson Lake ferrogabbro. It is still possible that the Fourmile Lake gabbro could have detached from the Dam Five gabbronorite, or from some unexposed intrusion from within the crust.

Finally, Miller and Chandler (1997) had speculated that the Houghtaling Creek troctolite and Sonju Lake intrusion may be genetically linked. They noted that the troctolite of the Houghtaling Creek troctolite is similar to the troctolitic section of the Sonju Lake intrusion in composition, mode and texture. Miller and Chandler (1997) suggested that the keel-shaped Houghtaling Creek troctolite might represent the dike-like conduit that fed the sill-shaped Sonju Lake intrusion to the south (Fig. 7.9). However, the 1098.62 ± 0.50 Ma $^{207}Pb/^{206}Pb$ age of the Houghtaling Creek troctolite determined by this study is significantly older than the 1096.1 ± 0.8 Ma age found by Paces and Miller (1993) for the Sonju Lake intrusion, thus disproving a possible link.

7.5 Periodicity of Main Stage MCR Magmatism

The results presented here still leave open questions about the periodicity of Beaver Bay magmatism and of intrusive magmatism in northeastern Minnesota as a whole. The current database provides reinforcing evidence for an approximate 2.5 Ma gap (based on $^{207}Pb/^{206}Pb$ ages) in intrusive activity during the main stage of MCR magmatism that was noted by the Paces and Miller (1993) study. A clear bimodal distribution of ages are now defined by Duluth Complex (and now early Beaver Bay Complex) intrusions at ~1098 Ma and late Beaver Bay intrusions ~1096 Ma (Figs. 7.6, 7.8). There are many other intrusions, however, within the Beaver Bay Complex that were evidently emplaced between the intrusion of the Houghtaling Creek troctolite (1098.62 ± 0.50 Ma, this study) and the next youngest dated intrusion - the Sonju Lake intrusion (1096.1 ± 0.8 Ma, Paces and Miller, 1993). Until these intrusions are dated, it will remain unclear whether this ~2.5 Ma gap is real or a phantom of the available data.

Detailed mapping in the southern and northern Beaver Bay Complex (Fig. 7.9; Miller, 1988; Miller et al., 1989; Miller et al., 1993; Miller et al., 1994; Boerboom and Miller, 1994; and Miller et al., 2006) imply that several intrusive suites occur between the emplacement of the Houghtaling Creek and Sonju Lake intrusions. These include the Finland granite, the Lax Lake gabbro, Blesner Lake diorite, and the Upper Manitou River gabbro (Fig. 7.7). The mafic components of these suites were termed the early gabbroic intrusions by Miller and Chandler (1997). Based on their similar compositional characteristics, they interpreted the early gabbroic intrusions to be comagmatic and at one point part of a continuous intrusive suite before becoming dismembered by younger intrusions of the Sonju Lake Intrusion and the Beaver River diabase dikes and sills (SLI and BRD, respectively, Fig. 7.7). Miller and Chandler (1997) further speculated that the largely buried Cloquet Lake layered series (CLLS, Fig. 7.7) is also correlative with the early gabbroic intrusions and actually is the original composite intrusion from which the other suites (LLG, BLD, and UMRG, Fig. 7.7) were dismembered.

The Finland granite was dated by Vervoort et al. (2007), who report a $^{207}Pb/^{206}Pb$ age of 1098.2±5.5 Ma. Unfortunately, the poor resolution of this date precludes using it to assess where the Finland granite fits in the BBC emplacement history. It is clear that the granophyric Finland granite predates the emplacement of the Sonju Lake intrusion and likely caused the Sonju's underplating by acting as a density barrier (Miller and Ripley, 1996). The Finland granite is evidently younger than the early gabbroic intrusions as it is found in sharp contact with the Lax Lake gabbro (Miller et al., 1993). Miller and Chandler (1997) suggested that a transgressive granophyric granite occurring in the Blesner Lake diorite intrusive suite and granophyric granites intersected in core in the Cloquet Lake layered series may also be correlative with the Finland granite, and like the early gabbro intrusions, were dismembered by the intrusion of the Sonju Lake intrusion and the Beaver River diabase.

Paces and Miller (1993) attempted to date the early gabbro intrusions by selecting a sample from the Lax Lake gabbro (LLG3). However, the five zircon fractions produced old and ambiguous ages, which the authors attributed to inheritance from an older source, Pb loss, or both. Until an age from one of the early gabbro intrusions is successfully obtained, the question of whether the apparent 2.5 Ma gap in intrusive magmatism is real or imagined remains unresolved.

7.6 Age of Endion Sill

Because of the inability to obtain an accurate age for the Endion sill, it remains unclear when this hypabyssal intrusion was emplaced into the subvolcanic pile. Several zircons yield discordant $^{206}Pb/^{238}U$ ages of 1132.69 ± 1.74 Ma, 1177.15 ± 1.50 Ma and 1043.72 ± 1.02 Ma, making it impossible to determine when this hypabyssal intrusion was emplaced. Curiously, the $^{206}Pb/^{238}U$ age for one of the more euhedral grains was 2654.82 ± 15.56 Ma. This Archean age may indicate the age of the source rock that partially melted to generate the Tischer Creek rhyolite flow, under which the Endion sill intruded. The inherited/contaminated zircon ages of the Endion sill are consistent with field and geochemical evidence for its strong contamination by the rhyolite flow which it underplated, partially melted, and assimilated (Ernst, 1960; Jerde, 1991). Unfortunately, underplating of subvolcanic mafic sill beneath rhyolite flows is common in the North Shore Volcanic Group (Miller and Green, 2002). Further attempts to find uncontaminated dateable samples from the Endion and related sills should probably focus on the lower mafic portions of these sheets. Until then, their age relationships to Duluth Complex and Beaver Bay Complex magmatism will remain unknown.

7.7 Rate of Emplacement of Layered Series Intrusions

The inability to differentiate between the various layered series intrusions has significant implications for the duration and timing of its emplacement. By using the $^{206}Pb/^{238}U$ dates for the Partridge River intrusion and Bald Eagle intrusion analyzed in this study as a time bracket for layered series emplacement, it appears as though the bulk of the layered series was emplaced over a period of less than one million years (Fig. 7.4). A reasonable estimate of the volume of mafic magma emplaced during the layered series can be obtained by dividing the layered series intrusion areas into three simplified sections, projecting them to depth using internal structure, inferring their areal extent by the limits of the gravity data of Chandler (2002), and using simple trigonometric relationships to obtain the intrusion thickness and volume (Fig. 7.10). Based on these estimates, it appears that at a minimum, 16,000 km^3 of mafic magma intruded during the emplacement of layered series alone (Table 7.2). This volume estimate is even more remarkable knowing that it does not take into account unknowable amounts of erosion or magmatism creating the anorthositic series and early Beaver Bay Complex.

Emplacement rates can be calculated by using the time interval between Partridge River and Bald Eagle intrusion obtained in the current study and the volume estimation calculation. With over 16,000 km^3 of mafic magma being intruded over a period of approximately 670 thousand years (the maximum error window of PRI and BEI ages), the emplacement rates were at least 0.024 km^3/yr. This is similar to extrusion rates of 0.02 to 0.05 km^3/yr calculated by Davis and Paces (1990) for the Copper City Flow-Greenstone Flow interval on the Keweenaw Peninsula and Isle Royale. These rates are consistent with or less than other extrusion rates reported for continental flood basalt provinces such as the Siberian Traps (~3 km^3/yr - Courtillot and Renne, 2003; Renne and Basu, 1991), the Deccan Traps (~2 km^3/yr - Courtillot and Renne, 2003), and the Columbia River Basalts (0.0154 km^3/yr – Tolan et al., 1989).

Table 7.2. Summary of layered series volume calculations. Variables x, y, w, y’, w’ and t refer to variables in Figure 7.10. Segment A is the northern segment, B the middle segment, and C the southern segment on the map in Figure 7.10

Segment	ϴ	x (km)	y (km)	w (km)	y' (km)	w' (km)	t (km)	Volume (km3)
A	20	68	5	15.5	5.3	16.5	1.7	1608.7
B	20	42	27	32	28.7	34.1	9.2	7635.7
C	25	88	10	22	11.0	24.3	4.2	6976.0
							TOTAL	16220.4

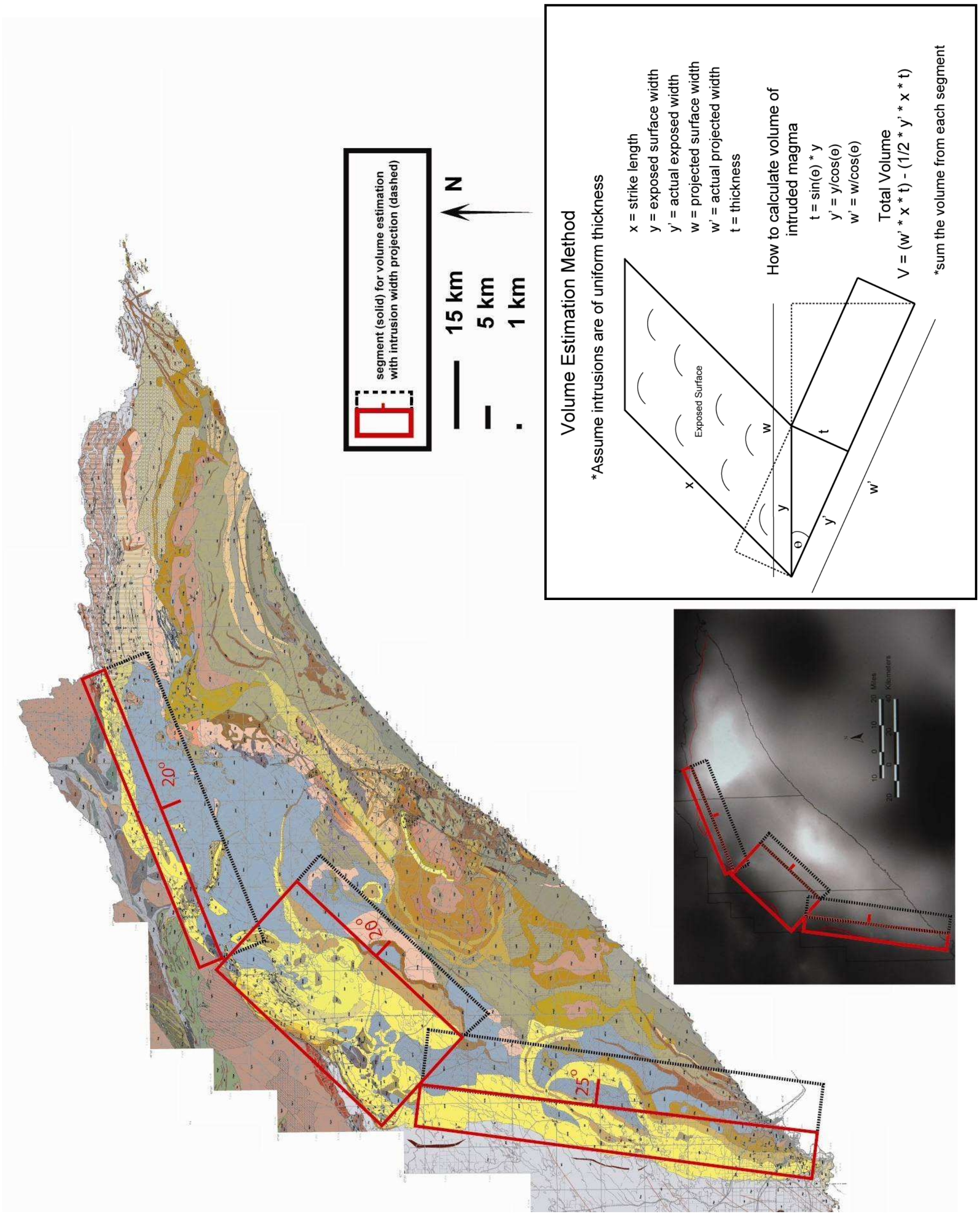

Figure 7.10. Method used to estimate the volume of mafic magma intruded during layered series emplacement. This estimate is likely conservative as it does not account for the massive amount of rock lost to erosion, or anorthositic rocks. Base map is modified from Miller et al. (2001), gravity map inlay taken from Chandler (2002).

8. Conclusions

As a result of the ages obtained in this study, several conclusions can be drawn about the temporal relationship of Duluth Complex and Beaver Bay Complex magmatism:

1) All layered series and anorthositic intrusions were emplaced at about 1098 Ma, with the bulk of layered series activity occurring within a window of 1.10 million years to 670 thousand years (1.10 Ma: max $^{207}Pb/^{206}Pb$ error window between PRI and BEI; 1097.98 ± 0.37 Ma and 1097.97 ±0.72 Ma, respectively, Fig. 7.4 – 0.670 Ma: max $^{206}Pb/^{238}U$ error window between PRI and BEI; 1095.94 ± 0.18 Ma and 1095.64 ± 0.19 Ma, respectively, Fig. 7.5). Despite the high-degree of precision, individual layered series intrusions cannot be differentiated using geochronologic data, and thus no direct support for the sequence of emplacement hypothesis of Miller and Severson (2002) was found.

2) Baddeleyite and zircon may not be analogous in light of new information. Precise zircon and baddeleyite ages (unpublished, Boise State Isotope Geology Laboratory) from the same anorthositic series sample yielded distinctly different ages (Fig. 7.2). As a result, the Tuscarora intrusion, which has a distinctly older $^{207}Pb/^{206}Pb$ age than the Partridge River intrusion (Fig. 7.4), has an unclear temporal relationship with other layered series intrusions until the differences in the zircon and baddeleyite systems are more fully understood.

3) The Houghtaling Creek troctolite has an indistinguishable age from layered series intrusions (Figs. 7.6, 7.8). This implies that Beaver Bay Complex magmatism was contemporaneous with layered series emplacement. In addition, the proposal by Miller and Chandler (1997) that the Houghtaling Creek troctolite might represent a feeder system for the 1096.1 ± 0.8 Ma Sonju Lake intrusion (Paces and Miller, 1993 – $^{207}Pb/^{206}Pb$ baddeleyite age) is impossible as the Houghtaling Creek troctolite is significantly older (Fig. 7.6).

4) The Wilson Lake ferrogabbro, interpreted by Miller and Boerboom (1994) to be older than the Houghtaling Creek troctolite, is distinctly younger than the HCT (Figs. 7.6, 7.8). This surprising result demonstrates that crosscutting relationships observed in the aeromagnetic data can be misleading (Fig. 7.7). In addition, the suggestion that the Greenwood Lake intrusion of the Duluth Complex is genetically linked to the plug-shaped Wilson Lake ferrogabbro (Miller and Severson, 2002) is implausible, since the distinctly older Bald Eagle intrusion crosscuts the Greenwood Lake intrusion.

5) The approximate two million year gap between Duluth Complex (and now early Beaver Bay Complex) magmatism and the later Beaver Bay Complex intrusions (Wilson Lake ferrogabbro, the Silver Bay intrusions, and the Sonju Lake intrusion) implied by Paces and Miller's (1993) data is still evident. However, more dating is needed from intrusions that span

the time gap between early and late Beaver Bay Complex intrusive activity to confirm this possible hiatus (Fig. 8.1).

6) A reasonable estimate based on the geometry of layered series intrusions indicate that over 16,000 km^3 of mafic magma intruded during the emplacement of the layered series (Fig. 7.10, Table 7.2). This volume estimate is quite surprising knowing that it does not take into account the unknowable amounts of erosion of layered series intrusions or the volume of magmatism associated with the anorthositic series and early Beaver Bay Complex. With over 16,000 km^3 of mafic magma being intruded over a period of around 670 thousand years, emplacement rates were at least 0.024 km^3/yr, which is similar or less than estimates for other large continental flood basalt provinces.

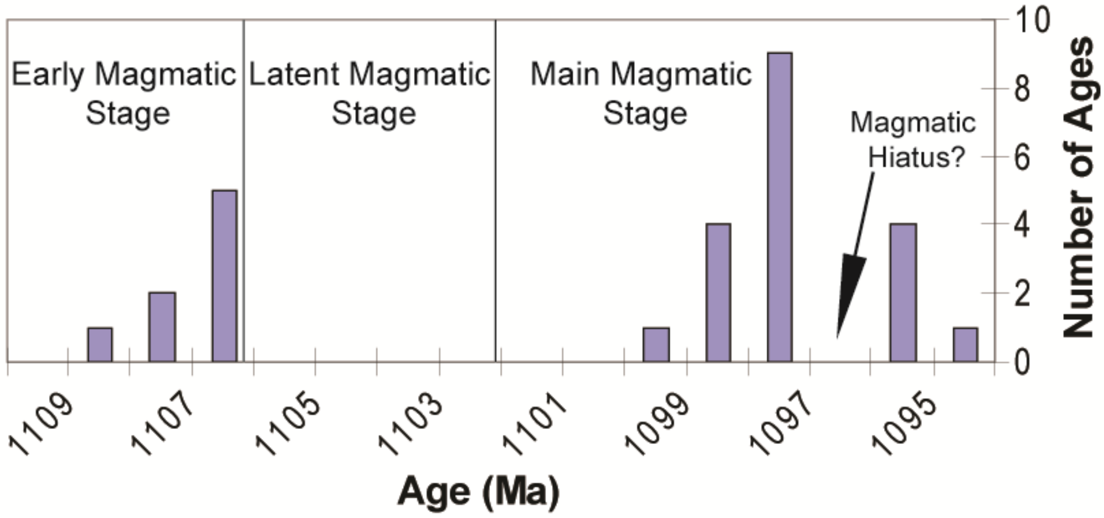

Figure 8.1. Distribution of all weighted mean $^{207}Pb/^{206}Pb$ ages for intrusions related to the Duluth Complex and Beaver Bay Complex. Data taken from Davis and Green (1997); Paces and Miller (1993); Vervoort et al (2007); Zartman et al (1997); and this study (2010)

9. References

Allen, D.J., Hinze, W.J., Dickas, A.B., Mudrey, M.G., Jr., **1997.** Integrated geophysical modeling of the North American Midcontinent rift system: new interpretations for western Lake Superior, northwestern Wisconsin, and eastern Minnesota. In: Ojakangas, R.W., Dickas, A.B., Green, J.C. (eds.), Middle Proterozoic to Cambrian rifting, central North America: *Geological Society of America Special Paper 312*, pp. 47-72.

Annells, R.N., **1973.** Proterozoic flood basalts of eastern Lake Superior: the Keweenawan volcanic rocks of the Mamainse Point area, Ontario. Geological Survey of Canada, Paper 72-10.

Baragar, W.R.A., **1978.** Michipicoten Island, Ontario, *in* Wanless, R.K., and Loveridge, W.D., eds., Rubidium-strontium isotopic age studies, Report 2 (Canadian Shield): *Geological Survey of Canada Paper 77-14*, pp. 40-43.

Behrendt, J.C., Green, A.G., Cannon, W.F., Hutchinson, D.R., Lee, M.W., Milkereit, B., Agena, W.F., Spencer, C., **1988.** Crustal structure of the Midcontinent rift system: results from GLIMPCE deep seismic reflection profiles. *Geology 16*, pp. 81-85.

Boerboom, T.J., and Miller, J.D., **1994.** Bedrock geologic map of the Siler Island Lake, Wilson Lake, and Western Toohey Lake Quadrangles, Lake and Cook counties, Minnesota: Minnesota Geological Survey Miscellaneous Map Series, M-81, scale 1:24,000.

Bonnichsen, B., **1971.** Outcrop map of southern part of Duluth Complex and associated Keweenawan rocks, St. Louis and Lake Counties, Minnesota: Minnesota Geological Survey Miscellaneous Map Series, M-11, scale 1:125,000.

Cannon, W.F., Green, A.G., Hutchinson, D.R., Lee, M.W., Milkereit, B., Behrendt, J.C., Halls, H.C., Green, J.C., Dickas, A.B., Morey, G.B., Sutcliffe, R.H., Spencer, C., **1989.** The North American Midcontinent rift beneath Lake Superior from GLIMPCE seismic reflection profiling. *Tectonics, v. 8*, pp. 305-332.

Cannon, W.F., and Nicholson, S.W., **1992.** Revisions of Stratigraphic Nomenclature within the Keweenawan Supergroup of Northern Michigan. *U.S. Geological Survey Bulletin, 1970-A*, pp. 1-8.

Cannon, W.F., **1992.** The North American Midcontinent Rift beneath the Lake Superior region with emphasis on its geodynamic evolution. *Tectonophysics, v. 213*, pp. 41-48.

Chandler, V.W., **2002.** Geophysical characteristics of the Duluth Complex and associated rocks, *in* Geology and mineral potential of the Duluth Complex and related rocks of northeastern Minnesota: Minnesota Geological Survey Report of Investigations 59, pp. 52-75.

Chaudhuri, S., **1972.** Radiometric ages of Keweenawan intrusions and extrusions in Michigan and adjacent areas. *Geological Society of America Abstracts with Programs, 4*, p. 470.

Chaudhuri, S., and Brookins, D.G., **1969.** Rb-Sr ages of late Precambrian rocks of Wisconsin. *Geological Society of America Abstracts with Programs, 1*, p. 32.

Condon, D., et al., **2007.** EARTHTIME: Isopotic tracers and optimized solutions for high-precision U-Pb ID-TIMS geochronology, Eos Trans. AGU, 88(52), Fall Meet. Suppl., Abstract V41E-06.

Costello, D.E., **2010.** Geology and Petrogenesis of the Tuscarora Intrusion of the Duluth Complex, Northeastern Minnesota. Unpublished Master's Thesis: University of Minnesota Duluth.

Courtillot, V.E., and Renne, P.R., **2003.** On the ages of flood basalt events, *Comptes Rendus Geoscience, v. 335,* pp. 113-140.

Davis, D.W., and Green, J.C., **1997.** Geochronology of the North American Midontinent rift in western Lake Superior and implications for its geodynamic evolution. *Canadian Journal of Earth Sciences, v. 34,* pp. 476-488.

Davis, D.W., and Paces, J.B., **1990.** Time resolution of geologic events on the Keweenaw Peninsula and implications for development of the Midcontinent Rift system. *Earth and Planetary Science Letters, v. 97*, pp. 54-64.

Davis, D.W., and Sutcliffe, R.H., **1985.** U-Pb ages from the Nipigon plate and northern Lake Superior. *Geological Society of America Bulletin, v. 96,* pp. 1572-1579.

Davydov, V.I., Crowley, J.L., Schmitz, M.D., and Poletaev, V.I., 2010. High-precision U-Pb zircon age calibration of the global Carboniferous time scale and Milankovitch band cyclicity in the Donets Basin, eastern Ukraine. Geochemistry Geophysics Geosystems 11, Q0AA04, doi:10.1029/2009GC002736.

Ernst, W.G., **1960.** Diabase-granophyre relations in the Endion Sill, Duluth, Minnesota. *Journal of Petrology, v. 1,* pp. 286-303.

Gardner, J.E., **1987.** Origin of the Endion Sill. Unpublished M.A. thesis: Washington University, St. Louis, 359 p.

Gerstenberger, H., and Haase, G., **1997.** A highly effective emitter substance for mass spectrometric Pb isotope ratio determinations, *Chemical geology, v. 136,* pp. 309-312.

Green, J.C., **1982.** Geology of Keweenawan extrusive rocks, *in* Wold, R.J., and Hinze, W.J., eds., Geology and tectonics of the Lake Superior basin: *Geological Society of America Memoir 156,* pp. 47-55.

Green, J.C., **1983.** Geologic and geochemical evidence for the nature and development of the middle Proterozoic (Keweenawan) Midcontinent rift of North America. *Tectonophysics, v. 94*, pp. 413-437.

Green, J.C., **2002.** Volcanic and sedimentary rocks of the Keweenawan Supergroup in northeastern Minnesota, *in* Geology and mineral potential of the Duluth Complex and related rocks of northeastern Minnesota: Minnesota Geological Survey Report of Investigations 59, pp. 94-105.

Green, J.C., Davis, D.W., and Schmitz, M.D., **2001.** Three new zircon dates for the Midcontinent Rift, North Shore, Minnesota: more data, more questions: Institute on Lake Superior geology, 47th Annual Meeting, Proceedings, v. 47, Program and Abstracts, p. 29.

Green, J.C., and Fitz, T.J., III, **1993.** Extensive felsic lavas and rheoignimbrites in the Keweenawan Midcontinent rift plateau volcanics, Minnesota: Petrographic and field recognition. *Journal of Volcanology and Geothermal Research, v. 54,* pp. 177-196.

Green, J.C., and Miller, J.D., **2008.** Bedrock Geology of the Duluth Quadrangle, St. Louis County, Minnesota: Minnesota geological Survey Miscellaneous Map Series, M-182, scale 1:24,000.

Green, J.C., Phinney, W.C., and Weiblen, P.W., **1966.** Geologic Map of Gabbro Lake Quadrangle, Lake County, Minnesota: Minnesota Geological Survey Miscellaneous Map Series, M-2, scale 1:31,680.

Heaman, L.M., Easton, R.M., Hart, T.R., Hollings, P., MacDonald, C.A., and Smyk, M., **2007.** Further refinement to the timing of Mesoproterozoic magmatism, Lake Nipigon region, Ontario. *Canadian Journal of Earth Sciences, v. 44,* pp. 1055-1086

Heaman, L.M., and Machado, N., **1992.** Timing and origin of midcontinent rift alkaline magmatism, North America: evidence from the Coldwell Complex. *Contributions to Mineralogy and Petrology, v. 110,* pp. 289-303.

Hinze, W.J., Allen, D.J., Fox, A.J., Sunwood, D., Woelk, T., and Green, A.G., **1992.** Geophysical investigations and crustal structure of the North American Midcontinent Rift system. *Tectonophysics, v. 213,* pp. 17-32.

Hollings, P., Fralick, P., and Cousens, B., **2007a.** Early history of the Midcontinent Rift inferred from geochemistry and sedimentology of the Mesoproterozoic Osler Group, northwestern Ontario. *Canadian Journal of Earth Sciences, v. 44,* pp. 389-412.

Hollings, P., Hart, T., Richardson, A., and MacDonald, C.A., **2007b.** Geochemistry of the Midproterozoic intrusive rocks of the Nipigon Embayment northwestern Ontario: evaluating the earliest phases of rift development. *Canadian Journal of Earth Sciences, v. 44,* pp. 1087-1110.

Hollings, P., Smyk, M., Heaman, L.M., and Halls, H., **2010.** The geochemistry, geochronology and plaeomagnetism of dikes and sills associated with the Mesoproterozoic Midcontinent Rift near Thunder Bay, Ontario, Canada. *Precambrian Research,* doi:10.1016/j.precamres.2010.01.012.

Hutchinson, D.R., White, R.S., Cannon, W.F., and Schulz, K.J., **1990.** Keweenaw Hot Spot: Geophysical evidence for a 1.1 Ga Mantle Plume Beneath the Midcontinent Rift System. *Journal of Geophysical Research, v. 96,* pp. 10,869-10,884.

Jaffey, A.H., Flynn, K.F., Glendenin, L.E., Bentley, W.C., Essling, A.M., **1971.** Precision measurement of half-lives and specific activities of ^{235}U and ^{238}U. *Physical Review,* C4, pp. 1889-1906.

Jerde, E.A., **1991.** Geochemistry and petrology of hypabyssal rocks associated with the Midcontinent rift, northeastern Minnesota. unpublished Ph.D. Thesis: University of California, Los Angelas, 305 p.

Jirsa, M.A., and Miller, J.D., **2004.** Bedrock geology of the Ely and Basswood Lake 30' X 60' quadrangles, northeast Minnesota: Minnesota geological Survey Miscellaneous Map Series, M-182, scale 1:100,000.

Klewin, K.W., and Shirey, S.B., **1992.** The igneous petrology and magmatic evolution of the Midcontinent rift system. *Tectonophysics, v. 213,* pp. 33-40.

Krogh, T.E., **1973.** A low contamination method for the hydrothermal decomposition of zircon and extraction of U and Pb for isotopic age determinations. *Geochemica Cosmochimica Acta, v. 37,* pp. 485-494.

Krogh, T.E., **1982.** Improved accuracy of U-Pb zircon ages by the creation of more concordant systems using an air abrasion technique. *Geochimica Cosmochimica Acta, v. 46,* pp. 637-649.

Krogh, T.E., Corfu, F., Davis, D.W., Dunning, G.R., Heaman, L.M., Kamo, S.L., Macahdo, N., Greenough, J.D., and Nakamura, E., **1987.** Precise U-Pb isotopic ages of diabase dykes and mafic to ultramafic rocks using trace amounts of baddeleyite and zircon. *In* Halls, H.C., and Fahrig, W.F. [eds.], Mafic dyke swarms. *Geological Association of Canada, Special Paper 34,* pp. 147-152.

Lightfoot, P.C., and Sutcliffe, R.H., Doherty, W., **1991.** Crustal contamination identified in Keweenawan Osler Group tholeiites, Ontario: a trace element perspective. *Journal of Geology, v. 99,* pp. 739-760.

Ludwig, K.R., **2003.** User's manual for Isoplot 3.00, 70 pp., Berkeley Geochronol. Cent, Berkeley, Calif.

Mattinson, J.M., **2005.** Zircon U-Pb chemical abrasion ("CA-TIMS") method: Combined annealing and multi-step partial dissolution analysis for improved precision and accuracy of zircon ages. *Chemical Geology, v. 220,* pp. 47-66.

Miller, J.D., **1988.** Geologic map of the Split Rock Point NE and Silver Bay quadrangles, Lake County, Minnesota: Minnesota Geological Survey Miscellaneous Map Series, M-68, scale 1:24,000.

Miller, J.D., **2004.** Petrology and PGE Potential of the Greenwood Lake Intrusion, Central Duluth Complex, Lake County, Minnesota: Minnesota Geological Survey Report of Investigations 62.

Miller, J.D., Boerboom, T.J., and Jerde, E.A., **1994.** Bedrock geologic map of the Cabin Lake and Cramer 7.5-minute Quadrangles, Lake and Cook Counties, Minnesota: Minnesota Geological Survey Miscellaneous Map Series, M-85, scale 1:24,000.

Miller, J.D., and Chandler, V.W., **1997.** Geology, petrology, and tectonic significance of the Beaver Bay Complex, northeastern Minnesota. *In*: Ojakangas, R.W., Dickas, A.B., Green, J.C. (eds.), Middle Proterozoic to Cambrian rifting, central North America: *Geological Society of America Special Paper 312*, pp. 73-96.

Miller, J.D., and Green, J.C., **2002.** Geology of the Beaver Bay Complex and related hypabyssal intrusions, *in* Geology and mineral potential of the Duluth Complex and related rocks of northeastern Minnesota: Minnesota Geological Survey Report of Investigations 59, pp. 144-163.

Miller, J.D., and Green, J.C., **2008.** Bedrock Geology of the West Duluth and Eastern Portion of the Esko Quadrangles, St. Louis County, Minnesota: Minnesota Geological Survey Miscellaneous Map Series, M-183, scale 1:24,000.

Miller, J.D., Green, J.C., and Boerboom, T.J., **1989.** Geology of the Illgen City quadrangle, Lake County, Minnesota: Minnesota Geological Survey Miscellaneous Map Series, M-69, scale 1:24,000.

Miller, J.D., Green, J.C., Boerboom, T.J., and Chandler, V.W., **1993.** Geologic Map of the Doyle Lake and Finland quadrangles, Lake County, Minnesota: Minnesota Geological Survey Miscellaneous Map Series, M-72, scale 1:24,000.

Miller, J.D., Green, J.C., and Jerde, E.A., **2006.** Bedrock geology of the Little Marais quadrangle, cook County, Minnesota: Minnesota Geological Survey Miscellaneous Map Series, M-172, scale 1:24,000.

Miller, J.D., Green, J.C., and Severson, M.J., **2002.** Terminology, nomenclature, and classification of Keweenawan igneous rocks of northeastern Minnesota, *in* Geology and mineral potential of the Duluth Complex and related rocks of northeastern Minnesota: Minnesota Geological Survey Report of Investigations 59, pp. 5-20.

Miller, J.D., Green, J.C., Severson, M.J., Chandler, V.W., and Peterson, D.M., **2001.** Geologic map of the Duluth Complex and related rocks, northeaster Minnesota: Minnesota geological Survey Miscellaneous Map Series, M-119, scale 1:2000,000.

Miller, J.D., Nicholson, S.W., and Cannon, W.F., **1995.** The Midcontinent Rift in the Lake Superior region. *in:* Miller, J.D., Jr., (Ed.), Field Trip Guidebook for the Geology and Ore Deposits of the Midcontinent Rift in the Lake Superior Region, Minnesota Geological Survey, Guidebook Series 20, pp. 1-22.

Miller, J.D., and Severson, M.J., **2002.** Geology of the Duluth Complex, *in* Geology and mineral potential of the Duluth Complex and related rocks of northeastern Minnesota: Minnesota Geological Survey Report of Investigations 59, pp. 106-153.

Miller, J.D., and Ripley, E.M., **1996.** Layered intrusions of the Duluth complex, Minnesota, USA. In: Cawthorn, R.G. (Ed.), Layered Intrusions. Elsevier Science, Amsterdam, pp. 257-301.

Miller, J.D., and Vervoort, J.D., **1996.** The latent magmatic stage of the Midcontinent rift: a period of magmatic underplating and melting of the lower crust: Institute on Lake Superior geology, 42nd Annual Meeting, Proceedings, v. 42, Program and Abstracts, pt. 1, pp. 33-35.

Miller, J.D., and Weiblen, P.W., **1990.** Anorthositic Rocks of the Duluth Complex: Examples of Rocks Formed from Plagioclase Crystal Mush. *Journal of Petrology, v. 31*, pp. 295-339.

Morey, G.B., and Green, J.C., **1982.** Status of the Keweenawan as a stratigraphic unit in the Lake Superior region, *in* Wold, R.J., and Hinze, W.J., eds., Geology and tectonics of the Lake Superior basin: *Geological Society of America Memoir, v. 156*, pp. 15-26.

Morey, G.B., Mudrey, M.G., Jr., **1972.** Keweenawan volcanic rocks in east-central Minnesota. In: Sims, P.K.,, Morey, G.B. (Eds.), Geology of Minnesota: A Centennial Volume. Minnesota Geological Survey, pp. 425-430.

Nicholson, S.W., Shirey, S.B., **1990.** Midcontinent rift volcanism in the Lake Superior region: Sr, Nd, and Pb isotopic evidence for a mantle plume origin. *Journal of Geophysical Research, v. 95*, pp. 10851-10868.

Nicholson, S.W., Shirey, S.B., Schulz, K.J., Green, J.C., **1997.** Rift-wide correlation of 1.1 Ga Midcontinent rift system basalts: implications for multiple mantle sources during rift development. *Canadian Journal of Earth Sciences, v. 34,* pp. 504-529.

Paces, J.B., and Miller, J.D., **1993.** Precise U-Pb Ages of the Duluth Complex and Related Mafic Intrusions, Northeastern Minnesota: Geochronological Insights to Physical, Petrogenetic, Paleomagnetic, and Tectonomagmatic Processes Associated With the 1.1 Ga Midcontinent Rift System. *Journal of Geophysical Research, v. 98*, pp. 13,997-14,013.

Palmer, H.C., and Davis, D.W., **1987.** Paleomagnetism and U-Pb geochronology of volcanic rocks from the michipicoten island, Lake Superior, Canada: precise calibration of the Keweenawan polar wander track. *Precambrian Research, v. 37,* pp. 157-171.

Peterson, D.M., and Severson, M.J., **2002.** Archean and Paleoproterozoic rocks that form the footwall of the Duluth Complex, *in* Geology and mineral potential of the Duluth Complex and related rocks of northeastern Minnesota: Minnesota Geological Survey Report of Investigations 59, pp. 76-93.

Queen, M., Heaman, L.M., Hanes, J.A., Archibald, D.A., and Farrar, E., **1996.** 40Ar/39Ar pholgopite and U-Pb perovskite dating of lamprophyre dykes from the eastern Lake Superior region: evidence for a 1.14 Ga magmatic precursor to Midcontinent Rift volcanism. *Canadian Journal of Earth Sciences, v. 33,* pp. 958-965.

Renne, P.R., and Basu, A.R., **1991.** Rapid eruption of the Siberian Traps flood basalts at the Permo-Triassic boundary. *Science, v. 253,* pp. 176-179.

Rogala, B., Fralick, P.W., Heaman, L.M., and Metsaranta, R., **2007.** Lithostratigraphy and chemostratigraphy of the Mesoproterozoic Sibley Group, northwestern Ontario, Canada. *Canadian Journal of Earth Sciences, v. 44,* pp. 1131-1149.

Schmitz, M.D., Bowring, S.A., and Ireland, T.R., **2003.** Evaluation of Duluth Complex anorthositic series (AS3) zircon as a U-Pb geochronological standard: New high-precision isotope dilution thermal ionization mass spectrometry results. *Geochimica Cosmochimica Acta, v. 67,* pp. 3365-3672.

Schmitz, M.D., and Schoene, B., **2007.** Derivation of isotope ratios, errors, and error correlations for U-Pb geochronology using 205Pb-235U-(233U)-spiked isotope dilution thermal ionization mass spectrometric data. *Geochemistry Geophysics Geosystems, v. 8*, Q08006, doi"10.1029/2006GC001492

Schoene, B., Crowley, J.L., Condon, D.J., Schmitz, M.D., and Bowring, S.A., **2006.** Reassessing the uranium decay constants for geochronology using ID-TIMS U-Pb data. *Geochimica Cosmochimica Acta, v. 70,* pp. 426-445.

Severson, M.J., and Miller, J.D., **1999.** Bedrock Geologic Map of Allen Quadrange, Minnesota: Minnesota Geological Survey Miscellaneous Map Series, M-91, scale 1:24,000.

Shirey, S.B., **1997.** Re-Os isotopic compositions of Midcontinent rift system picrites: implications for plume - lithosphere interaction and enriched mantle sources. *Canadian Journal of Earth Science, v. 34,* pp. 489-503.

Shirey, S.B., Klewin, K.W., Berg, J.H., and Carlson, R.W., **1994.** Temporal changes in the sources of flood basalts: Isotopic and trace element evidence from the 1100 Ma old Keweenawan Mamainse Point Formation, Ontario, Canada. *Geochimica Cosmochimica Acta, v. 58,* pp. 4475-4490.

Silver, L.T., and Green, J.C., **1972.** Time constraints for Keweenawan igneous activity. *Geological Society of America Abstracts with Programs, 4,* pp. 665-666.

Tolan, T.L., Reidel, S.P., Beeson, M.H., Anderson, J.L., Fecht, K.R., and Swanson, D.A., **1989.** Revisions to the estimates of the areal extent and volume of the Columbia River Basalt Group. *Geological Society of America Special paper 239,* pp. 1-20.

Van Schmus, W.R., **1992.** Tectonic setting of the Midcontinent Rift system. *Tectonophysics, v. 213*, pp. 1-15.

Van Schmus, W.R., Green, J.C., Halls, H.C., **1982.** Geochronology of Keweenawan rocks of the Lake Superior region: a summary. In: Wold, R.J., Hinze, W.J. (Eds.), Geology and Tectonics of the Lake Superior Basin. *Geological Society of America Memoir 156*, pp. 165-171.

Van Schmus, W.R, and Hinze, W.J., **1985**. The Midcontinent Rift System. *Annual Review of Earth and Planetary Sciences, v. 13,* pp. 345-383.

Vervoort, J.D., Wirth, K., Kennedy B., Sandland, T., and Harpp, K.S., **2007.** The magmatic evolution of the Midcontinent rift: New geochronologic and geochemical evidence from felsic magmatism. *Precambrian Research, v. 157,* pp. 235-268.

Weiblen, P.W., **1965.** A funnel-shaped gabbro-troctolite intrusion in the Duluth Complex, Lake County, Minnesota. Ph.D. thesis: University of Minnesota, p. 161.

Weiblen, P.W., and Morey, G.B., **1980.** A summary of the stratigraphy, petrology, and structure of the Duluth Complex. *American Journal of Science, v. 280-A,* pp. 88-133.

Zartman, R.E., Nicholson, S.W., Cannon, W.F., Morey, G.B., **1997.** U-Th-Pb zircon ages of some Keweenawan Supergroup rocks from the south shore of Lake Superior. *Canadian Journal of Earth Sciences, v. 34,* pp. 549-561.